personal buildup for

Force Motors Limited Library

MTZ worldwide 1/2012, as epaper released on 21.12.2011
http://www.mtz-worldwide.com

content:

page 1: Cover. p.1

page 2: Contents. p.2

page 3: Editorial. p.3

page 4: Peter Schoeggl, Andreas Haimann, Leo Ress: Electrification in Motorsports. p.4-11

page 12: Steve M. Sapsford, Tim Yates, Richard Farquhar: The V8 Engine for McLaren´s new MP4-12C. p.12-17

page 18: Wolfgang Maus, Rolf Brück, Roman Konieczny, Peter Hirth: The Future of Exhaust Aftertreatment Design for Electrified Drive Trains. p.18-25

page 26: Richard Bauder, Jan Helbig, Henning Marckwardt, Halit Genc : The new 3.0-Litre TDI Biturbo Engine from Audi - Part 1: Design and Engine Mechanics . p.26-33

page 34: Jürgen Stehlig, James Taylor, Rene Dingelstadt, David Gurney: Variable-length Air Intake Module for Turbocharged Engines. p.34-41

page 42: Carsten Enge, Ralf Sternberg, Wolfgang Tschiggfrei: Enhancing Efficiency in Calibrating Diesel Engines for Low Temperatures. p.42-47

page 48: Matthias Kroll, Gero Seydler: Noise Absorption Close to the Engine with Positive Thermal Effects. p.48-52

page 53: Research Peer Review. p.53

page 54: Christina Artmann, Hans-Peter Rabl, Martin Faulstich : Online Oil Dilution Measurement at Gasoline Engines. p.54-59
page 60: Christoph Heinz, Stefan Kammerstätter, Thomas Sattelmayer : Prechamber Ignition Concepts for Stationary Large Bore Gas Engines. p.60-65

www.MTZonline.com

MTZ WORLDWIDE

01 January 2012 | Volume 73

CATALYST SYSTEM for Electrified Drive Trains

ENHANCING EFFICIENCY in Calibrating Diesel Engines for Low Temperatures

OIL DILUTION Measurement at Gasoline Engines

THE FUTURE OF SPORTS ENGINES

CONTENTS

COVER STORY

THE FUTURE OF SPORTS ENGINES

4, 12 I Sports car and racing car powertrains are in some cases experiencing an almost revolutionary change. As in series-production vehicles, reducing fuel consumption is becoming increasingly important and new drive technologies are being introduced. Our cover story examines the current and future development trends.

COVER STORY

SPORTS ENGINES

4 Electrification in Motorsports
Peter Schoeggl, Andreas Haimann, Leo Ress [AVL]

12 The V8 Engine for McLaren's New MP4-12C
Steve M. Sapsford, Tim Yates [Ricardo], Richard Farquhar [McLaren]

DEVELOPMENT

CATALYSTS

18 The Future of Exhaust Aftertreatment Design for Electrified Drive Trains
Wolfgang Maus, Rolf Brück, Roman Konieczny, Peter Hirth [Emitec]

DIESEL ENGINES

26 The New 3.0-l TDI Biturbo Engine from Audi – Part 1: Design and Engine Mechanics
Richard Bauder, Jan Helbig, Henning Marckwardt, Halit Genc [Audi]

AIR MANAGEMENT

34 Variable-length Air Intake Module for Turbocharged Engines
Jürgen Stehlig, James Taylor, Rene Dingelstadt, David Gurney [Mahle]

ENGINE MANAGEMENT

42 Enhancing Efficiency in Calibrating Diesel Engines for Low Temperatures
Carsten Enge, Ralf Sternberg, Wolfgang Tschiggfrei [IAV]

ACOUSTICS

48 Noise Absorption Close to the Engine with Positive Thermal Effects
Matthias Kroll, Gero Seydler [Isolite]

RESEARCH

53 Peer Review

MEASURING TECHNIQUES

54 Online Oil Dilution Measurement at Gasoline Engines
Christina Artmann, Hans-Peter Rabl [University of Applied Sciences Regensburg], Martin Faulstich [Technical University of Munich]

GAS ENGINES

60 Prechamber Ignition Concepts for Stationary Large Bore Gas Engines
Christoph Heinz [MTU Friedrichshafen], Stefan Kammerstätter, Thomas Sattelmayer [Technical University of Munich]

RUBRICS I SERVICE

3 Editorial
47 Imprint, Scientific Advisory Board

PASSIONATELY EFFICIENT

Dear Reader,

Vehicle development is focusing increasingly strongly on efficient overall systems. We are researching into new technologies and expanding our perspective from local emissions to so-called "well to wheel" energy use. We are experiencing a huge increase in complexity, alternative powertrains are expanding the modular system for the drive train and the combination possibilities are becoming almost infinite. And for the consumer in particular, it is becoming more and more difficult to understand the complex technologies and to see the benefits of one particular drive system over another.

One might assume that emotionality has taken a back seat, that sports cars are seen as being out of date and can therefore no longer be used to boost a car maker's image. But in fact the opposite is true. An emotional vehicle in particular can help to explain complex technology and to illustrate the effect of a certain powertrain configuration. It is hardly surprising, therefore, that the major development trends from large-volume production – such as downsizing or electrification – can be found more and more often in sports cars and racing cars.

Spectators at a 24-hour race will see the advantage of a hybrid system if the car has to stop for fuel less often. At the same time, they will realise that none of the fascination of a racing car is lost even when it is powered by a hybrid or diesel engine. This was proven by Audi and Peugeot in Le Mans, for example, or by Porsche with the 911 GTR R Hybrid. And these were not simple marketing ploys by the manufacturers. A racing team wants to win, and a road-going sports car needs to be fast – and new technologies help in that respect too. Increasingly, what were initially purely efficiency measures are also proving to be a potential benefit for vehicle dynamics.

MTZ is starting the New Year with a cover story dedicated entirely to sports car and racing car engines, probably the most emotional aspect of a car. While preparing the articles, I met many people who are very aware of their role as a multiplier and who are working very passionately at keeping fascination alive even in highly efficient drive systems.

I wish you all the best for 2012 – as well as a lot of pleasure and passion in your work.

RUBEN DANISCH, Vice Editor-in-Chief
Wiesbaden, 28 November 2011

ELECTRIFICATION IN MOTORSPORTS

The electrified powertrain keeps entering in motorsports as well. Hybrid drives are used in Formula 1 since 2009 and for 2013 the FIA plans a special race series for electric vehicles. At present, therefore there is a strong wave of innovation, in which it is still unclear which technologies will prevail. AVL describes various systems and their advantages and disadvantages. Based on simulations the impact on performance parameters, lap time, speed and duration of the race gets clear.

AUTHORS

DR. PETER SCHOEGGL
is Deputy Vice President for the Business Field Racing, Engineering and Technology Powertrain Systems at AVL List GmbH in Graz (Austria).

DIPL.-ING. ANDREAS HAIMANN
is Project Manager Racing in the Vehicle Department for Engineering and Technology Powertrain Systems at AVL List GmbH in Graz (Austria).

LEO RESS
is Senior Technical Advisor – Racing in the Vehicle Department for Engineering and Technology Powertrain Systems at AVL List GmbH in Graz (Austria).

HYBRID IN MOTORSPORTS

Hybrid-powered vehicles are used in Formula 1 only since 2009, in the LMP Series since 2011. For 2013, the FIA plans the introduction of a new and very innovative electric race series, called Formula E. In current and future reglements, electric powertrains will be favored to promote electric mobility in motorsports. This way, the principal disadvantage of electric powertrains, the low specific energy density of the storage media, should be compensated.

From 2009 until 2013, relatively low electric performances of 60 kW max are used in Formula One; the retrievable energy per lap is limited to 400 kJ. The permitted boost duration of 6.66 s is mostly used in combination with an adjustable rear wing to enable or prevent overtaking maneuvers. Starting in 2014, the FIA regulations for Formula One will allow the electric power to double to 120 kW and a maximum energy of 4 MJ. Up to 2 MJ kinetic energy per lap can be stored in the battery and additional energy can be produced via an engine/generator, connected to the turbocharger. With this connection of combustion engine and hybrid drive, a high number of strategy varieties for performance and energy management are possible.

Since 2011, hybrid drives are also allowed in the LMP series. The electric energy, released during two braking maneuvers is limited to 500 kJ; the electric power of the hybrid drive is not limited. In contrary to the Formula One, an electric four-wheel drive is allowed in the LMP series. Other race series are also considering allowing hybrid systems.

CHARACTERISTIC OF RACING VEHICLES

Naturally, racing vehicles are operated close to the dynamic limit of the car; Braking and acceleration phases alternate constantly. While accelerating, the kinetic energy of the vehicle increases and is usually converted into heat during the following braking phase. This characteristic fits the hybridization perfectly; recuperation of energy while braking and release of the saved energy while accelerating. The performance characteristics for power and energy depend on the race track profile, the vehicle weight, the aero performance and the tire grip.

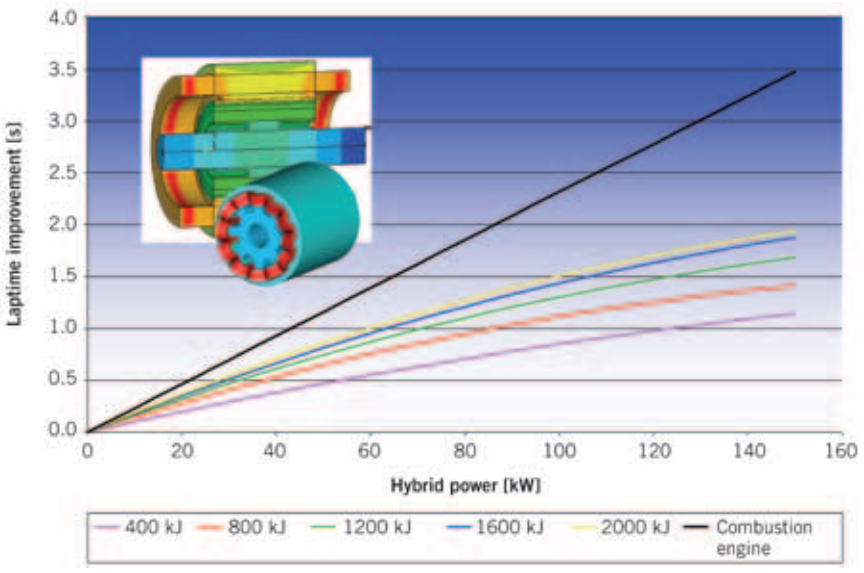

❶ Influence of KERS power and energy on lap time (Circuit Spa)

The braking power of a Formula One vehicle amounts to more than 2400 kW [1] at top speed and the released energy at a 300 to 100 km/h braking maneuver is more than 2000 kJ. This braking energy is lost without hybrid technology. But even with hybrid technology only part of it can be recuperated, because electric generator- and storage power are limited.

According to current Formula 1 regulations [2], only a maximum of 60 kW of electric power may be used during braking and accelerating, which is only a fraction of the possible 2400 kW. There are limits to propulsion and braking ability at low speeds due to tire slip. In this area, either the braking power has to be reduced or only part of the engine power can be used. The full power from recuperation can only be transferred as soon as the power of the engine gets too low to maintain a propulsion-ideal longitudinal tire slip. In 2009, hybrid technology appeared under the name of KERS for the first time in the Formula One. KERS stands for Kinetic Energy Recovery System; the permitted power during charging and discharging was 60 kW max, the energy rendered per lap was limited to 400 kJ. The Formula One KERS system is limited to interaction with the rear tires only. In the LMP, an energy recovery system (called STSYS) is allowed since 2011 and the system may interact with both, front or rear tires [3]. ❶ shows the influence of KERS power and energy on lap time by means of a simulation.

SYSTEMS FOR ENERGY RECOVERY

The development of KERS systems started as early as 2006, right after finalization of the 2009 regulations. A few different technologies where considered which are described in the following.

ELECTRICAL SYSTEMS

Here, merely electric components are used: an engine/generator, a battery and an electric inverter incl. electronic control unit. The 60 kW KERS engine weighs only 5 to 6 kg and is usually liquid cooled. Liquid cooling or heating is also preferred for the battery cells. The weight of the entire KERS system is around 20 to 30 kg. The entire electric system has significant advantages when it comes to packaging and weight distribution.

Only the electric engine has to be linked directly with the vehicle drive train, all other components can be connected by partially thick wires and placed at advantageous positions throughout the vehicle. However, negative influences on aerodynamics are inevitable due to necessary cooling surfaces. For the power pack, mistakenly called batteries most of the time, the specific power is important. With special Li-Ion or Li-Po power packs, values of more than 5 kW/kg are achievable, ❷.

For the use in the Formula 1, special cell types where developed which are usually replaced after every race. Starting in 2014, batteries have to be used for five races, just like every other drive train component. A principal alternative to batteries are capacitors, so called Super-Caps. With them, specific power of over 10 kW/kg can be achieved. However, due to a higher internal resistance, Super-Caps generate a lot of heat and need significantly more cooling. Also, the specific energy is relatively low; therefore Super-Caps could not be established in Formula 1.

Li-Ion batteries react sensitive to fast charge- and discharge cycles. The even charge balance of all cells has to be closely monitored. If this is not the case, cells are overloaded and destroyed. Fully electrical KERS systems where developed by Magneti Marelli – for example. Key components such as electric engines where partly developed by the teams themselves [5].

MECHANICAL SYSTEMS

The oldest form of energy storage is the flywheel. The modern flywheel runs with very high revs exceeding 60,000 rpm; the high centrifugal forces are controlled by composite fibers. A purely mechanical system was developed by a company called “Flybrid” [6]. The demanded storage capability of 400 kJ was achieved with a mass of about 5 kg. The flywheel is linked to the drive train by a continuously variable transmission. The CVT transmission is necessary to connect the mass either braking or accelerative to the drive train. It can be controlled electronically via transmission control.

ELECTROMECHANICAL SYSTEMS

The two earlier mentioned systems do have their disadvantages. Especially the storage of energy with high-powered Li-Ion power packs, their life-span and reliability were critical factors for a long time. The electromechanical system tries to combine the advantages of the two systems; it is electromechanical storage. The CVT transmission and the battery are no longer necessary. The new system consists of an electric motor at the drive train, a power unit with electrical control unit and energy storage by means of a flywheel. The advantage of such systems lies in increased life-span compared to batteries. A Disadvantage is the space requirement of the flywheel, which is very critical for open wheel race cars.

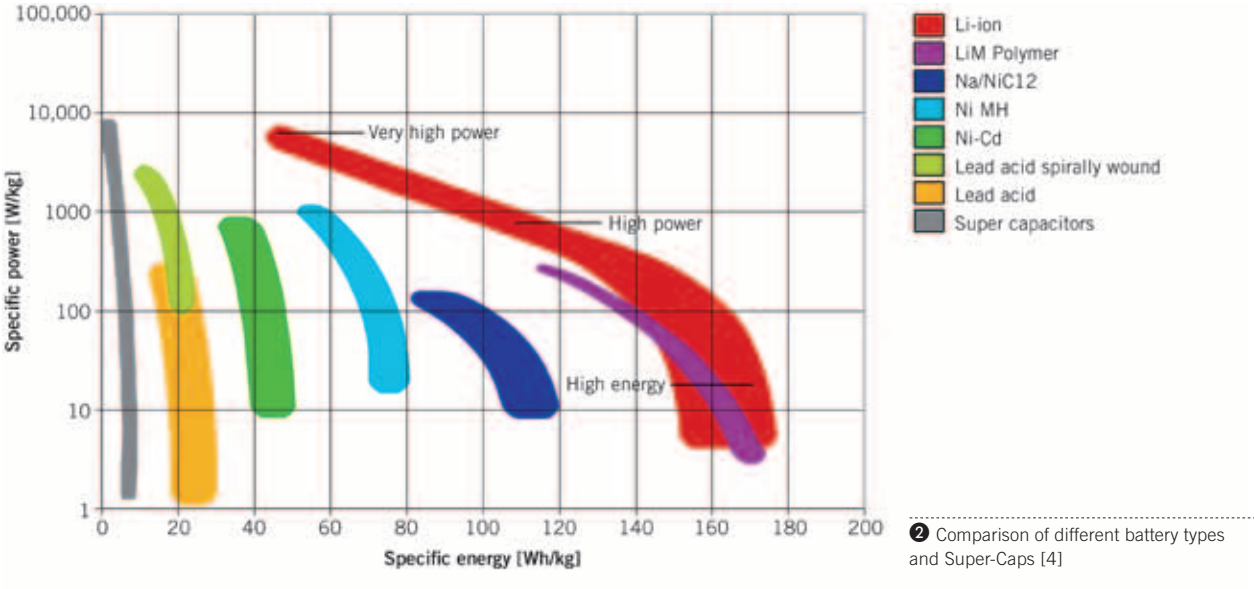

❷ Comparison of different battery types and Super-Caps [4]

COMBINATION OF FLYWHEEL STORAGE WITH A SECOND ELECTRIC ENGINE

Similar to the mechanical system, a flywheel is used which is now accelerated or decelerated by a second electric motor. The second one works in opposition to the aggregate at the combustion engine. The idea works like this: if the aggregate is used as a generator on the combustion engine, the second machine acts as a motor and accelerates the inertia; if the machine on the combustion engine acts as an electric motor, the other one acts as a generator to draw energy out of the inertia. The system is quite conventional; the only disadvantage comes from the installation of the second electric machine which increases the weight. A system like that was developed by Magneti Marelli and Flybrid in cooperation [7].

THE ROTOR OF THE SECOND E-MACHINE ACTS AS INERTIA STORAGE

A real innovative solution can be realized if the rotor of the 2nd E-machine operates as inertia storage. The basic idea is similar to the passive inertia; high revving composite wheels are running in a housing with a vacuum atmosphere. The innovation is the implantation of magnetic particles into the composite material so it can be electrically activated and operated like a rotor of an electric machine. At the moment there are two suppliers that offer such systems: WHP (Williams Hybrid Power) [8] and Dynastore from Compact Dynamics [9].

RACING APPLICATIONS – FORMULA 1

Starting in 2009, KERS was used by the top teams most of the time. All successful systems were fully electrical. The gain of lap time was strongly dependent on the characteristics of the actual circuit and the expected advantages of the system where only partly obtained.

In the 2010 season KERS was not used in the Formula One, based on an agreement of the FOTA teams in order to keep the costs low. In 2011, KERS was used again, but with slightly adapted regulations:

- The size of the front tires has been reduced by 1 inch to adapt the tire dimension to the new weight distribution
- The minimum total car weight including the driver has been increased to 640 kg
- The weight distribution has been fixed at 46 % at the front and 54 % at the rear with a variation of maximal 0.5 % in all directions, to allow an easier vehicle adaption to the new Pirelli tires.

Many teams use the Magneti Marelli KERS system in 2011 [10]. However, the top teams will continue using their own components to best suit their car. In 2014, regu-

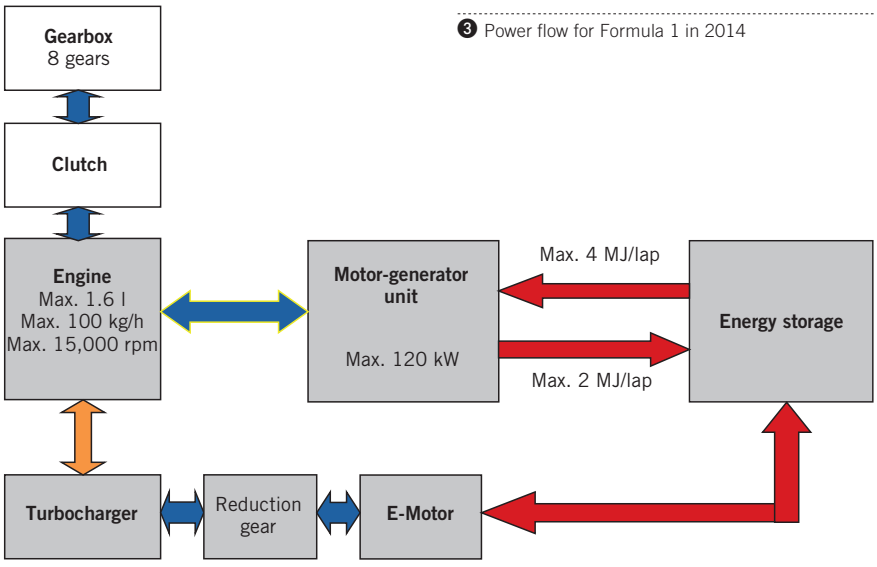

❸ Power flow for Formula 1 in 2014

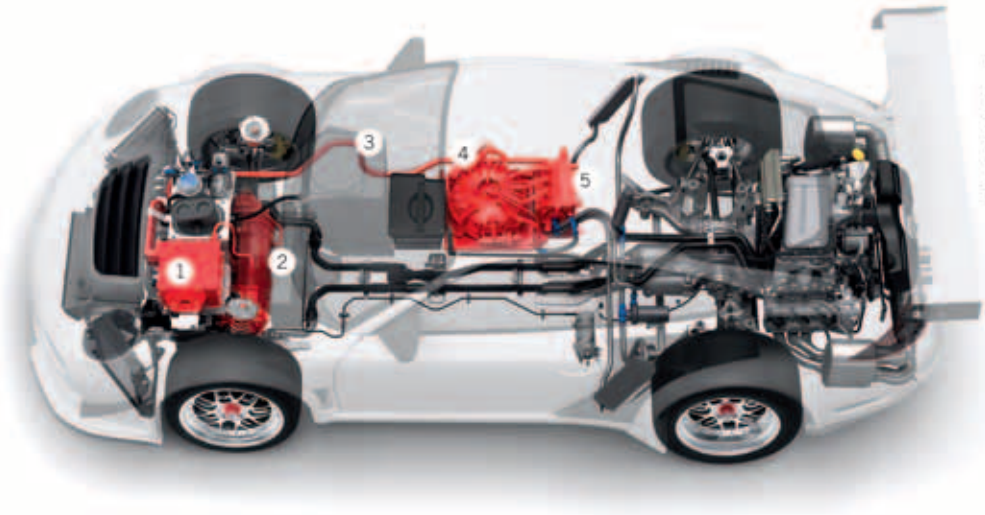

1. Power electronics
2. Portal shaft with two electric motors
3. High-voltage cable
4. Electrical flywheel battery
5. Power electronics

❹ Drive train at the front axle of the Porsche GTR 3 Hybrid [12]

lation adaptions will result in big changes in the Formula 1 [11]; in the following are extracts of these new regulations:

: electric drive power 120 kW (now called ERS)
: energy output from storage to ERS of 4 MJ max per lap
: energy recovery from drive train in recuperation 2 MJ max per lap
: combustion engine displacement 1.6 l, V6 turbo charged, the shaft of the turbo charger may be connected to the second E-machine, maximum rev 15,000 rpm, fuel consumption 100 kg/h max over 10,500 rpm. Direct fuel injection must be used; injection pressure limited to 500 bar.

A diagram for the power flow of the 2014 systems can be seen in ❸.

LMP

Since 2011, hybrid vehicles are also allowed in the LMP1 series. The regulations [3] allow the electric drive train (called STSYS) on front or rear axle. The released energy between two braking maneuvers is limited to 500 kJ, but there is no power limitation. Also, the fuel cell volume of the STSYS vehicles was adapted to the standard drive train, which increased the competitiveness of hybrid vehicles dramatically. However, in 2011 no competitive vehicles were to be seen, but Peugeot completed a series of tests with a hybrid drive train in October 2011. Its expected to see that vehicle in Le Mans 2012; as well as a hybrid-powered Audi and Toyota.

SPORTS AND TOURING CARS

At the 24 h race at the Nürburgring in 2010, a Porsche GT3 R Hybrid, equipped with the WHP flywheel system, was leading for many hours. The concept of this particular vehicle differed strongly from the usual WHP system used in the Formula 1, ❹.

In contrary to Formula One cars where the rear wheels are activated by KERS, Porsche has installed two electric machines at the front end. To use KERS on the front wheels has some advantages; the additional power can already be used at low speeds while the rear wheels are still operating at the slip limit caused by the power of the combustion engine. The earlier the additional power is activated the more time can be gained. Furthermore, the braking power is stronger at the front wheels and the braking stability is higher if the rear wheels are unloaded by the additional inertia to charge the storage system.

In ❺ the vehicle stability while braking around the vertical axis with and without KERS for rear-wheel drive only is demonstrated. With an open wheel car with aerodynamic downforce, the braking balance should change over the vehicle speed. A constant, additional electrical power will further change the longitudinal force balance, unfortunately towards an unfavorable direction; this results in a significantly lowered braking stability while braking on the limit.

In other motorsports categories, hybrid systems have hardly been used. In 2007, a Toyota Supra Hybrid won the 24 h of Tokachi [13], but this result was rarely perceived in Europe. In the future, hybrid powered vehicles will be introduced in many different other racing series and the regulations of the most important ones are adapted currently. The new rules will favor the use of hybrids in motorsports. Topics like electrical four-wheel drive and torque vectoring will be of interest and the storage charging at part load of the combustion engine will be used.

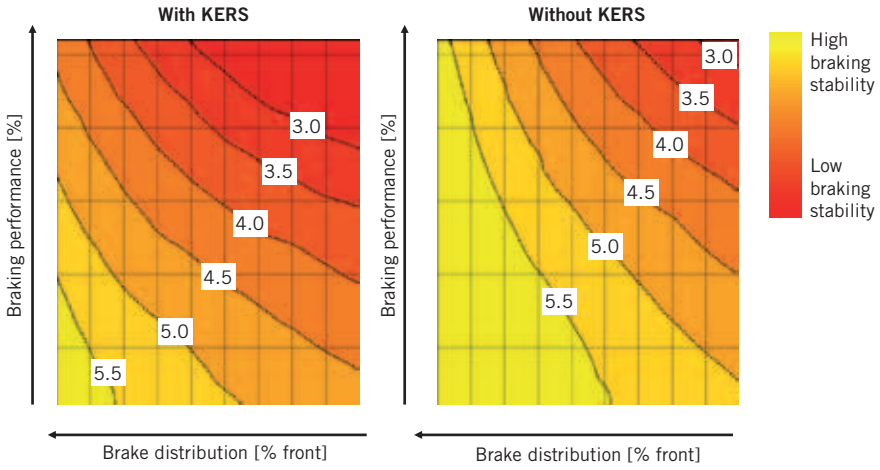

❺ Vehicle stability around the vertical axis with and without KERS (AVL simulation)

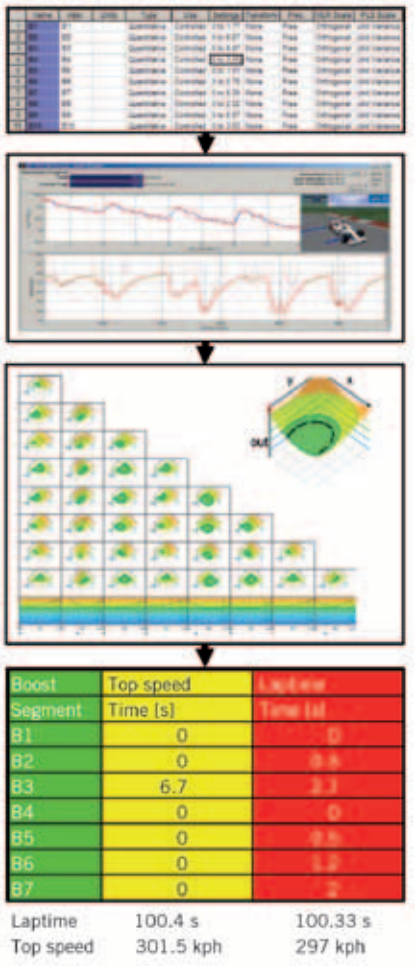

❻ Simulation for optimum race strategy (AVL simulation)

RACE STRATEGY

KERS can be used for different objectives: To realize the best lap time in qualifying and part of the race or to gain the best top speed in order to overtake or to avoid being overtaken.

❻ shows the process on how to generate the optimum race strategy by the utilization of advanced simulation tools. Thereby the entire vehicle including tires, the driver behavior and the race track are simulated. A DoE concept is used in order to reduce the number of runs. This way, it needs only about 50 simulated laps to define the best boost strategy for the best lap time or the best top speed. The whole procedure will take about two hours. With further increased ERS power as it will be possible from 2014 on, the braking balance based on stability criteria should be included.

ELECTRICAL VEHICLES IN MOTORSPORTS

For 2013, the Federation of international motorsports commission FIA plans the introduction of a racing series for pure electrical vehicles [14]. In order to give that racing series an innovative character, the regulations were drawn up quite freely. This way, the most creative engineers will have a high level of freedom.

The target will be to push the development for the critical components of an electric drive train, in particular the batteries, the electric motors and the electronic controls. To promote the electric drive train, a new variable aerodynamic was permitted. On the basis of that, downforce and drag can be adjusted to the optimum; low drag for the straights, high downforce for cornering. Main issues for the new rules are:

- number of electric motors free; four-wheel drive possible
- weight of the rolling chassis minimum 540 kg, batteries max 300 kg, total vehicle weight min 780 kg
- aerodynamics and bodywork free in design, downforce and drag adjustable by the driver
- safety cell on the level of Formula 1.

The plan is, to first start with race durations of of 15 to 20 min. This duration shall be extended later on continuously, based on the expected rapid development of the components and especially the storages.

PERFORMANCE AND DURATION OF RACES

The rules for the E-Racers contain an additional point compared to well-known racing leagues; the stored energy is limited by the mass of the battery. ❼ shows a comparison between energy density of different sources [15].

Just looking at the energy content of gasoline compared to batteries, highlights the challenges of electric propulsion. Gasoline has 80 times the energy density of a current state of the art Li-Ion battery.

To use the available energy in the best way, the developers and designers of the vehicle will face high demands. It is essential to optimize variables like motor power, aerodynamics, power distribution, recuperation as well as the strategy behind the usage of energy.

The simplest control of the energy consumption can be done by restricting the used engine power. This alone will not lead to a winning concept. One of the attributes of the electric propulsion is the recuperation. At each brake application a part of the kinetic energy of the vehicle can be used to recharge the accumulator. For a short time the electric engine is capable of taking increased thermal stress to generate even more energy.

Nevertheless, just 15 to 20 % of the used energy can be recuperated. A further aspect with high influence is aerodynamics. In using variable components, the top

❼ Specific energy of various energy sources

SPECIFIC ENERGY	MJ/kg	kWh/kg
DOUBLE LAYER CAPACITOR	0.02	0.0055
FLYWHEEL	0.18	0.05
LEAD BATTERY	0.11	0.03
NICD BATTERY	0.14	0.039
NIMH BATTERY	0.36	0.10
ZEBRA BATTERY	0.43	0.119
LI-ION BATTERY	0.5	0.139
ZINC-AIR BATTERY	1.2	0.333
LI-AIR BATTERY	3.6	1.000
NATURAL GAS	22.7	6.306
METHANE	24.3	6.750
GASOLINE	43	11.945
DIESEL	45.4	12.612
HYDROGEN	142	39.447

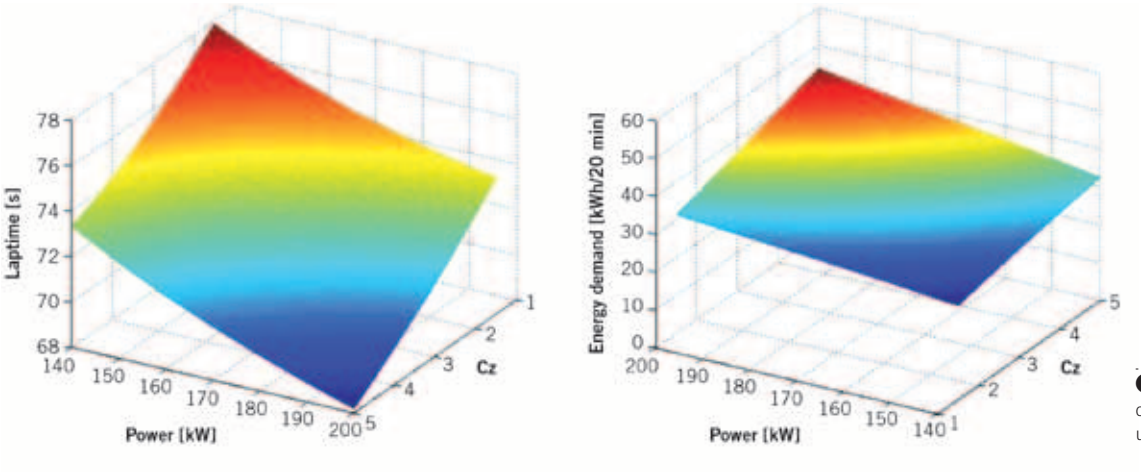

❽ Relationship power, down force, energy usage (Circuit Pau)

speed and therefore the energy efficiency will be increased by 40 %. With the higher downforce, clearly decreased lap times can be achieved and besides the increased cornering speeds later braking and earlier acceleration is possible. Later braking and earlier acceleration lead to an increased percentage of full throttle and therefore also energy usage. But with reduced engine power quicker lap times can still be achieved. ❽ shows the relationship between lap time, engine power, downforce (Cz) and energy usage. To find the best compromise, a lot of detail work will be necessary. In addition, the optimum will vary from track to track.

PROJECT E-RACER

Some Teams already started the development of electric powered race cars. Toyota, Formulec and Fondtech follow very different approaches [16]. It can be anticipated that this new racing league will come up with many new vehicle concepts, ❾.

FUTURE PROSPECTS

Already in 2009, within the Formula 1 rules valid at that time, KERS increased the performances in the top motorsport racing league. Today not even midfield results are achievable without KERS. From 2014 on the portion of electric propulsion power will be doubled and therefore a perfect system will be even more important for good results. In Le Mans the first competitive hybrid vehicles will be expected in 2012. The most important step for the electrification follows in 2013, when purely electric powered race cars fight for the victory.

In Formula 1 more or less the same technologies are currently used for the hybrid components, for Formula-E the level of innovation will be stronger in the first year of introduction. Without the highest level of engineering in the area of energy storage, e-motors, controller and also aerodynamics nobody will be successful.

Out of that, motorsports will be the platform for innovations and marketing of the future generations of electromobility.

REFERENCES

[1] www.brembo.com/racingworld/F1championship/circuitidentitycards
[2] FIA Reglement KERS (www.fia.com)
[3] ACO – Technical Regulations 2011
[4] www.hybrid-autos.info/Energiespeicher/Elektrischer-Speicher
[5] Baritaud, T.: Ferrari Gestione Sportiva, Hybrid Systems in Sports Cars, 21st International AVL Conference Engine and Environment, Sep. 10th – 11th, 2009, Graz, Austria
[6] www.flybridsystems.com/technology/originalF1System
[7] Magneti Marelli Press Release: Magnetti Marelli and Flybrid Systems to collaborate on KERS energy storage for Motorsport, 29 April 2009
[8] www.WilliamsHybridPower.com/technology/whps-flywheel-technology
[9] Sontheim, J.: Kinetischer Speicher für Hybridfahrzeuge. In: ATZ 110 (2008), No. 3
[10] Schmidt, M.: Hybrid-Rückkehr spaltet die Formel 1, Auto Motor und Sport Online, Sept. 8th 2010
[11] FIA Reglement 2014 (www.fia.com)
[12] Armbruster, D.: GT3 R Hybrid: Technologieträger und Race Lab, 22nd International AVL Conference Engine and Environment, Sept. 9th – 10th, 2010, Graz, Austria
[13] Collins, S.: The KERS of Le Mans, Racecar Engineering, July 2009, Vol. 19, No. 7, pp. 55
[14] Auto Motor Sport, Issue 19/2011, Editorial "Strom Aufwärts"
[15] Wikipeda, Energy Content
[16] Colins, S.: Bright Sparks, Racecar Engineering, November 2011, Vol. 21, No. 11, pp. 28

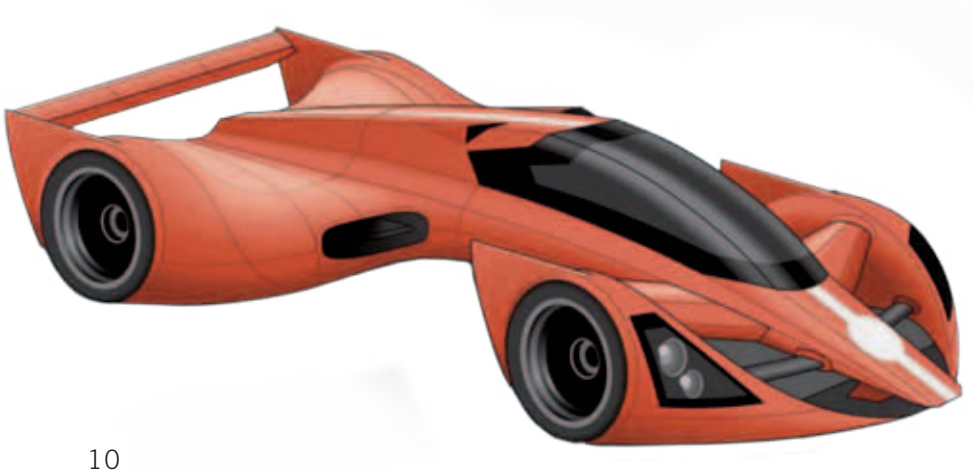

❾ E-Racer concept 2013 [14]

STOP LOOKING. START FINDING.

ATZ ONLINE. KNOW MORE. GO FURTHER.

Information that inspires is the root of innovation. Staying up to date helps accelerate development. And substance is what makes knowledge valuable. ATZonline is the place to go when you want to know what's happening in our industry and to get information that is unique in its depth. ATZ, MTZ, ATZelektronik, ATZproduktion and ATZautotechnology subscribers get access to a complimentary archive of industry articles as well as specials and whitepapers. All articles are well researched, with background and insider information.

No need to look any further – get your competitive advantage on
www.ATZonline.com

ATZ online

THE V8 ENGINE FOR MCLAREN'S NEW MP4-12C

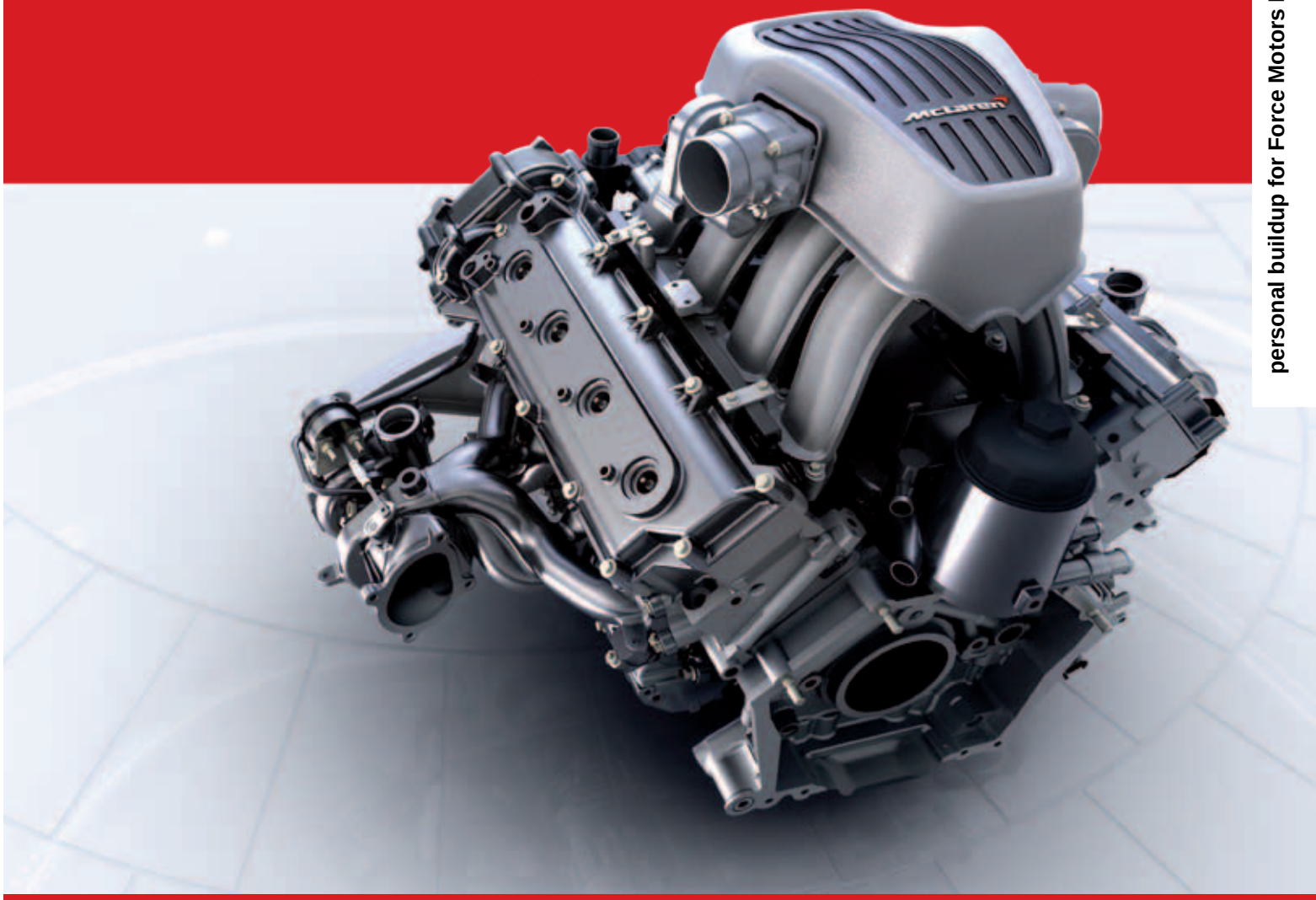

The 441 kW, 3.8 l turbo-charged V8 engine that powers McLaren's new MP4-12C supercar was designed by McLaren in collaboration with Ricardo who will also manufacture it. The engine reconciles ambitious performance targets with good fuel economy and CO_2 emissions at only 279 g/km.

AUTHORS

STEVE M. SAPSFORD
is Global Market Sector Director High Performance Vehicles and Motorsport at Ricardo plc in Shoreham by Sea (Great Britain).

TIM YATES
is Operations Director at Ricardo UK Ltd in Shoreham by Sea (Great Britain).

RICHARD FARQUHAR
is Function Group Manager Powertrain at McLaren Automotive in Woking, Surrey (Great Britain).

DEVELOPMENT TARGETS

When McLaren decided to use its own engine in the new MP4-12C this was the beginning of the new M838T engine. Its underlying architecture of a 90 degree V8 turbo-charged gasoline engine with 4-valve technology was derived from a race engine. However, despite its larger displacement the base engine concept could not meet either McLaren's performance or fuel economy targets, nor could it get anywhere near a noise, vibration and harshness (NVH), and sound quality acceptable for a road engine. ❶ gives an overview of what the new engine was expected to deliver and how those requirements were met.

The parameters in ① outline an engine that has the power to give a supercar superior driving dynamics. At the same time the challenging targets demanded a very modern engine that shares some traits with the most recent passenger car engine technology in order to achieve excellent fuel economy and low emissions. Ricardo was entrusted with the responsibility to develop and design the final engine, to develop and install the production line and to establish the global supply chain for the 1100 individual engine components – all of which had to be completed within 18 months. Therefore the development work necessitated a comprehensive simultaneous engineering linking engine and manufacturing design.

Probably the most fundamental single decision was to follow a technology path based upon downsizing and turbo-charging. Typically it would take a naturally aspirated engine with 5 to 5.5 l of swept volume to achieve the targeted power and torque. In fact other current supercar engines in the same league have roughly that displacement. Bringing this down to just 3.8 l means downsizing the engine by 30 to 40 %. While this is not unheard of in a passenger car engine, the demanding requirements of immediate response and a high rpm range extending up to 8500 rpm poses considerable challenges in the case of a supercar engine.

To be able to achieve all of the targets within the 18 month timeline involved a core team of 80 engineers and a total of 400 experts worldwide contributing to individual tasks at certain points. A half dozen of Ricardo's proprietary CAE simulation tools were utilized to identify the correct technology options with a target of being right first time wherever possible. This paper outlines the new M838T's main features and explains how they contributed to the final engine properties.

BASE ENGINE DESIGN AND OIL FLOW

To support excellent vehicle performance through minimum engine weight and a low center of gravity (CoG) the longitudinal all-aluminum V8 engine consists of a very low bedplate, a short block (just 201 mm high) with ladder design and the cylinder heads. Dry sump lubrication ensures a reliable oil

ATTRIBUTE	TARGET	ACHIEVED
POWER	441 kW at 7000 rpm	441 kW at 7000 rpm
TORQUE	600 NM at 3000 rpm	600 NM at 3000 rpm
MASS	< 200 kg	199 kg
CO_2 (VEHICLE)	< 300 g/km	279 g/km
BSFC (AT 1500 rpm/2.62 bar BMEP)	352 g/kWh	346 g/kWh
TRANSIENT RESPONSE (AT 50 % LOAD AND 3000 rpm INPUT: 100 % THROTTLE)	0.5 s to 75 % Desired boost	0.45 s to 75 % Desired boost
MAXIMUM SPEED	8500 rpm	8500 rpm
IDLE SPEED	850 rpm	600 rpm
EMISSIONS	EU 5/ULEV2	EU 5/ULEV2

❶ Engine development targets and results

ENGINE ATTRIBUTE	
FORMAT	90° V8, bi-turbo, ladder frame, dry sump, flat plane crankshaft
MATERIAL	All aluminum
BANK STAGGER	20 mm
DISPLACEMENT	3799 cm^3
BORE X STROKE	93 x 69.9 mm
COMPRESSION RATIO	8.7:1
BORE SPACING	108 mm
POWER	441 kW at 7000 rpm
TORQUE	600 Nm at 3000 to 7000 rpm
VALVE TRAIN	32 valve, DOHC, finger follower, chain drive to cam via intermediate gear, cam to cam gear drive, quad cam phasers
REDLINE RPM	8500 rpm
L X W X H	623 x 705 x 465 mm
WEIGHT	199 kg

❷ Core engine features

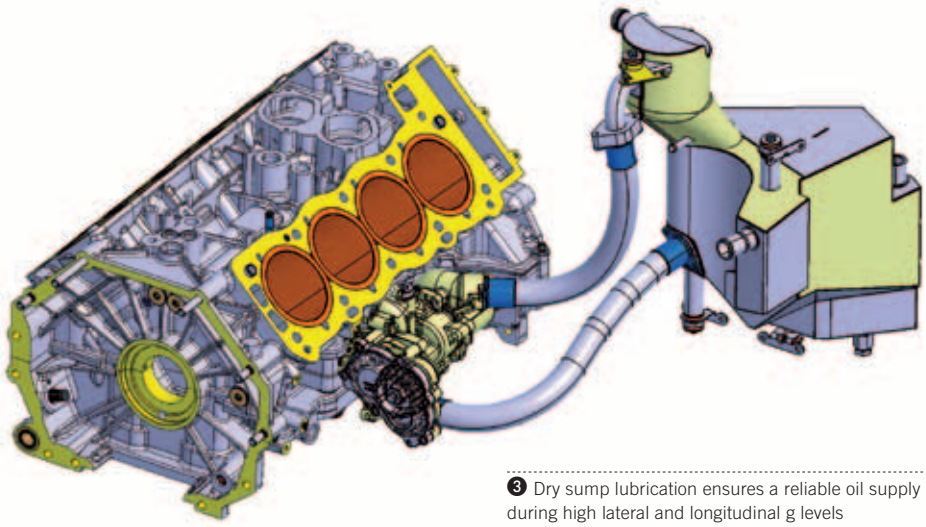

❸ Dry sump lubrication ensures a reliable oil supply during high lateral and longitudinal g levels

supply despite high lateral and longitudinal g levels. Moreover it facilitated a bedplate design which brings the centerline of the crank shaft down to just 131 mm above vehicle underfloor. At the same time the bed plate provides the rigidity needed for the high combustion loads. ❷ lists core engine parameters.

The flat bedplate of the crank case contains the cast-in engine oil drain passages and ducts which transport the oil to the three scavenging pumps. There is no inter-bay breathing as the sections are sealed off from one another around the crank shaft, and the cylinder head and chain case are also isolated from the crank bays. One oil drainage area combines the oil flow from cylinders 1 and 5 plus 4 and 8. The second oil drainage area connects cylinders 2 and 3 plus 6 and 7. Oil drainage section number three feeds the oil from the cylinder heads, the front end and timing drive back to the dedicated scavenging pump. This design avoids pumping compressed air in the crank case from one section to another. Instead the air is simply compressed within one section and will subsequently expand after the power stroke ("gas spring" effect). As the engine speed goes up, this strategy to reduce pumping work and internal losses becomes particularly beneficial as it increases real world fuel economy.

The three scavenging pumps transport the oil to an external reservoir that holds approximately 5.5 l of engine oil, ❸. Compared to a wet sump design the aluminum tank saves 1.5 kg. Exploiting the greater level of cross-section design freedom, the tank is shaped to facilitate tight integration into the chassis. A plastic oil filter and cooler module is located in the "V" between the banks. By using plastic, the unit saves 0.8 kg of weight per engine. Importantly, this weight saving is high up on the engine thereby contributing to the low overall CoG.

Axially guiding the con rods from the small ends reduces weight and dimensions of the crank shaft. As there is no axial thrust control on any of the connecting rod big ends, the differing thermal expansion of the aluminum block and the steel crank shaft will not result in lateral distortion. Instead the big end is free to adapt to the instantaneous block and crank shaft movements. By avoiding any iron inserts as part of the main bearings, the thick all-aluminum bearings achieve excellent conformability.

To ensure sufficient piston cooling, oil jets are located in the short block. This design feature provides an example for the need to closely link engine and assembly design: During the regular feedback sessions it became clear that the ideal location for the oil jets clashed with assembly requirements. In order not to compromise piston cooling, special tooling was developed which allowed the oil jets to be mounted after fitting the piston and con rod without a risk of the jets being damaged.

During early development, all oil and coolant passages were integrated into the engine block to minimize the number of "T" joints and to achieve excellent sealing integrity. This was also done by using a picture frame sealing design. As an example the two-layer steel cylinder head gasket extends forward to also cover the chain drive.

A 3 plate electrical thermostat controls the engine operating temperature by adjusting the coolant flow to the instantaneous conditions. During cold start the thermostat provides a no-flow condition to speed up the vehicle warm-up and to provide faster cabin heating. As the coolant temperature rises, stepped phases of coolant flow are activated to control the engine operating temperature. For normal driving in the part load regime the thermostat ensures a sufficiently high engine temperature to reduce friction. During high load on the other hand, maximum cooling is activated.

POWER CELL UNIT

The short block contains high-grade aluminum, Nikasil-coated top-hung cylinder liners. The wet liners sit on a register and are additionally supported by a structure at the bottom and sealed by two O-rings. During assembly the liners are clamped by the cylinder head. This design facilitates excellent cooling as there is only the liner wall thickness that separates combustion chamber and coolant. Also there is comparatively little liner distortion as the liners are fairly free to move inside the short block during firing. Nevertheless the block's design ensures a good rigidity with little blow-by.

The forged aluminum pistons with 93 mm diameter bore on a short stroke of only 69.9 mm enable adequate exhaust bridge cooling and unrestricted exhaust valve sizing. As a consequence the bottom end structure of the short block could be reduced in height, which contributed to the target of a low CoG. Following this path also saved around 4 kg of mass per engine in comparison to a long stroke design with conventional pressed-in liners. The pistons are sealed against the spiral-hone finished cylinder running surface by a ring pack with a nitrided steel ring in the anodized top groove and a standard cast-iron ring in the second groove.

Managing the high combustion loads of the supercar engine required a lot of full-block analysis and detail optimization. Fully integrated fired engine simulation revealed areas of concern as some liner cracking could be seen initially at an extremely high speed of 9000 rpm. ❹ shows the critical areas before (top) and after the design optimization of the contact between the liner and the block (bottom).

CYLINDER HEADS

An engine of this size and performance creates a huge amount of thermal load plus there is a massive amount of gas flow to handle. Designing the complex aluminum cylinder heads, which include secondary air passages for emissions control adding to the complexity, required optimized cooling. Again this necessitated a closed-loop feedback between simulation tool-based cylinder head design and design for manufacturing: Thermo-mechanical FE analysis predicted that the coolant's flow velocity was not sufficient to remove the heat from the exhaust valve bridge. The initial sand casting core for the cooling passage was therefore dropped. Three steps of optimization succeeded in speeding up the coolant flow close to the flame plate by drilling the coolant passages just 8 mm down from the flame plate – a method typically found in diesel engines – with an associated improvement in the robustness of the core. ❺ shows the predicted temperature levels at the exhaust valve bridge prior to and after re-designing the coolant passages.

AIR INTAKE, MIXTURE PREPARATION AND VALVE TRAIN DESIGN

To reduce the mass at the top of the engine, the intake manifold is an injection-molded plastic part made from standard PA 66 GF30. On top of saving around 3.8 kg per engine, compared to an aluminum design, the plastic intake manifold also has a particularly good surface quality on the inside which improves flow characteristics by reducing wall losses.

The M838T works with external mixture preparation: Four solenoid valve fuel injectors with eight spray holes are located in the ports upstream of the inlet valves of each bank. A fuel rail feeds the fuel to the injectors. The shape of the ports results in a tumble motion of the mixture which adds to the preparation quality.

The valve train features double overhead hollow-cast cam shafts (DOHC)

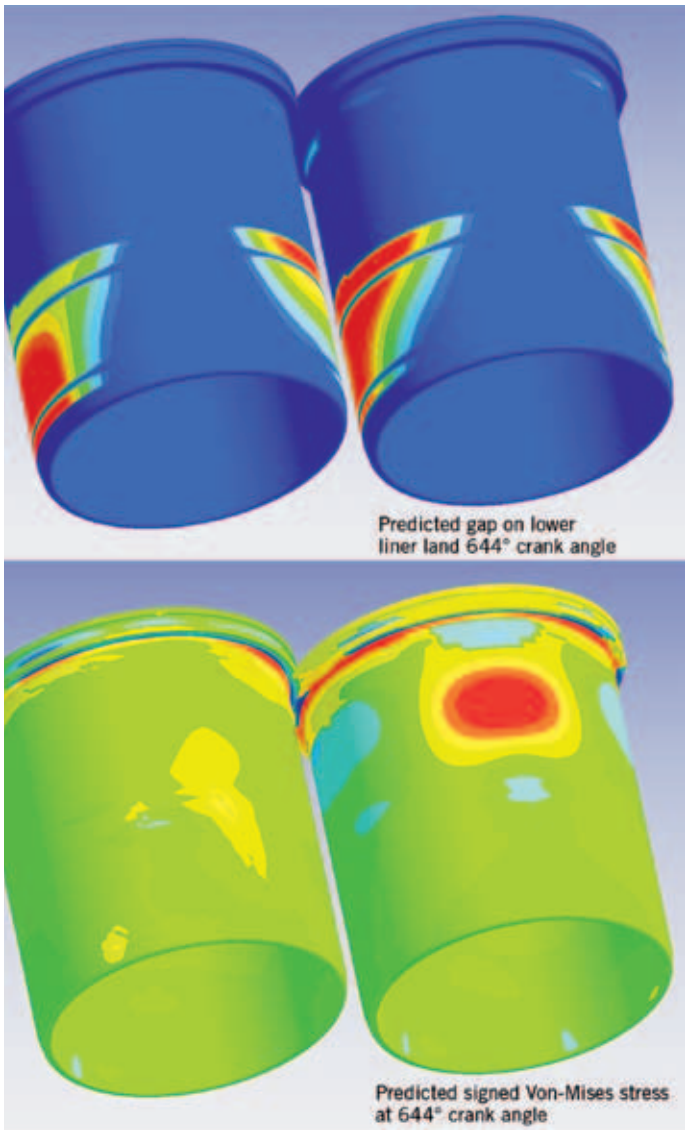

❹ The initial liner design showed cracking at 9000 rpm; changes to the contact areas between liner and block solved the issue

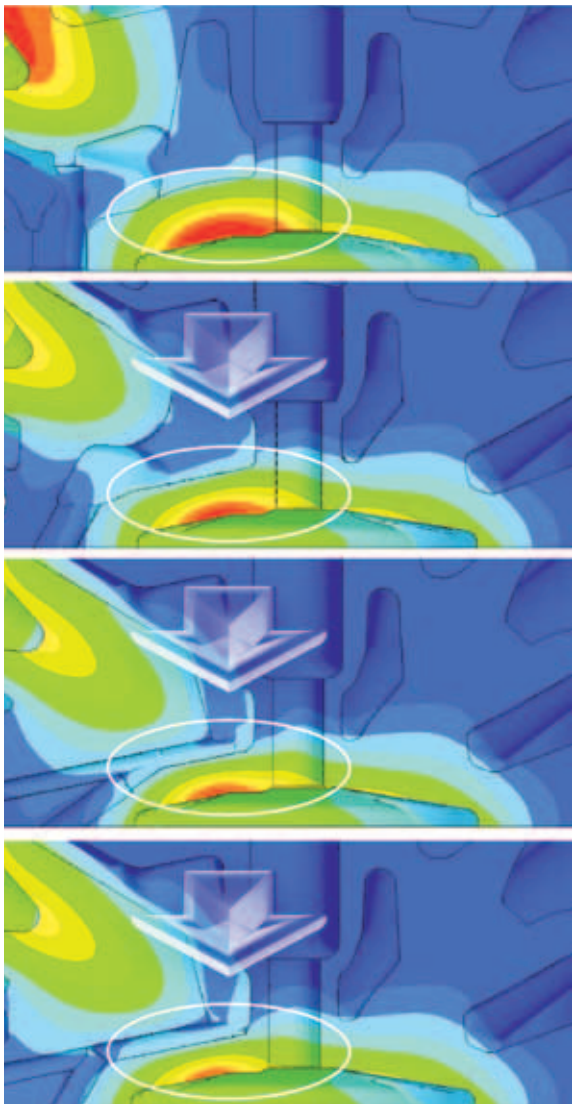

❺ CAE predicted overly high temperatures at the exhaust valve bridge (top). Design and manufacturing method were changed in several iterations to accelerate the coolant flow (bottom)

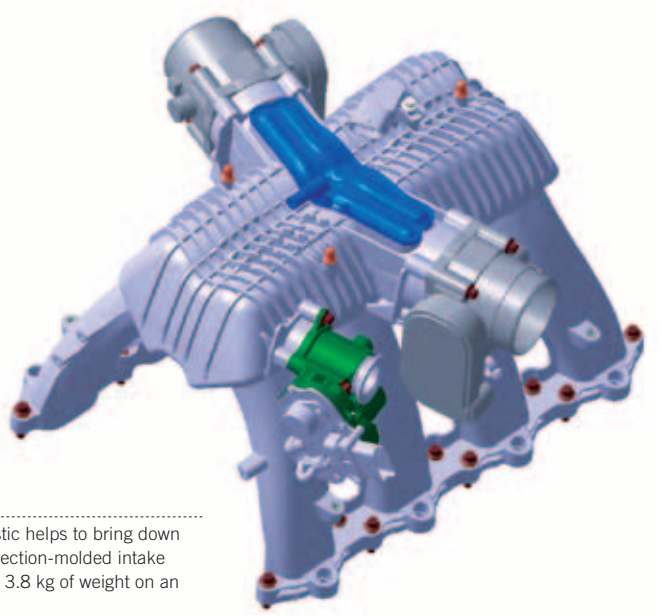

❻ The targeted use of plastic helps to bring down the center of weight; the injection-molded intake manifold for instance saves 3.8 kg of weight on an aluminum design

which are chain driven from the front end. End pivoted finger followers control the valve lift to the designed cam profiles while ensuring low moving mass and high stiffness. Owing to the wide engine speed range requirement and the targeted EU 5 and ULEV2 legislations, quad cam phasers (one phaser per camshaft) are used to achieve enough valve timing variability in order to control emissions, fuel economy and driveability throughout the wide speed range.

Single piece plastic cam covers help to reduce the weight of the cylinder head assembly by around 2.3 kg, ❻. Using magnesium as an alternative to plastic was ruled out at an early analysis stage for NVH concerns. Using plastic for the cylinder head cover offers another advantage: Owed to the material's thermal inertia very little heat is transferred upwards from the cylinder head to the air intake and the fresh charge.

From day one of the development process it was clear that the valve train would be central to achieve the targeted performance. Many features had to be put in place before the valve train met the performance and NVH targets. On the one hand, a light, low-inertia valve train was required to achieve good dynamics. On the other hand four large valves with 6-mm stems were needed per cylinder and there was to be absolutely no restriction by the exhaust valve size. To allow for the heat level, sodium-cooled valves are used on the exhaust side.

Also the valve spring was optimized for the high speed range. To bring down valve train friction, the valve train was designed with a single spring instead of a duplex spring. During simulation this caused some concern when the initial set-up was taken above maximum speed: At 9000 rpm there was not only a loss of contact between cam and follower going on, but there was also some spring surge, and even valve seat bounce occurring before the valve reached a steady state. Subsequent CAE design work and analysis solved the issue and led to a single tapering beehive valve spring, which is light weight and low in friction.

The shim design was also changed to achieve the desired valve lash precision at reduced assembly time: The shim, cam journals, cam base circles, and follower height are measured and the best fit of 34 grades of shim is subsequently chosen to be fitted during assembly.

ENGINE CONTROL

While the class-leading engine controller (ECU) together with the overall control strategy is fairly much on a gasoline standard, the level of vehicle integration is not. The MP4-12C has a highly networked engine, transmission, body, and chassis control, supervised by a top-level controller. Therefore, when the driver changes between the four modes "normal", "sport", "track", and "winter", this impacts many on-board system parameter settings from the pedal map, to the gearbox response right through to a stiffer chassis feel.

During the development and validation two test beds were constantly dedicated to getting the calibration right and balance of performance, function, emissions, economy and noise. Again the challenge was not so much to integrate parameters such as valve and injection timing, and waste gate control, but to fulfill the emissions legislation across the range of dynamic capabilities of this engine. Among the achievements was a reduction of the idling speed down to 600 rpm which was only possible through a very stable combustion. Controlling knock is achieved by a combination of limiting the compression ratio and the ECU that applies the required advancing, retarding, and enrichment strategies. Four knock sensors are located on the block between cylinder pairs, where they pick up the signals for the ECU.

BI-TURBO CHARGING

Two oil and water cooled turbo chargers are located at the two exhaust manifolds of each bank and extend sideways into a free space offered by an upper, middle, and lower chassis beam. The turbo chargers, with pneumatically actuated waste gates, run at up to 170,000 rpm and are designed for gas temperatures of up to 950 °C. They deliver up to 2 bar of charge air pressure. Big intercoolers downstream of the compressor bring down the temperature of the charge air.

During development the high-end engine speed target necessitated detailed trimming of the compressor and turbine entry and housing geometry. A lot of computational fluid dynamics (CFD) modeling was done to refine the manifold and turbo charger entry in particular. The development target was to get full boost support from 3000 rpm onwards without any choking occurring at full engine speed.

FRONT END DRIVE AND ANCILLARIES

The ancillaries are driven from the crankshaft via chain drives. A sprocket on the shaft transfers the power upwards to two separate chain drives branching off to the right and left, and another one further up to the valve trains. To support the CoG target the ancillary components are mounted low, and in line with the engine.

On the right side of the engine (bank A) three scavenging pumps and the oil feed pump are located on a common shaft. The drive from the front end is passed on from the oil pump shaft via a step-up gearbox to the alternator. This configuration places the considerable mass of the generator at a very low position. On the left side of the engine (bank B) another chain drive powers the coolant pump unit. Its two integrated pumps feed a main high-temperature circuit and the smaller low-temperature circuit. Via a direct pass-through drive the power is transferred from the coolant pump unit to the HVAC compressor.

SOUND DESIGN

Controlling noise sources and noise quality was a major part of the development program. The base engine in the mule vehicle did not meet the sound quality expected from a supercar driven on the road. One of the first changes undertaken was to replace the original gear drive of the ancillary system by a chain drive to get rid of a lot of high-pitched rattle and thus minimize the base engine noise character, ❼. The intake system was also modified and a sound generator added. The sound generator takes pressure pulsation from the intake and passes them on to the inside of the vehicle in a controlled way. This serves to control the amount of engine feedback to the cabin at cruising. Depending on the driving mode, the sound feedback is progressively increased and the character changed. While this is partly a comfort function it is also an important element of feeding back to the driver how the engine responds to his torque demand at the pedal. A new exhaust system controls the sound quality to the vehicle's environment by lifting the noise and adding to its sonorous quality, which is an important factor of the branding for a supercar.

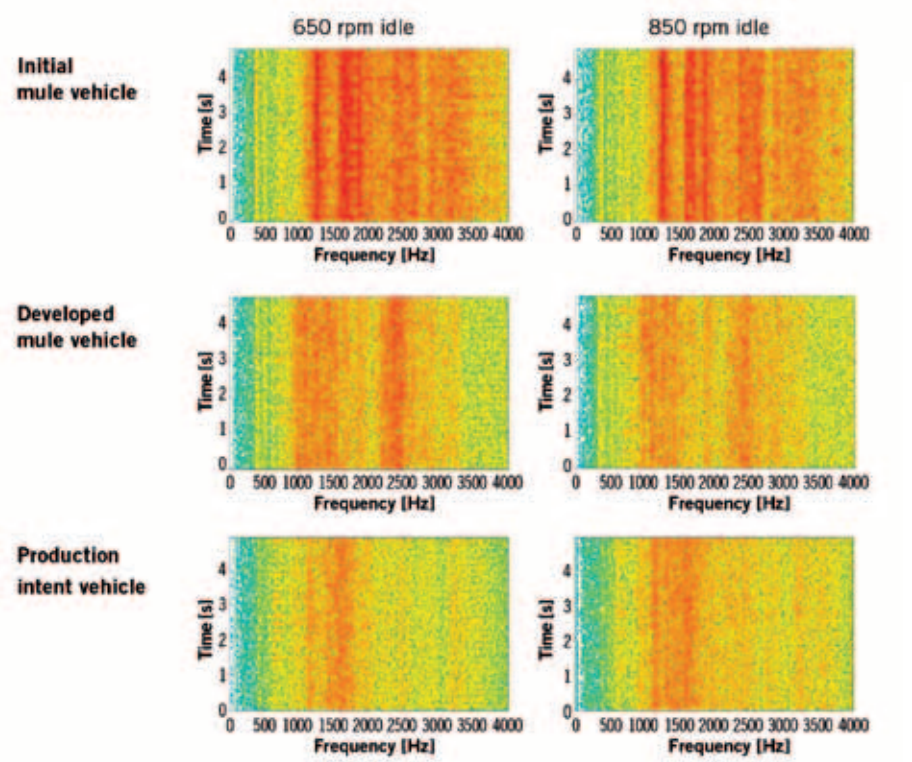

❼ Sound design included substantial design changes such as the switch from a gear drive at the front end to a chain drive

CONCLUSIONS

Due to the challenging targets there were no out-of-the box solutions for the engine. An extensive use of CAE and analysis tools served to identify the optimal technology options and to design the final engine within the tight timeline. At the end of the engine development program all the ambitious targets were met or exceeded. The M838T has a very high speed capability for a turbo-charged engine and responds immediately to the driver's request for acceleration – even when compared to a naturally aspirated engine. Intense optimization work achieved a good balance of hardware interaction, control interaction and calibration changes to achieve this transient response. The M838T's class-leading performance, ❽, is combined with a class-leading CO_2 emission level of just 279 g/km and an average consumption (NEDC) of 11.7 l. As the compact and lightweight engine sits very low in the car it supports excellent driving dynamics.

❽ The plotted kW per l put the downsized engine significantly above the trend line

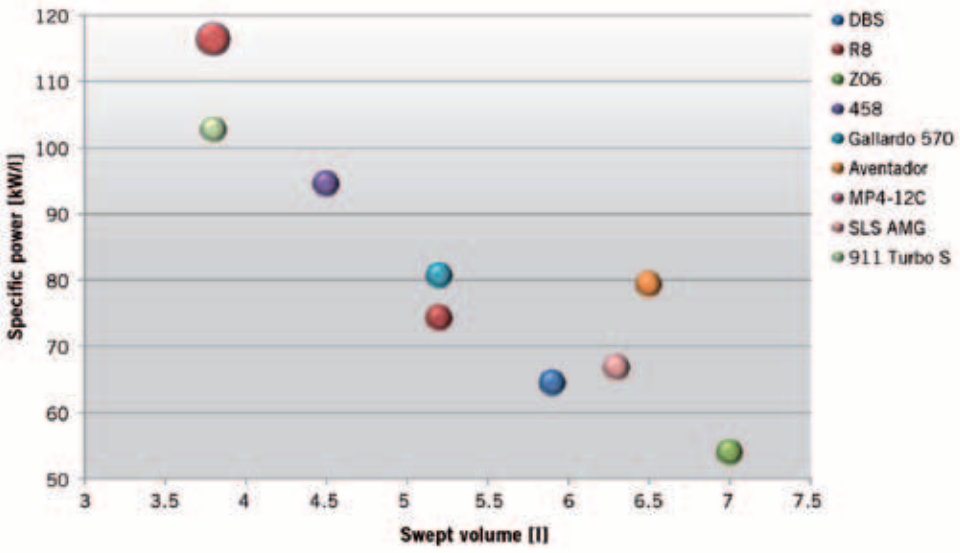

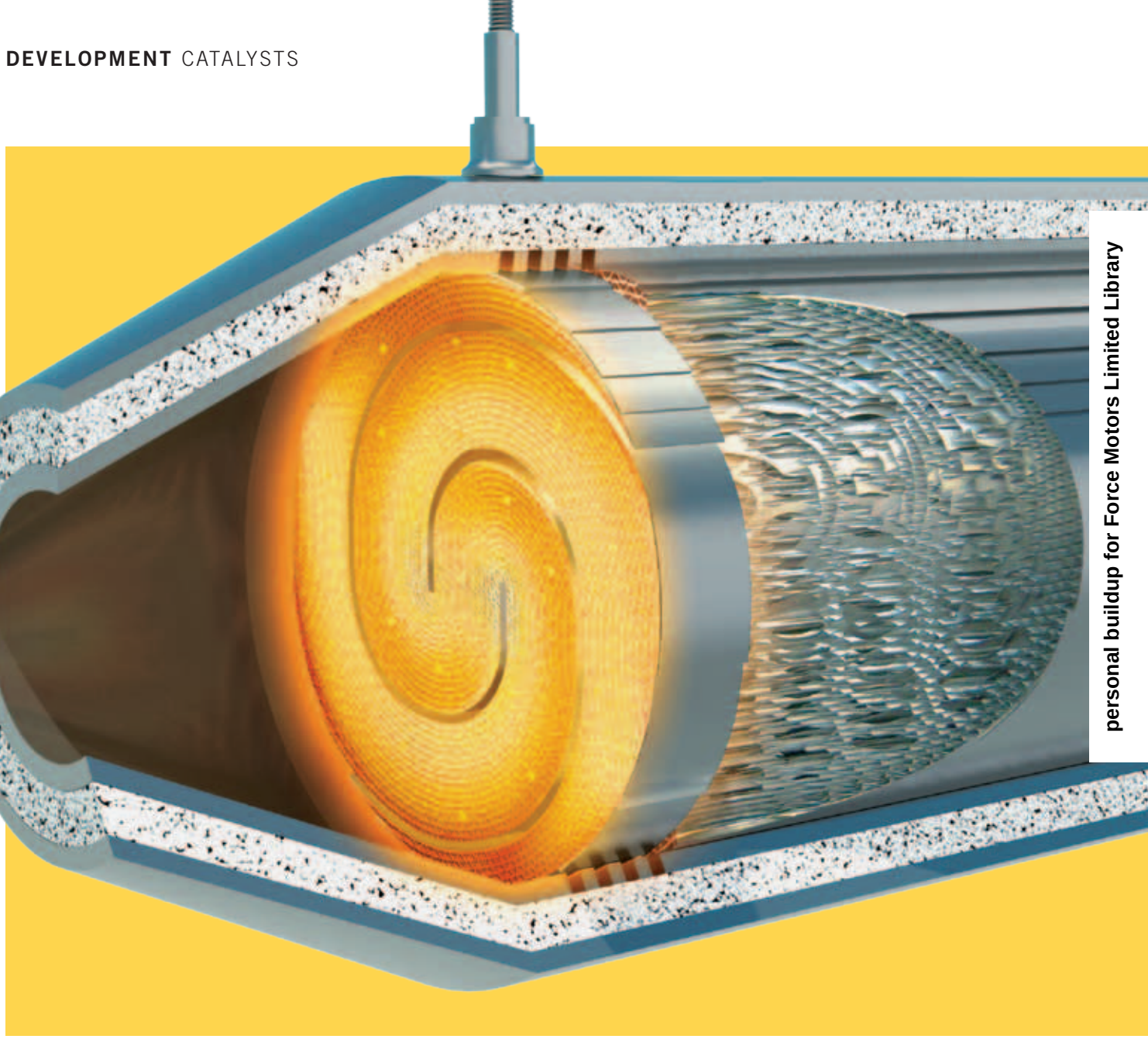

EFFECTS OF ELECTRIFICATION

The debates on CO_2 emissions and fuel consumption portray electric vehicles as a political solution [1, 2]. However, the range of these vehicles is severely limited by available power capacities, especially in real driving conditions [3]. Electrified drivetrains up to electric vehicles with range extenders, provide an alternative. When used in conjunction with an electric motor, combustion engines have very different requirements for catalytic converter systems [4] particularly in view of the 'zero emissions' image of electric vehicles. At present, 'electrification of the drivetrain' generally refers to drive systems such as mild hybrids, full hybrids and electric vehicles with or without a range extender. In view of the power density and the charging times of modern batteries it still seems sensible to add a combustion engine to an electric vehicle unless it was driven exclusively in urban areas or for short distances. Apart from passenger cars, this particularly applies to vans and light-duty and heavy-duty commercial vehicles, which have a considerably higher power requirement per kilometre travelled. For instance, a heavy-duty commercial vehicle uses approximately 1 kWh/km when travelling at constant speed on a motorway, which is seven times as much as a passenger car in the NEDC.

The advantage of electric vehicles that is often emphasized is that they do not produce any emissions. This is however only true locally and does not consider the emissions produced to generate the electricity. The internal combustion engine at operating temperature that is equipped with a high-performance exhaust gas aftertreatment system by contrast can emit lower pollutant levels than present in the surroundings. The remaining challenge is to reduce or eliminate the cold-start emissions, especially in hybrid vehicles that have frequent engine starts. New catalyst concepts and operating strategies are needed for this.

THE FUTURE OF EXHAUST AFTER-TREATMENT DESIGN FOR ELECTRIFIED DRIVETRAINS

Combustion engines used as range extenders in electric vehicles in consequence of their increased number of cold starts make high demands on the exhaust gas aftertreatment systems. Emitec has developed and optimised a range extender catalyst system which reduces cold start emissions up to 90 %, especially by preheating and thermal insulation.

AUTHORS

DIPL.-ING. WOLFGANG MAUS
is Chairman Board of Management at the Emitec GmbH in Lohmar (Germany).

DIPL.-ING. ROLF BRÜCK
is Managing Director Research, Development & Application at the Emitec GmbH in Lohmar (Germany).

DIPL.-ING. ROMAN KONIECZNY
is General Manager Application Light Duty at the Emitec GmbH in Lohmar (Germany).

DIPL.-CHEM.-ING. PETER HIRTH
is Head of Research, Development & Test Dept. at the Emitec GmbH in Lohmar (Germany).

LIMITING CONDITIONS FOR THE USE AND OPERATION OF CATALYST SYSTEMS

The type of electrified drivetrain has an enormous impact on the operating conditions of the catalyst system. For example, when used in urban areas or for short distances vehicles with a range extender are likely to stop for extended periods, resulting in a number of real cold starts. By contrast, the combustion engine is likely to run most of the time in extra-urban cycles or when the vehicle is driven at higher loads.

The development of suitable technologies for the different drive systems requires a detailed overview of real-life load conditions. The basic data for the strategies used to optimise these technologies is supplied by an analysis of engine on and off times for each cycle with prevailing engine speeds and loads and corresponding exhaust gas mass flows, emissions and exhaust gas and catalyst temperatures.

RANGE EXTENDER

The off times and heating times shown in ❶ are based on the typical operating conditions of a range extender that are partly analogous to [5]. In electric-only mode the battery is discharged up to a certain limit capacity before the combustion engine is started to provide both driving power and

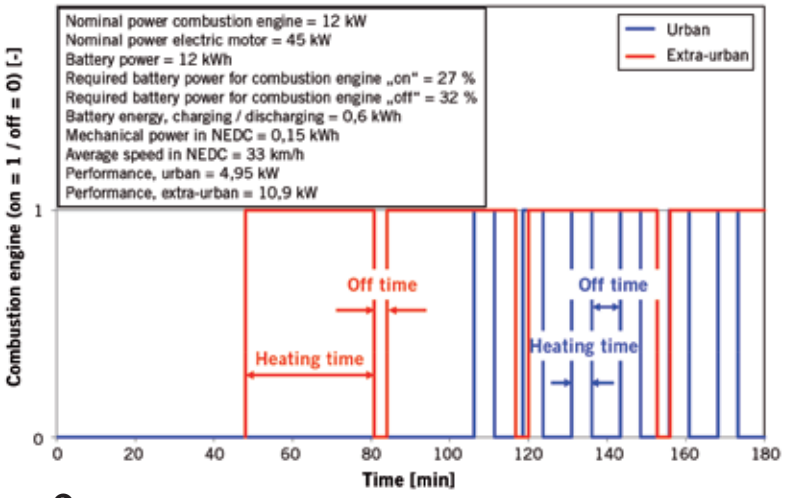

❶ Combustion engine running times and off times in a vehicle with a range extender for two scenarios

charge the battery. Several NEDC cycles were run in sequence for both the urban and the extra-urban scenario. The power demand in the extra-urban cycle was more than twice that of the urban cycle. The calculation started with a full battery subject to the limiting conditions shown in ①. The battery charge was not allowed to drop below 27 %, at which point the combustion engine was started. The engine was switched off again as soon as the battery had been charged to 32 %. Depending on the load profile (urban or extra-urban) there will be little power left to recharge the battery so that engine off times become increasingly shorter. In this example they are approximately seven minutes in urban cycles but already less than three minutes in extra-urban cycles. Similarly, there are five engine starts per hour in the urban cycle whereas there are only two in the extra-urban cycle. Depending on the duration the engine off time was followed by either cold starts or warm starts. The longest off time, which was approximately 50 min in the extra-urban cycle (approximately 105 min in the urban cycle), was the period during which the battery capacity fell from 100 % to the lower limit of 27 % for the first time.

THE RANGE EXTENDER CONCEPT

The limiting conditions described above combined with the demand for a zero emissions concept result in the following important requirements for a catalyst in hybrid or range extender vehicles:

: Catalyst heating before the engine starts
: Heating function inside the catalyst
: Optimised insulation to delay cooling during long engine off times.

HEATING BEHAVIOUR IN COLD STARTS – E-CATALYST WITH PRE-HEATING FUNCTION

Despite engine-based catalyst heating approximately 80 % of total emissions are still produced during cold starts when the catalyst has not yet been brought to operating temperature entirely. This is the challenge faced by zero emissions vehicles with a combustion engine.

An effective method to increase cold start efficiency is the use of an electrically heated catalyst, ❷. This has already been applied in serial production [6, 7]. For the hybrid applications described, an additional advantage is the ability to heat up the catalyst volume to lightoff temperature even before engine start.

Heat is created within the said short heated disc and has to be transferred to the main catalyst downstream in order to make sure that a catalytically active volume is provided. One option is to transfer the heat via the air flow produced by a secondary air pump or the electrically driven engine. The achievable temperature of the exhaust gas downstream of the heated disc

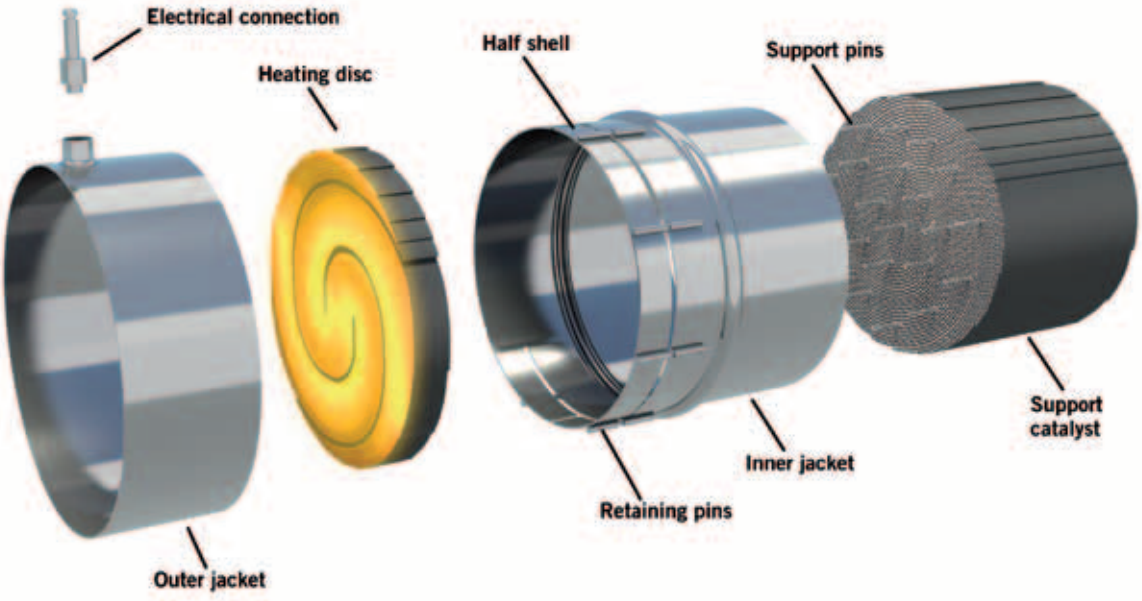

❷ Assembly of electrically heated catalyst

depends on the air mass flow and the electric heating output (1 kW electrical energy can heat a massflow of 36 kg/h by 100 K). The heating rate of the catalyst downstream of the heated disc is determined by the air mass flow, ❸. The lower the air mass flow the higher the catalyst temperature that can be achieved with the same heating output. However, a lower air mass flow also means that it takes longer to heat the entire length of the catalyst.

③ shows the heating behaviour of the main catalyst as a function of the exhaust gas mass flow at a heating output of 2 kW. At a mass flow rate above 5-10 kg/h a large partial volume (> 50 %) of the main catalyst (140 mm axial length) can be heated to and above the light-off temperature by pre-heating the heated catalyst before the engine starts. As a result, it should be possible to convert most of the emissions after the engine starts while an optimum air mass is expected.

This was verified by subsequent emissions calculations using the same catalyst system. The results of these calculations are shown in ❹, which contains the calculated cumulative HC emissions for each specified pre-heating time (between 10 and 60 seconds), plus another 90 s in the EU cycles, with additional variation in the air mass flow.

Unsurprisingly, longer pre-heating (in the periods observed) reduces emissions while there also seems to be an optimum air mass flow in the region of 10 to 15 kg/h that is associated with minimum emissions at times exceeding 10 s. The HC emissions achieved in the calculation for the overall test are in the order of 1.6 mg of HC per km based on the assumption that the catalyst would not cool down below light off in the subsequent stages of the test.

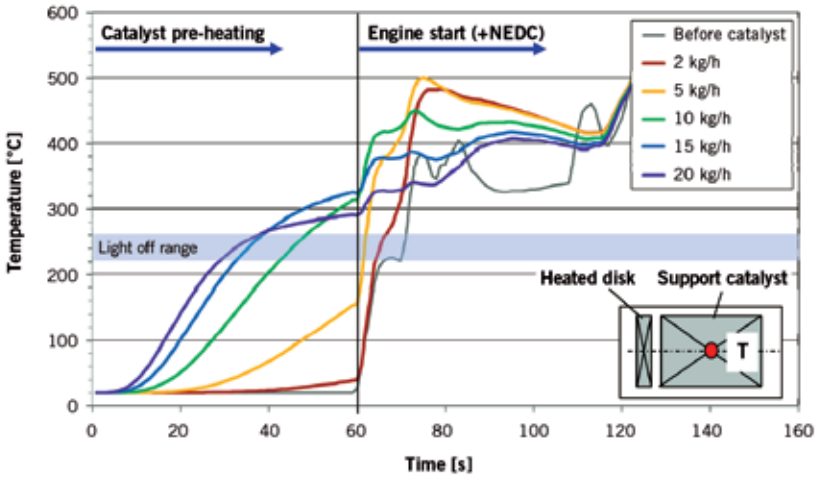

❸ Heating behaviour of the main catalyst as a function of the exhaust gas mass flow at a heating output of 2 kW (at the axial centre of the support catalyst; Ø 98.4 x (8 + 140) mm / 600 cpsi)

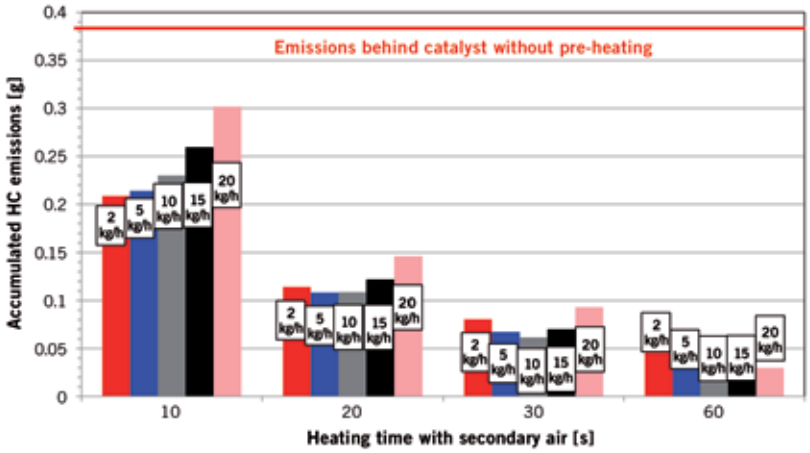

❹ Calculated cumulative HC emissions for different pre-heating times (between 10 and 60 s), plus a further 90 s after engine start in the EU cycle, with additional variation in the air mass flow between 2 and 20 kg/h

COOLING BEHAVIOUR DURING ENGINE OFF TIMES – MINIMISATION OF HEAT LOSS

Several factors relating to cooling behaviour have to be taken into account and addressed by appropriate design measures [8]. Assuming that the engine is always operated at load and otherwise uncoupled, this essentially concerns radial and axial heat conduction in the substrate and convection and radiation to the environment, ❺.

Heat conduction inside the substrate and especially heat transfer to the boundaries (mantle, front and end faces) should be reduced to a minimum to limit heat loss. Additional insulation in the outer mantle area can reduce heat loss even further. ❻ shows all of the measures that were implemented in the development of the range extender design.

Consequently, most of the chosen measures constrict conductive heat dissipation both in a radial and in an axial direction. They include discontinuous areas in the radial section of the catalyst matrix close to the mantle and close to the axial front and end faces that interrupt heat conduction. Another approach involves measures that thermally decouple the mantle from the matrix in a radial direction through the use of a coating with poor thermal conductivity and/or air gaps. The mantle itself was thermally decoupled from the exhaust system in an axial direction. In addition, a special insulation material was used for the radial insulation of the catalyst mantle and the cones.

❼ shows the influence of the insulation as measuring results in the form of volume fractions of the catalyst matrix, which, starting from a core temperature of 400 °C, are still above a notional light-off temperature of 230 °C and hence still catalytically active. Clearly, referencing to a substrate without any insulation, the introduction of radial insulation (thickness = 5 mm) already delays the cooldown of the substrate significantly. The combination of radial and axial decoupling with the described insulation measures made it possible to almost double the time for cooling down the substrate.

The example of the scenario highlighted above, ①, shows that the engine off times during the urban cycle would allow the

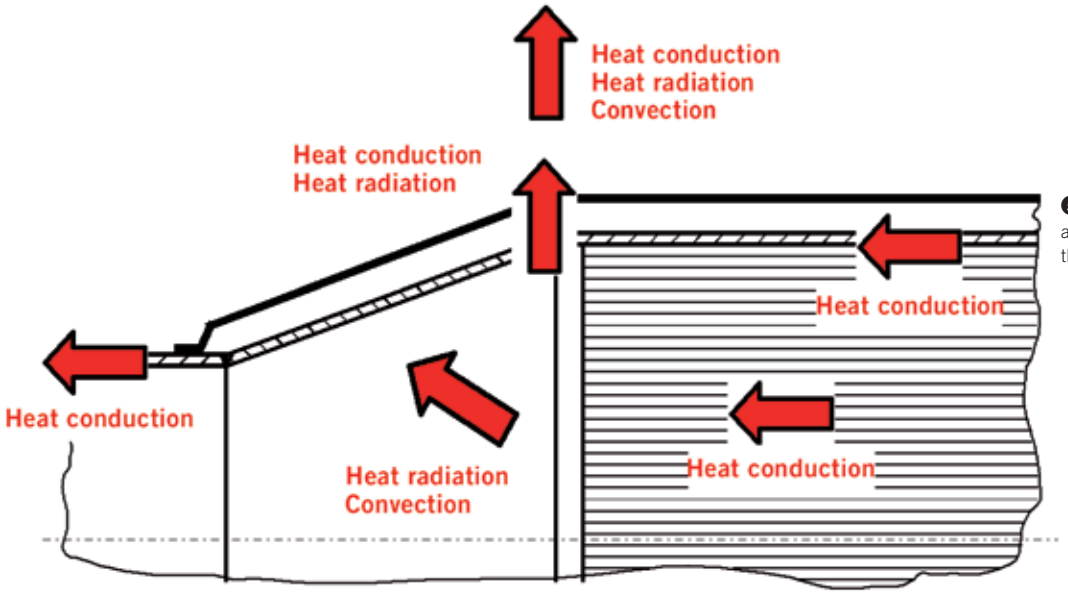

❺ Heat transfer mechanisms in the catalyst, its insulation and its integration in the exhaust system

catalyst to cool down with a corresponding effect on emissions. This could be prevented or lessened by the measures described above.

OPTIMISED OPERATING STRATEGY – VEHICLE TESTS

The aim of the tests performed on the vehicle was to demonstrate low-emission engine starts for various limiting conditions. At the same time, the tests were also meant to validate the simulated results discussed above. To this end, an electrically heated catalyst with a heating output of 1.8 kW was installed close to the engine of the test vehicle. The catalyst measured Ø 98.4 x (8 + 140) mm / 600 cpsi. The tests described in this section were carried out with the aid of a secondary air pump in order to examine the effect of different mass flows.

Initial tests were based on an NEDC cold start. The temperatures in the electrically heated catalyst were recorded by a number of thermocouples fitted behind the heated disc and inside the downstream main catalyst. ❽ shows the temperature curve of a measuring point located at a depth of 15 mm in the main catalyst for an NEDC cold start with different pre-heating times and different mass flows during the pre-heating phase. ❾ shows the corresponding temperatures at an axial depth of 70 mm in the main catalyst.

As shown in ⑧, a mass flow of 15 kg/h and a pre-heating time of 30 seconds are not quite enough to raise the temperature at an axial depth of 15 mm to the catalyst light-off range by the time the engine starts but a few seconds later. However, this is still at least 13 seconds earlier than

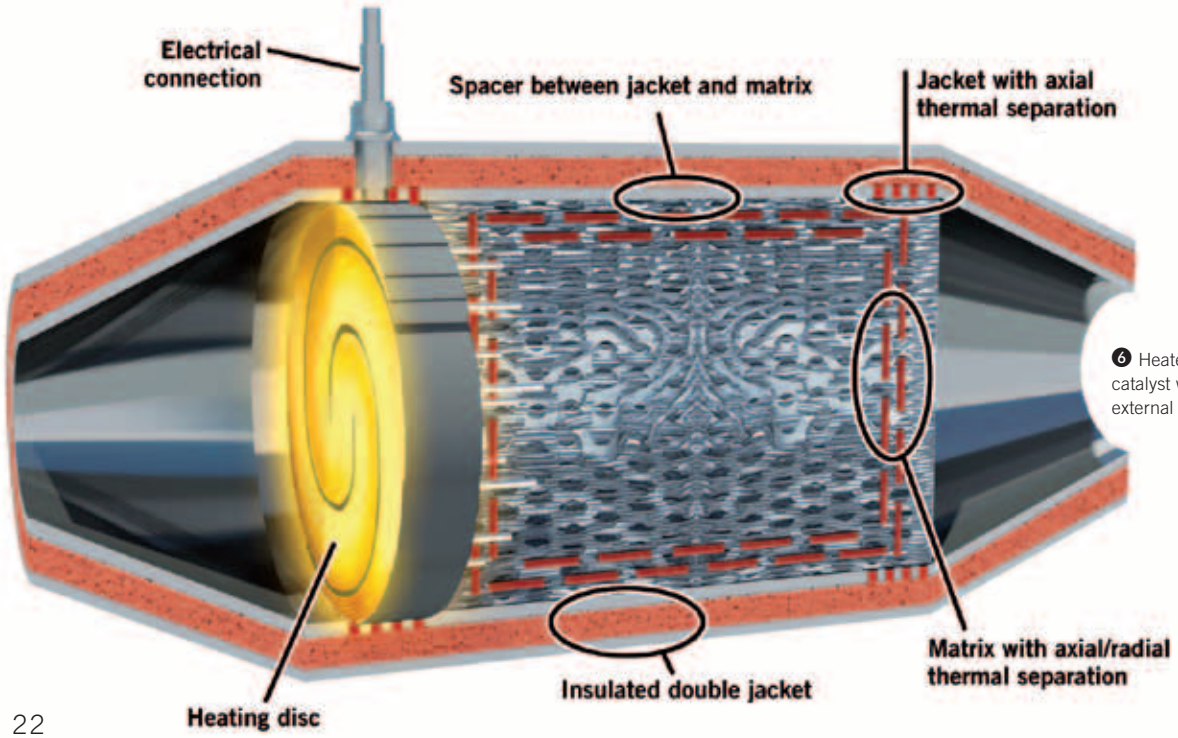

❻ Heated range extender catalyst with internal and external insulation

without heating. By doubling the mass flow to 30 kg/h it becomes possible to produce a temperature of approximately 300 °C at the measuring point when the engine starts and so ensure light off. Any further increase in the mass flow shows no significant effect at this measuring point.

A much bigger impact is produced by extending the heating time from 30 to 45 s with an average mass flow (30 kg/h). This raises the temperature at the measuring point by another 150 °C, which is substantially above the light-off range.

Looking at the temperatures at the centre of the support catalyst, ⑨, it becomes clear that without active heating measures the heat is transferred to this point only after the first acceleration peak. Depending on the scenario pre-heating can bring half of the catalyst volume up to the light-off temperature before or during the first acceleration.

⑩ shows the effect of these measures on emissions. Compared to normal cold starts, a pre-heating time of 30 s and a mass flow of 15 kg/h during the pre-heating phase can reduce HC emissions during cold starts by approximately 80 % from 0.8 g to 0.15 g. CO emissions can be reduced to a similar extent.

SUMMARY

This paper describes the development and optimisation of a new catalyst concept, the range extender catalyst, its design criteria and effect on tailpipe emissions, especially when used in petrol engines. Typical requirements for an aftertreatment system based on the conceivable operating modes of a range extender combustion engine primarily include catalyst heating before the engine starts. This can be achieved, for example, by installing an electric heating device inside the catalyst. Optimised insulation to delay catalyst cooling for as long as possible during longer engine off times is at least as important.

The range extender catalyst concept was presented as a step towards meeting these challenges. The design includes an electric pre-heating function and is particularly effective at minimising heat loss to the environment. As a result, it is able to maintain the catalyst system at operating temperature for almost twice as long as a system without any insulation.

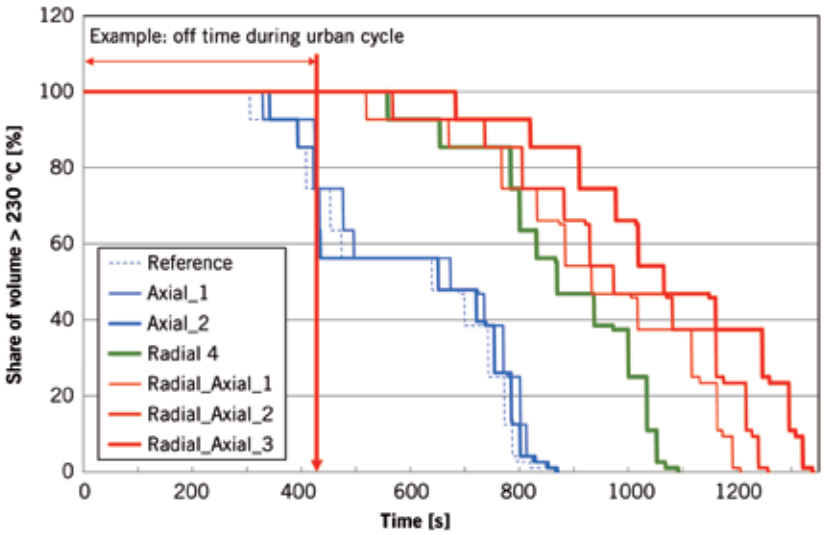

❼ Parts of the catalyst structure that are above the light-off temperature of 230 °C, various types of radial and axial insulation

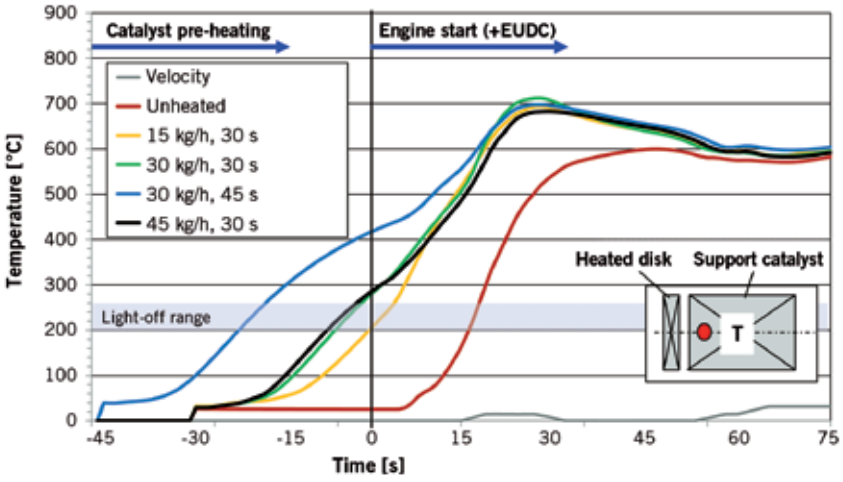

❽ Temperatures in the support catalyst at an axial depth of 15 mm for various cold start strategies in the NEDC (Ø 98.4 x (8 + 140) mm / 600 cpsi)

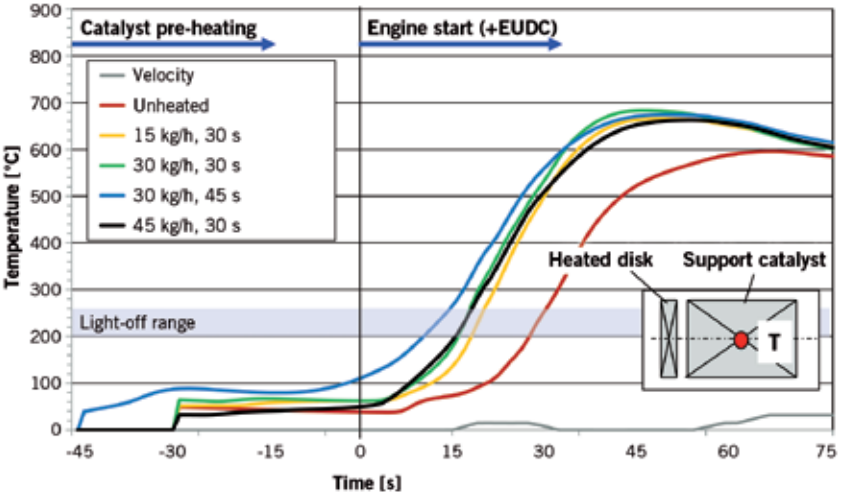

❾ Temperatures in the support catalyst at an axial depth of 70 mm for various cold start strategies in the NEDC (Ø 98.4 x (8 + 140) mm / 600 cpsi)

❿ The effect of the pre-heating strategy on HC emissions in NEDC cold starts

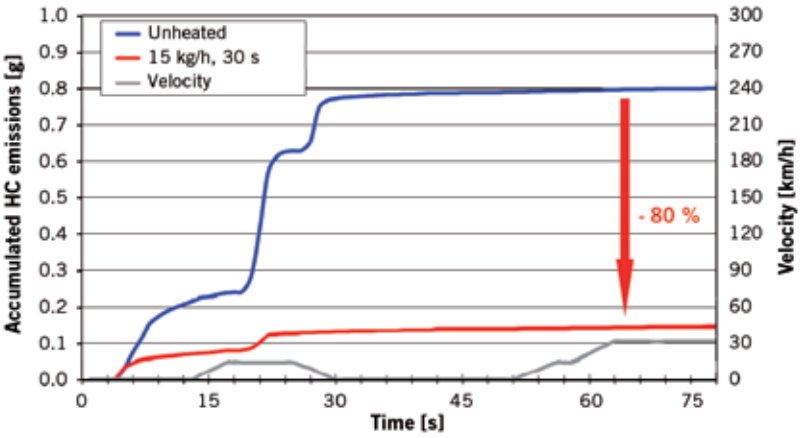

Mathematical simulations and correlating measurements were used to establish optima for the limiting conditions during catalyst pre-heating, that is, air mass flow and heating time, which each reduce emissions to a minimum. The electrically heated catalyst system was able to cut cold start emissions by between 80 and 90 % during the measurement and the simulation.

This paper described a basic concept, which after further refinement and optimisation could have the great potential to become the catalyst technology for future range extender drive systems.

REFERENCES

[1] Zetsche; D.: „Auf dem Weg zur emissionsfreien Mobilität? Möglichkeiten und Grenzen des elektrischen Fahrens."; Aachener Motorenkolloquium 2009

[2] Hadler; J.: „ Gegenwärtige und zukünftige Antriebstechnologien im Spannungsfeld globaler Anforderungen"; Aachener Motorenkolloquium 2009

[3] Forst; R.: „Elektromobilität bei Opel – Die Zukunft des Verkehrs"; Aachener Motorenkolloquium 2010

[4] Zikoridse; G.: „Konzeptstudie zur Realisierung einer Abgasnachbehandlung beim Betrieb eines Range-Extenders"; Innovationsforum Feinstaubarmes Fahrzeug, Klettwitz 2011

[5] Hartmann, B.; Renner, C.: "Autark, Plug-in oder Range-Extender? Ein simulationsgestützter Vergleich aktueller Hybridfahrzeugkonzepte"; 18. Aachener Kolloquium Fahrzeug- und Motorentechnik, 2009

[6] Küper; P.-F.; Maus, W.; Swars, H.; Brück, R.; Kaiser; F.-W.: "Ultra-Low Power Electrically Heated Catalyst System"; SAE 940465; 1994

[7] Hanel, F.-J.; Otto, E.; Brück, R.: "Electrically Heated Catalytic Converter (EHC) in the BMW Alpina B12 5,7 Switch Tronic", SAE 960349, 1996

[8] Breuer, J.; Brück, R.; Diewald, R.; Hirth, P.: "Temperature Examinations on a Metal Catalyst System"; SAE 971028, 1997

12th Stuttgart International Symposium

Automotive and Engine Technology

VEHICLE TECHNOLOGY
Aerodynamics, new vehicle concepts, driving dynamics and driver assistance systems

VEHICLE POWERTRAIN
Hybrid technology, alternative fuels, spark-ignition and diesel engines, engine management and modelling

VEHICLE ELECTRONICS
Electric vehicles, software and design, modelling and simulation

13 and 14 March 2012
Stuttgart I Germany

FKFS

ATZ live
Abraham-Lincoln-Straße 46
65189 Wiesbaden I Germany

Phone +49 (0)611 / 7878 – 131
Fax +49 (0)611 / 7878 – 452
ATZlive@springer.com

PROGRAM AND REGISTRATION
www.ATZlive.com

THE NEW 3.0-L TDI BITURBO ENGINE FROM AUDI

PART 1: DESIGN AND ENGINE MECHANICS

With the arrival of the V6 TDI biturbo engine, Audi is adding a high-performance version with two-stage turbocharging to its V6 TDI engine line-up. At the heart of the engine lies a new turbocharger system from Honeywell Turbo Technologies (HTT), capable of boosting power output to 230 kW and delivering 650 Nm maximum torque. By adopting all the efficiency measures from the basic V6 TDI monoturbo engine, a combination of excellent performance and extremely good fuel consumption figures has been achieved. In the following design and the mechanics of the new engine are described, the topics of thermodynamics and application will be dealt with in a second section in the MTZ 2.

AUTHORS

DIPL.-ING. RICHARD BAUDER
is Head of Diesel Engine Development at Audi AG in Neckarsulm (Germany).

DIPL.-ING. JAN HELBIG
is Head of Diesel Engine Mechanics Development at Audi AG in Neckarsulm (Germany).

DR.-ING. HENNING MARCKWARDT
is Head of Mechanics Development for Biturbo Diesel Engines at Audi AG in Neckarsulm (Germany).

DIPL.-ING. HALIT GENC
is Design Engineer in the Diesel Engine Development at Audi AG in Neckarsulm (Germany).

DESCRIPTION OF THE ENGINE AND INSTALLATION IN THE VEHICLE

Alongside the V8 TDI which is used in the Audi A8 and Q7, the new V6 TDI biturbo engine represents the top-of-the-range diesel engine option for the new Audi A6 and the A7. The objective of the development of this engine was to set new standards in the realm of sporty diesel vehicles, by means of an outstanding, dynamic build-up of torque and extraordinarily free-revving characteristics. The intention was to combine excellent performance with good fuel consumption figures, which has been achieved by adopting the following efficiency measures from the basic engine:

: thermal management
: frictional optimization measures
: weight reduction
: eight-speed automatic transmission
: start/stop system.

Other requirements for the engine's development were that it should be built on the existing assembly line for the basic engine at the engine plant in Győr, and that it should utilize the maximum number of common parts offering the benefits of synergy with the V6 TDI monoturbo [1-4].

The 46 kW increase in power output compared with the A8 version of the basic engine was achieved primarily by means of a new turbocharging system combined with optimized charge air cooling, as well as modifications to the fuel injection system. The heart of the new engine, the turbocharger system, is located at the rear of the inner V of the engine, and in the clearance space above the gearbox, which can be seen in the cover figure in the partial section view from the rear [5].

❶ shows the installation of the V6 TDI engines in the C series. The installation of the V6 TDI monoturbo engine can be seen in ① (left), while ① (right) shows the biturbo. In both pictures it is possible to see the limiting contours of the plenum chamber and the bonnet, as well as the position of the gearbox and exhaust system. In ① (left) can be seen the combined close-oupled oxidation catalytic converter with diesel particulate filter (DPF), which is positioned behind the turbocharger. The exhaust leaves the turbocharger to the left, as seen in the direction of travel; it is turned through 180° and then flows through the DPF to the right-hand side of the gearbox. The exhaust system is not visible; it runs past the gearbox on the right, as seen in the direction of travel, and into the underbody. In the case of the biturbo, the installation space for the DPF has been used for the high-pressure turbocharger. The exhaust system does not cross over the gearbox but runs where it can be seen in ① (right), on the left-hand side of the gearbox. The oxidation catalytic converter can be seen; the DPF has been relocated into the underbody. Additionally the vacuum unit for the turbine switching valve and the electric actuator for the variable turbine geometry (VTG) of the small turbocharger can be seen. ① makes very clear the major challenge of fitting a V engine with two-stage sequential turbocharging into the vehicle's restricted engine compartment.

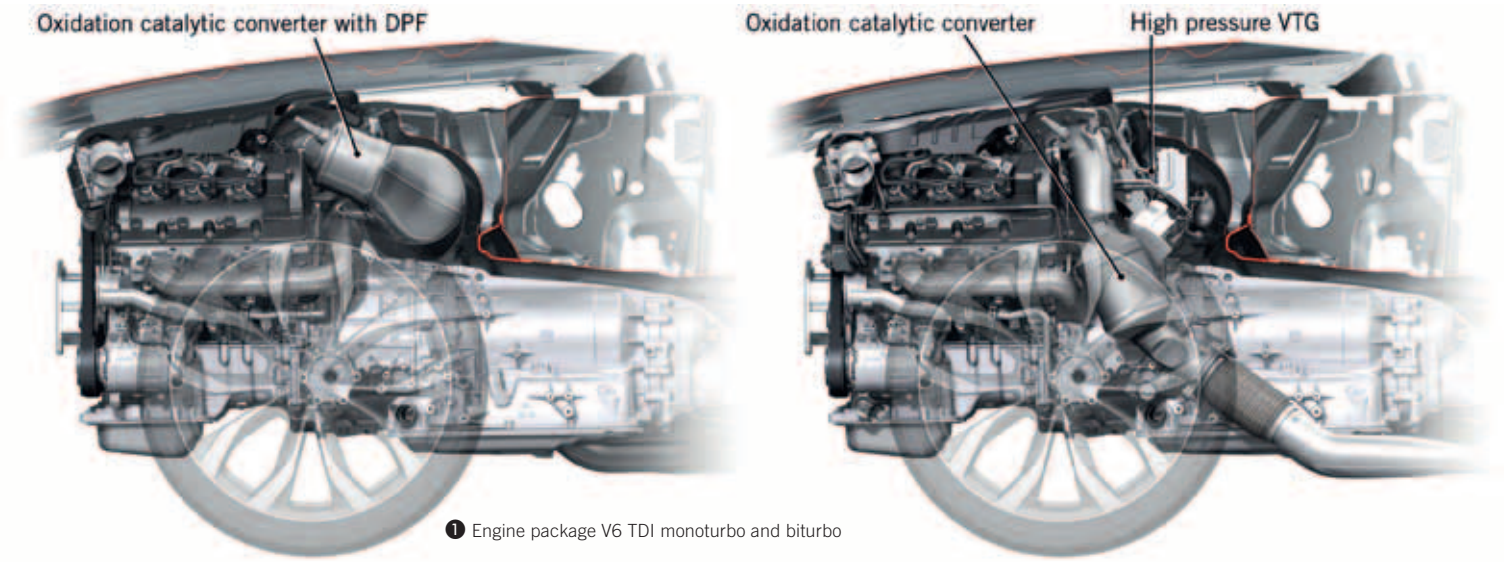

❶ Engine package V6 TDI monoturbo and biturbo

❷ lists the main dimensions and characteristic data of the engine. The main geometrical dimensions match those of the basic engine. In order to deliver the high performance reliably in operation, the cylinder heads and the piston assembly including piston cooling have been enhanced. This article looks into these assemblies in more detail.

The oil and water pumps have also been revised. The oil pump has been adapted to meet the engine's increased demand for oil resulting from the improved splash oil cooling of the pistons and the second turbocharger. As in the case of the basic engine, the pump is a controllable vane pump with its volumetric flow increased by widening the rotor by approximately 25 %. As a further measure in response to the increased engine cooling required, a higher-capacity water pump has been fitted. In the case of the V6 TDI biturbo, a closed plastic rotor with a diameter of 72 mm and three-dimensionally curved vanes is used. As a result the volumetric flow has been increased by approximately 30 % at the design point in comparison with the basic engine, with a simultaneous 7 % improvement in efficiency at the same operating point.

FEATURE	UNIT	
DESIGN	–	V6 engine with 90° V-angle
CAPACITY	cm^3	2967
STROKE	mm	91.4
BORE	mm	83.0
STROKE/BORE	–	1.10
COMPRESSION RATIO	–	16.0:1
DISTANCE BETWEEN CYLINDERS	mm	90
CRANKSHAFT	–	Forged, four bearings
MAIN BEARING DIAMETER	mm	65.0
CON-ROD BEARING DIAMETER	mm	60.0
CON-ROD LENGTH	mm	160.5
VALVE DIAMETER (INLET)	mm	28.7 (2x)
VALVE DIAMETER (EXHAUST)	mm	26.0 (2x)
FUEL INJECTION SYSTEM	–	Common rail, 2000 bar (Bosch CRS 3-20) with piezo injectors and high-pressure pump CP4.2
TURBOCHARGER	–	HTT Garrett GT 1749 with VTG (HP turbocharger) HTT Garrett GT 3067 with waste gate (LP turbocharger) Vacuum-controlled turbine switching valve
FIRING SEQUENCE	–	1, 4, 3, 6, 2, 5
NOMINAL POWER OUTPUT	kW	230 kW from 3900 to 4500 rpm
TORQUE	Nm	650 from 1450 to 2800 rpm
EMISSIONS STANDARD	–	EU5
WEIGHT TO DIN 70020 GZ	kg	209
ENGINE LENGTH	mm	437.0

❷ Main dimensions and characteristic data of the V6 TDI biturbo engine

CYLINDER HEAD

The cylinder head is subject to dynamic loading while the engine is running due to the cylinder pressure, as well as thermo-mechanical loading due to temperature variation. The peak pressure has not been increased in comparison with the basic engine, though it is utilized across a wider engine speed range under full load, so increasing the overall loading. The thermal loading of the cylinder head rises as the cylinder power output increases. ❸ shows the maximum material temperature between the exhaust valves 1 mm below the surface of the combustion chamber plate. The two columns on the left depict the temperatures of the 150 kW and 184 kW versions of the basic engine under full load with a one-part water chamber in the cylinder head. When this unmodified geometry is used for the V6 TDI biturbo the temperature rises to a critical level – with the increased risk of cracking of the combustion chamber plate as a result of thermo-mechanical fatigue after running for lengthy periods.

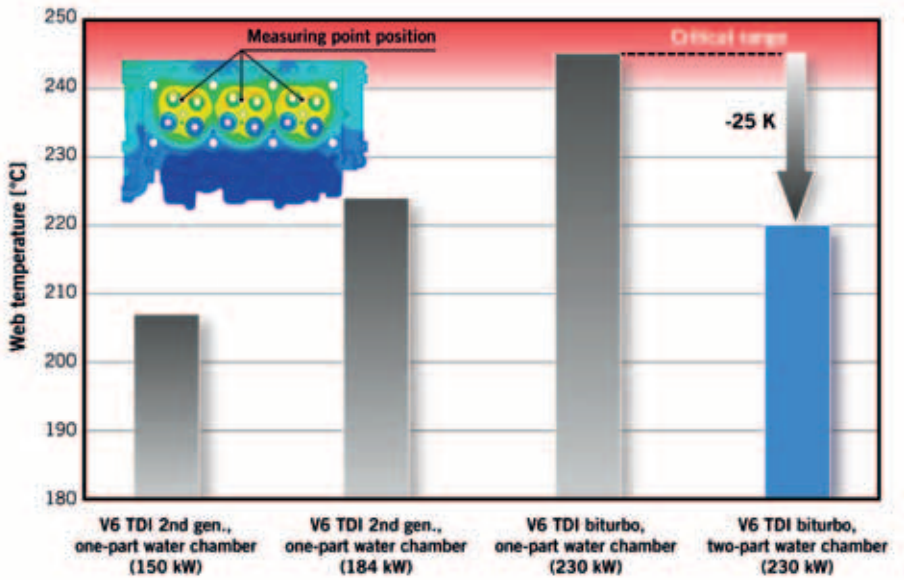

❸ Cylinder head material temperatures at 4500 rpm and 95 °C coolant temperature

For this reason, a cylinder head with a two-part water chamber has been developed for the high-performance engine, ❹. The water chamber is divided into top and bottom sections, each supplied by way of separate feeds from the engine block. This arrangement enables a higher volumetric coolant flow (cooling jet) to be directed through the lower water chamber, which cools the areas between the valves and the injector seat. The upper water chamber is adjusted to allow lower volumetric flow by means of restrictor bores in the cylinder head gasket. The cooling of the lands

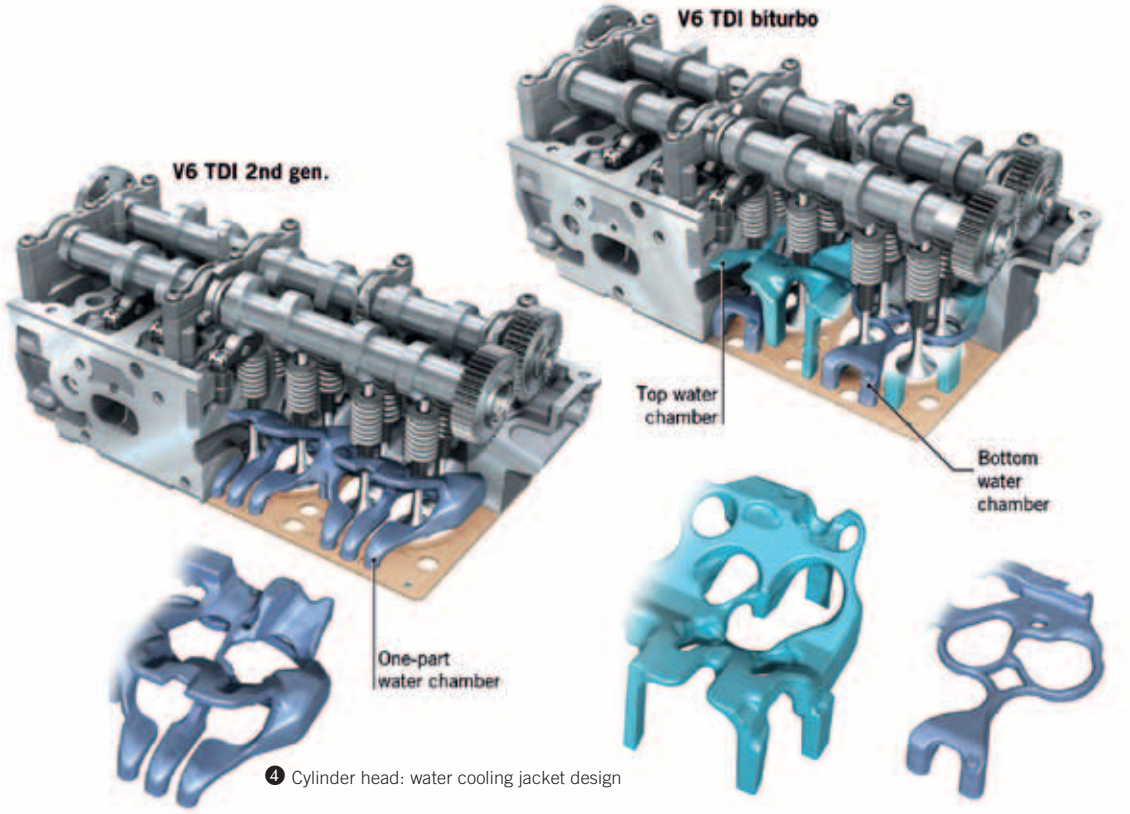

❹ Cylinder head: water cooling jacket design

between the cylinders is carried out from the cylinder head, as in the basic engine. The pressure difference between the upper and lower sections of the water chamber is used to propel the coolant. The principle of cross-flow cooling has been retained, as has the separate head-block cooling of the basic engine, controlled by the thermal management system [1, 3]. This solution has enabled the maximum temperature to be lowered by 25 K, ③.

The separation of the two coolant jackets results in an intermediate deck in the cylinder head, which stiffens the structure and enhances its strength. In the area of the injector seat, for example, high assembly and dynamic tensions are overlaid with high temperatures. Calculations show an improvement in the safety and security which have been achieved at this point by switching to the two-part water chamber with intermediate deck, despite the higher stress loads in the V6 TDI biturbo. The new head concept thus combines high mechanical strength with very low temperatures for an engine of this performance class, and as such also points the way ahead for future high-performance design concepts.

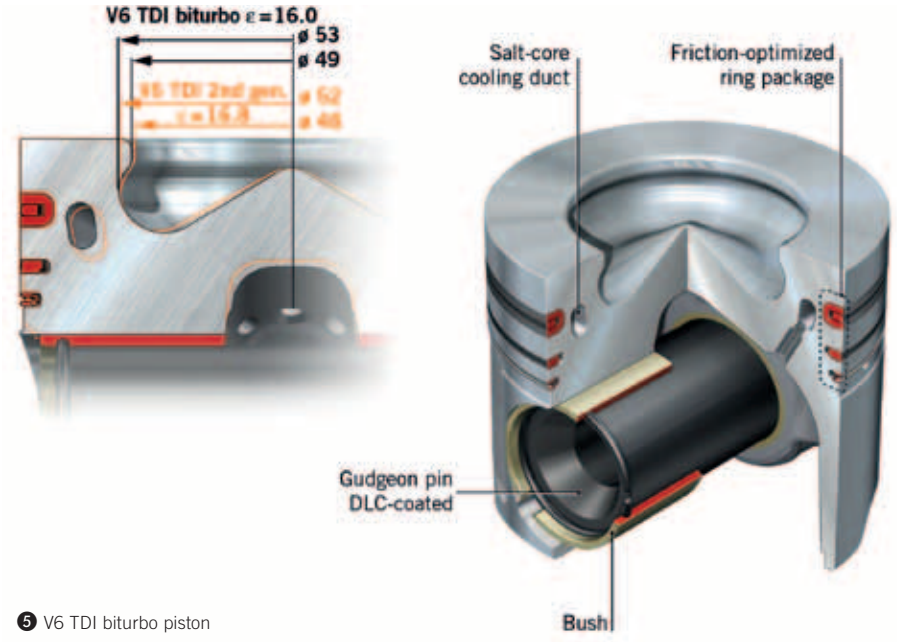

❺ V6 TDI biturbo piston

PISTONS

The major increase in power output from the engine also meant that the pistons needed to be optimized. The basic engine in all its versions features a piston with salt-core cooling ducts and a piston pin running in aluminium. The compression ratio is 16.8:1. The compression ratio of the V6 TDI biturbo has been reduced to 16.0:1 by enlarging the piston bowl, ❺. The position of the cooling duct has been moved slightly upwards and towards the first ring groove.

To improve strength, the V6 TDI biturbo is fitted with a bushed piston with a DLC-coated (diamond-like carbon) piston pin. The DLC layer alleviates the tendency of the pin to seize and reduces the friction in this area. By using bushes with moulded

bores, the pressure distribution between the pin and the piston is evened out and the risk of hub cracking is avoided. These measures enabled the pin diameter of the basic engine to be retained, meaning that the con-rod could also be retained as a shared component. The ring package is frictionally optimized as in the case of the basic engine. The higher positioning of the cooling duct and the optimized splash oil cooling enabled the bowl rim temperature to be significantly reduced relative to the piston of the 184 kW engine, ❻. This design offers potential for further power increases.

❻ Influence of optimized piston cooling on piston temperatures: maximum bowl rim temperature at 4000 rpm

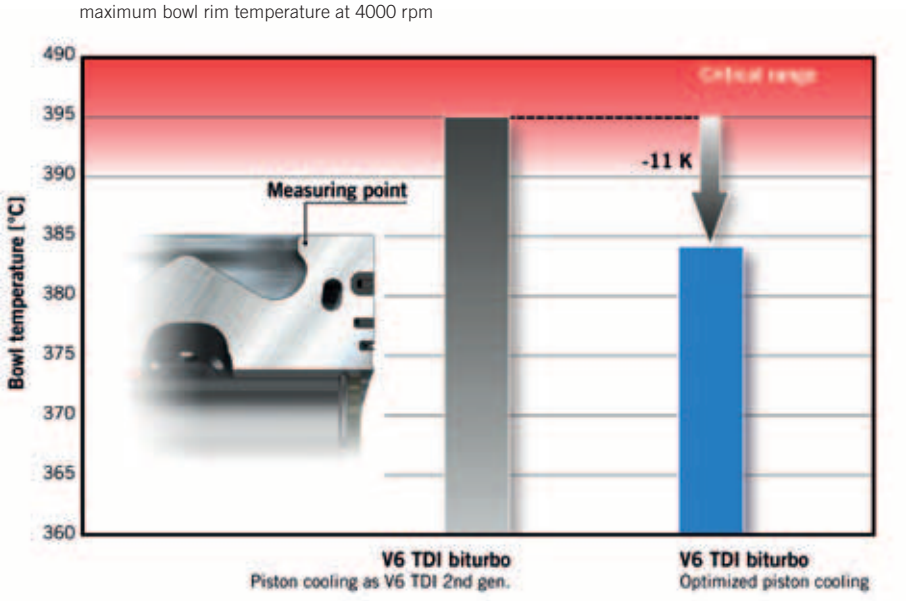

TURBOCHARGING SYSTEM

❼ presents a schematic view of the component layout in the two-stage turbocharging system. On the air side, the fresh air flowing in via the air filter and clean air system is pre-compressed by the low-pressure compressor across the entire map range. In the high-pressure compressor, the pressure of the air-mass flow is increased further. The air is then cooled in the intercooler and routed into the engine via the throttle valve, central swirl flap and intake manifold. A self-regulating compressor bypass valve is installed in parallel to the high-pressure compressor. This valve opens depending on the compressor output of the low-pressure turbocharger and the resultant pressure ratio upstream and downstream of the high-pressure compressor. The compression of the low-pressure stage is then sufficient to set the required charge pressure.

On the exhaust side, the high-pressure and low-pressure turbines are configured in series and both fitted with a bypass or wastegate. The bypass of the high-pressure turbine has a large cross-section, which can be infinitely adjusted by way of a turbine switching valve which is pneumatically actuated with vacuum. When the turbine switching valve is closed, the entire exhaust gas flow is partially relieved by way of the high-pressure turbine and then flows through the low-pressure turbine. The high-pressure turbocharger features VTG with an electric actuator motor. When this reaches its speed limit, the turbine switching valve is opened. In this case only part of the exhaust gas mass flow is then relieved by way of the high-pressure turbine; most is routed via the turbine bypass directly to the larger low-pressure turbine. The low-pressure turbocharger is fitted with a wastegate which regulates the charge pressure at high exhaust gas mass flow rates.

❽ shows the turbocharging system design as implemented for the V6 TDI biturbo engine. The low-pressure turbocharger is housed in the rear area of the inner V while the high-pressure turbocharger, rotated 90°, is positioned behind the engine above the gearbox. The key component of the turbocharging system is the turbine housing of the high-pressure turbocharger, via which the exhaust gas mass flows are distributed within the system. It incorporates the flange for connec-

❼ Schematic view of the V6 TDI biturbo turbocharging system

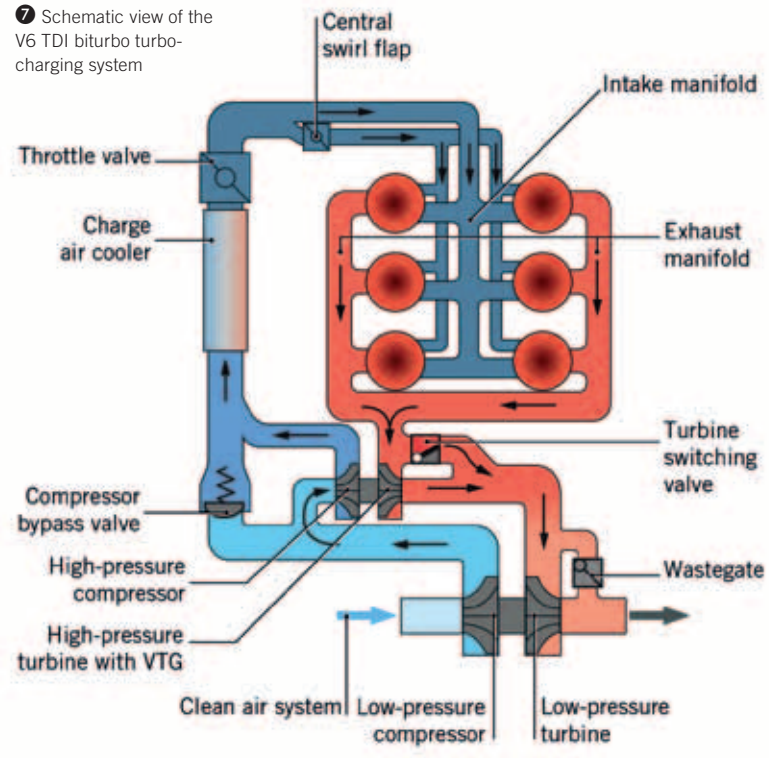

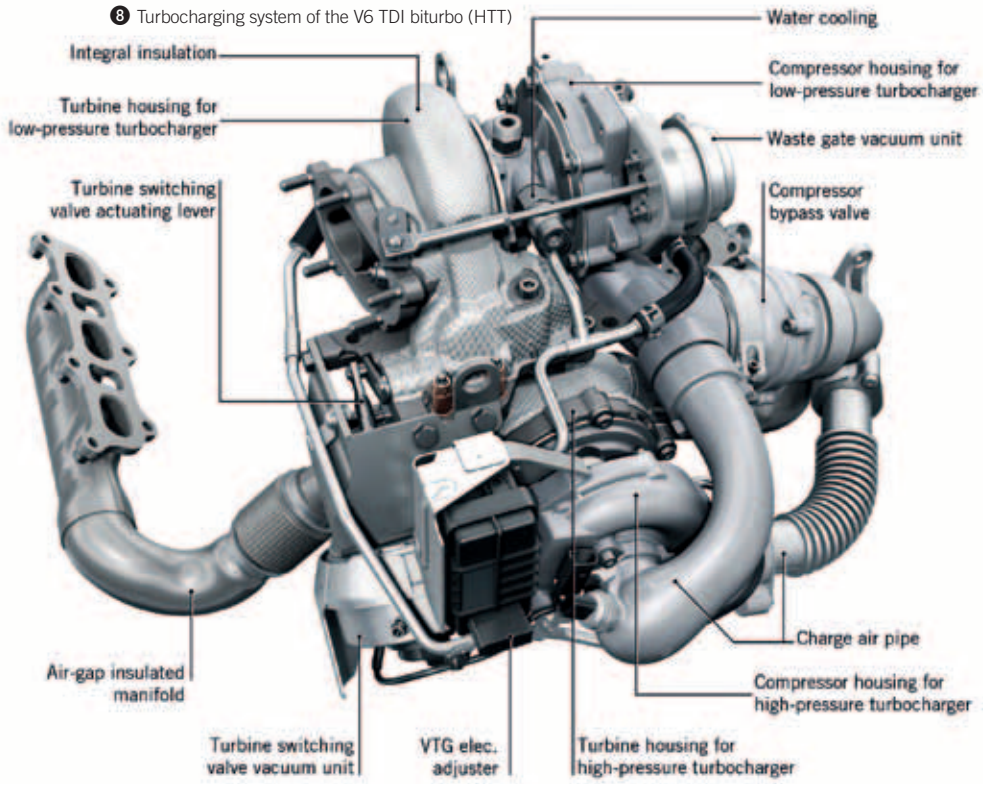

❽ Turbocharging system of the V6 TDI biturbo (HTT)

tion of the exhaust manifold by way of a Y-piece as well as the flanges for the high-pressure turbine bypass, the low-pressure turbocharger and the exhaust gas recirculation line. The turbine switching valve, including seat and shaft, is housed in the turbine housing of the low-pressure turbocharger.

All the other components are grouped around these key components. On the left as seen in the direction of travel is the large vacuum unit, with position feedback for the turbine switching valve, and the electric actuator for the high-pressure turbocharger. On the right are the compressor bypass valve, the vacuum unit to actuate the wastegate and the charge air ducting. The compressor bypass valve is designed so as to widen its cross-section rapidly on non-stationary acceleration and yet still prevent unintentional opening due to engine vibration. The pressure losses occurring at the compressor bypass have been reduced by optimizing the geometry of the valve cone down to a minimum. The center housings of both turbochargers are water-cooled. The water and oil supply is provided via external lines.

The turbine housing of the high-pressure turbocharger is the most complex cast component of the turbocharger assembly. The areas of the component that are subjected to hot exhaust gases change depending on the position of the exhaust flap. This results in inhomogeneous temperature distribution and therefore in thermal stresses in the component. In the course of design optimizations carried out on the component, the number of cores was reduced from 16 to eight and at the same time the thermal stresses in critical areas were reduced to a non-critical level. ❾ shows the number and layout of the cores in the casting mould before and after optimization.

With two-stage turbocharging, the responsiveness of the engine is dictated by the tight closure of the turbine switching valve. Even the tiniest leaks will lead to significant loss of enthalpy for the high-pressure turbine. Consequently, special attention was paid during the development process to the seal achieved by the turbine switching valve. To evaluate the seal achieved by the turbine switching valve, a pressure difference of 2.5 bar is applied by way of the flap valve on the component test rig and the resultant volumetric flow leakage is determined. In an early phase of the project, two different turbine switching valve designs were compared in with regard to leakage:

: a centrally mounted changeover flap valve (butterfly design)
: a side-mounted changeover flap valve (swing valve design).

The tests carried out revealed at an early stage that, in its new condition, the swing valve offered significant advantages over the butterfly design in terms of the seal achieved, ❿. The leakage of the swing valve design as new is many times less than that of the butterfly design. It also proved much better over lengthy running periods. As the swing valve also offers major benefits in terms of flow pressure losses because it is moved fully out of the bypass duct, Audi chose to develop this solution for series production. The large bypass flap in combination with the high turbine intake pressures do however require high actuator forces in order to prevent the flap from opening of its own accord, even under transient operating

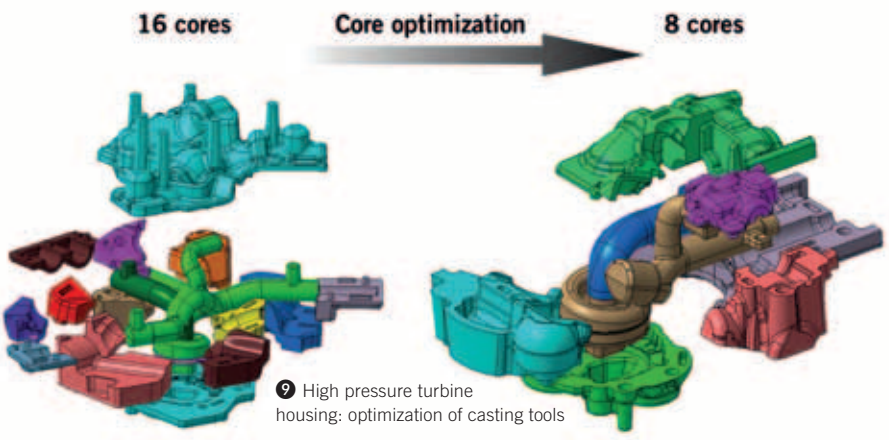

❾ High pressure turbine housing: optimization of casting tools

⓾ Turbine switching valve leakage behaviour

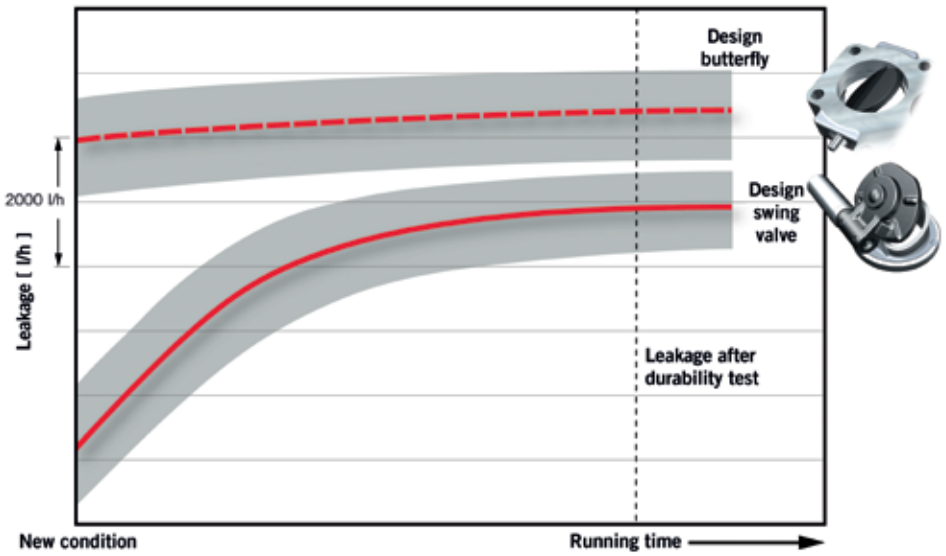

conditions. In order to satisfy these requirements a special long-stroke vacuum unit with a large effective cross-section has been developed. The unit has a position feedback feature in the form of a position sensor inside the unit, which has had to be adapted to the long stroke of the unit.

To assess the influence of the seal achieved by the exhaust flap, acceleration was measured on a vehicle with new components and with components at the end of endurance testing. The defined maximum permissible leakage quantities at the end of endurance testing guarantee minimal time lag under acceleration in comparison with new components. This is key to the excellent dynamic responsiveness of the engine throughout the life of the vehicle.

SUMMARY

With the V6 TDI biturbo, Audi has launched its most powerful six-cylinder diesel engine to date. The engine gives the C-segment cars extraordinarily sporty performance along with low fuel consumption, supplementing the range of Audi V-engines below the V8 TDI and V12 TDI. The two-stage turbocharging system has been implemented in the restricted space available with no need for compromise in terms of thermodynamic design and long-term mechanical durability. The higher loading on the engine compared with the basic engine has been taken into account by means of optimization measures which open up potential for further increases in power output for both the biturbo and monoturbo designs.

REFERENCES

[1] Bauder, R.; Bach, M.; Fröhlich, A.; Hatz, W.; Helbig, J.; Kahrstedt, J.: Die neue Generation des 3.0 TDI Motors von Audi – emissionsarm, leistungsstark, verbrauchsgünstig und leicht [The new-generation 3.0 l TDI engine from Audi – low emissions, high performance, good fuel economy and lightweight design]. 31st International Vienna Motor Symposium, 2010

[2] Bauder, R.; Kahrstedt, J.; Zülch, S.; Fröhlich, A.; Streng, C.; Eiglmeier, C.; Riegger, R.: Der 3.0 l V6 TDI der zweiten Generation von Audi – konsequente Weiterentwicklung eines effizienten Antriebes [The second-generation 3.0 l V6 TDI from Audi – consistent further development of an efficient power unit]. 19th Aachen Colloquium Automobile and Engine Technology, 2010

[3] Bauder, R.; Fröhlich, A.; Rossi, D.: Neue Generation des 3,0-l-TDI-Motors von Audi, Teil 1 – Konstruktion und Mechanik [New-generation Audi 3.0 l TDI engine, part 1 – design and mechanical components]. In: MTZ 71 (2010), No. 10

[4] Kahrstedt, J.; Zülch, S.; Streng, C.; Riegger, R.: Neue Generation des 3,0-l-TDI-Motors von Audi, Teil 2 – Thermodynamik, Applikation und Abgasnachbehandlung [New-generation Audi 3.0 l TDI engine, part 2 – thermodynamics, application and exhaust treatment]. In: MTZ 71 (2010), No. 11

[5] Bauder, R.; Eiglmeier, C.; Eiser, A.; Marckwardt, H.: Der neue High Performance Diesel von Audi, der 3.0 l V6-TDI Biturbo [The new high-performance diesel from Audi, the 3.0 l V6 TDI biturbo]. 32nd International Vienna Motor Symposium, 2011

We make connections – worldwide.

The trade journal for adhesives and sealing technologies.
Test it and order your own print- or e-magazine at

www.adhesion.com

adhesion ADHESIVES & SEALANTS

VARIABLE-LENGTH AIR INTAKE MODULE FOR TURBOCHARGED ENGINES

Customers have always wanted good performance and dynamics from their vehicles. One solution for cars with naturally aspirated engines is an air intake module with variable runners. For turbocharged gasoline passenger car engines, however, variable runner-length air intake modules have never been used. Yet, the constantly increasing requirements placed on engines call for new methods. Mahle has investigated the combination of turbochargers and variable-length runners and found some interesting advantages with respect to dynamics and fuel consumption.

AUTHORS

JÜRGEN STEHLIG
is Director of the Product Development Segment Air Intake Modules at Mahle Filter Systems in Stuttgart (Germany).

JAMES TAYLOR
is Principal Engineer in the Thermodynamic and Application department at Mahle Powertrain Ltd in Northampton (Great Britain).

RENE DINGELSTADT
is Project Manager in the Corporate Advanced Engineering at Mahle International GmbH in Stuttgart (Germany).

DR. DAVID GURNEY
is Principle Engineer Simulation, Research & Development at Mahle Powertrain Ltd. in Northampton (Great Britain).

MOTIVATION

Driven by rising expectations for lower fuel consumption and emissions, turbocharged downsizing concepts have taken center stage for passenger car gasoline engines. In order to increase customer acceptance, these engines need better low-end torque and optimised responsiveness. Single-stage turbocharged engines represent a compromise between turbochargers designed for dynamics and low-end torque on one hand, and those designed for efficiency at rated power on the other. Potential optimisation steps include turbochargers with variable turbine geometry, or a combination with a second turbocharging unit or charging concept. Driven by increasing demands on costs, performance, and fuel consumption, Mahle is breaking new ground and has investigated the solution described below.

The combination of an exhaust gas turbocharger and the proven technology of an air intake module with variable runner lengths is intended to join the advantages of both individual technologies and to achieve additional positive effects:

: exhaust gas turbocharger designed for higher engine speeds, for reducing pump losses and therefore fuel consumption
: cooling charge air at medium and high engine speeds, for additional fuel savings
: resonance charging with the runner, for greater torque at low engine speeds and better responsiveness.

TEST SETUP

Starting with a mass-production, four-cylinder downsizing engine, the following adjustments were made:

: replacement of the exhaust camshafts to optimise exhaust valve opening time
: use of a mass production exhaust gas turbocharger designed for medium and high speeds.

Torque is limited to 225 Nm in the range from 1500 to 4500 rpm, in order to maintain charge air reserves, ❶. The rated power of the test engine is 112 kW. Conditions for testing:

: ignition point offset 1° CA from knock limit
: charge air temperature before cooler: maximum 180 °C
: maximum turbocharger speed: 210,000 rpm.

The variable runner length was produced as a laser sintered air intake module, made of the following components:

❶ Torque curve of the test engine with series runner length

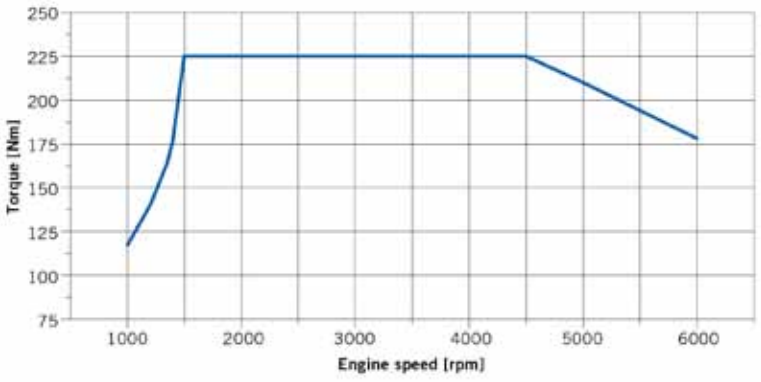

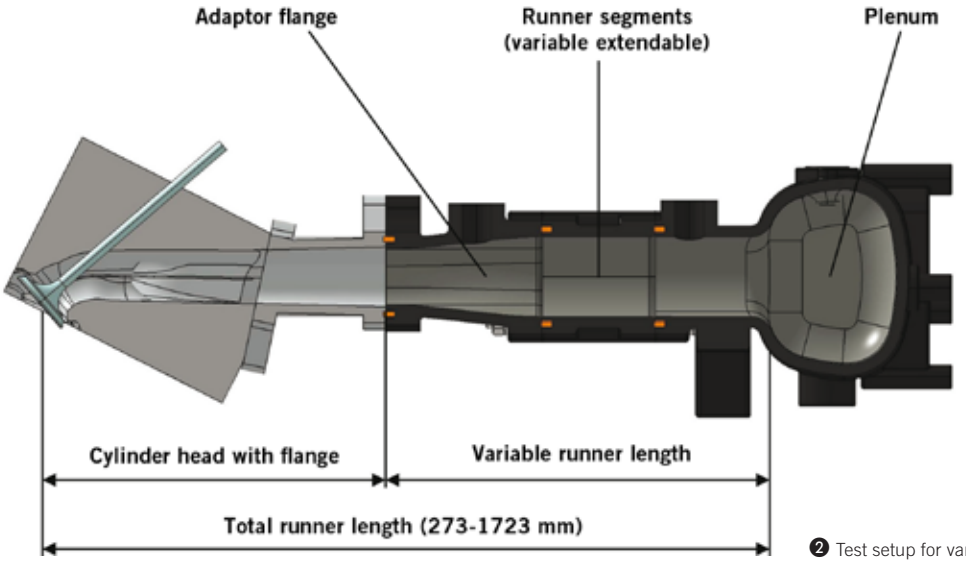

❷ Test setup for variable-length runner

: plenum
: runner segments (of different lengths, interchangeable)
: adapter flange.

The inner surfaces were painted in order to produce a flow-optimised surface. The runner lengths given here refer to the distance from the interface between the plenum and runner, to the intake valve. These were between 273 mm (current mass production application) and 1723 mm, ❷.

The charge air pipe length between the charge air cooler and the throttle valve was constant across all tests.

❸ Intake pressure curve and valve lift

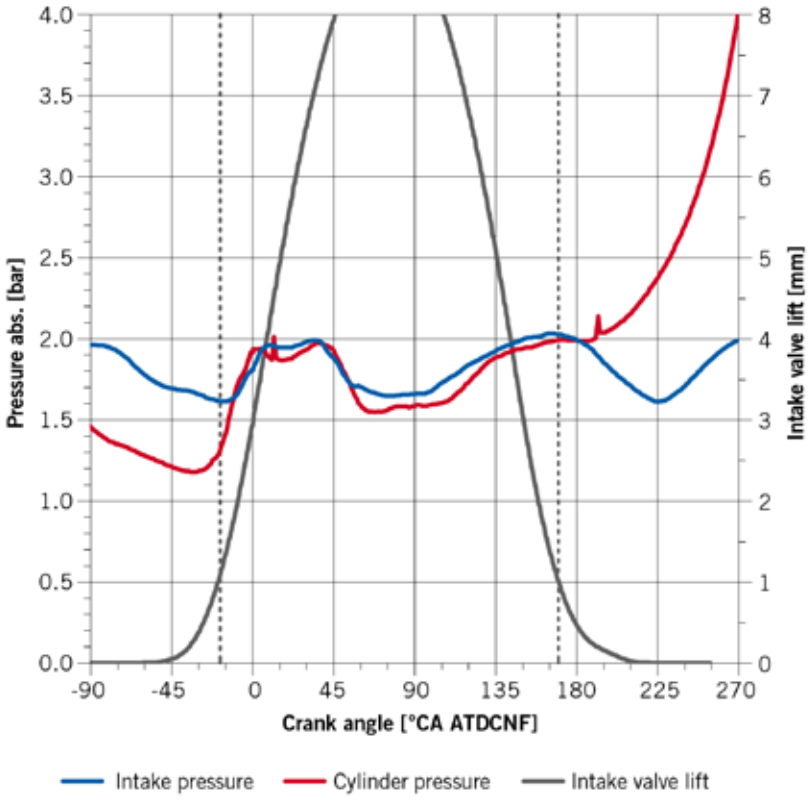

INCREASED TORQUE AT LOW ENGINE SPEEDS

Tests for increased torque were performed at the low speed range between 1000 and 1500 rpm. In the basic configuration, the turbocharger provides very little charge air pressure, even with the wastegate closed, which means that the torque achieved in this speed range is not satisfactory.

Tests of variations in the intake timing and different runner lengths demonstrate the potential of this variability in turbocharged gasoline engines. The ratio of fuel to air was set to stoichiometric for all cases. The ignition point was set so as to optimise the efficiency whenever possible, or at one degree of crank angle from the knock limit. Similarly to resonance runner charging in naturally aspirated engines, the air charge can also be increased in a turbocharged engine if the runner length and intake closing point are optimally tuned to the engine speed.

As ❸ indicates, in the tuned state, the closing point of the intake valve coincides with a pressure peak of the air pressure wave in the runner. This increases the air mass entering the combustion chamber. When the injection quantity is adapted accordingly, this leads to increased torque values, just as in a naturally aspirated engine.

The following additional effect occurs in a turbocharged engine: the greater volumetric efficiency increases the engine pressure ratio (plenum pressure/exhaust pressure), leading to an increase in the turbine speed. The

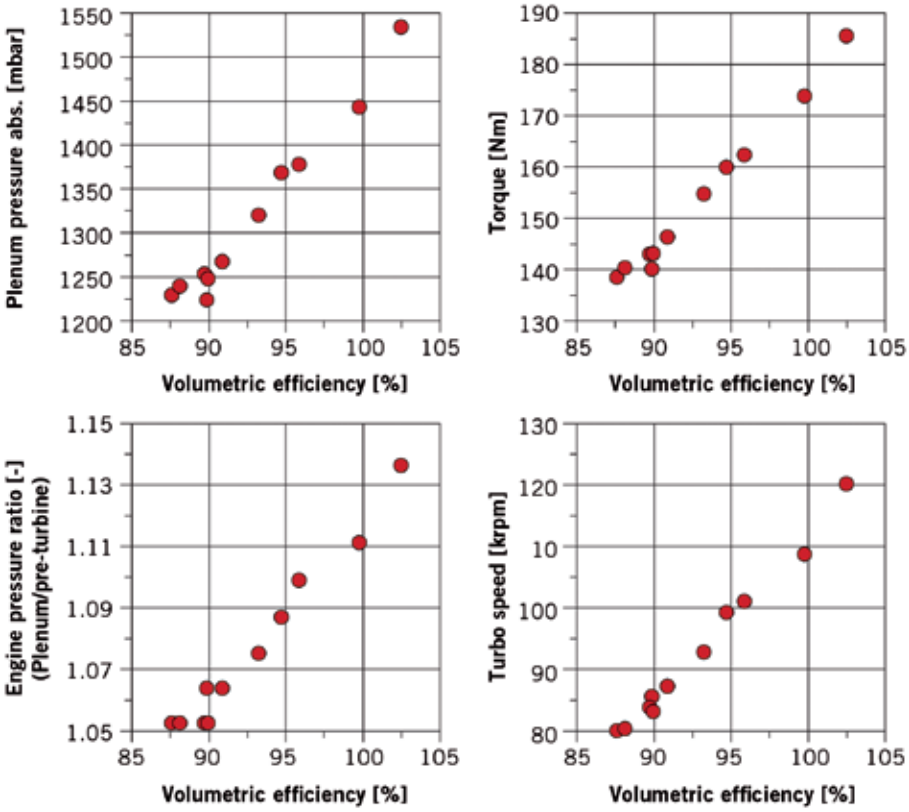

❹ Investigating optimal runner lengths

turbocharger can thus raise the air mass flow until an equilibrium or the nominal torque is reached, in which case the wastegate opens. This additional air mass flow is cooled by the charge air cooler. The dependencies of volumetric efficiency to plenum pressure, torque, engine pressure ratio, and turbine speed are shown in ❹, using the example of 1200 rpm. The individual points represent different runner lengths.

The optimum of all the runner lengths measured is shown in ❺. It describes which combination of runner length and engine speed had the greatest increase in torque. It was possible to demonstrate an increase in torque of over 35 % at 1350 rpm. Four different runner lengths allow significant improvement in the torque curve. The torque was increased by 60 Nm over the base version at 1350 rpm, and the nominal torque is already available at 1400 rpm.

POTENTIAL OF VARIABLE RUNNER LENGTHS AT HIGH ENGINE SPEEDS

Tests at medium and high engine speeds were intended to demonstrate the additional potential of varying the runner length. Because the wastegate is open in this case, the goal is not to further increase the torque. Instead, the intent is to reduce fuel consumption at a constant torque.

In the speed range of the nominal torque, intake air is available in sufficient quantity. Reduced fuel consumption can be achieved essentially by lowering the intake air temperature. The runner length effect therefore does not lead to an increase in pressure and the associated temperature increase, as it does at lower engine speeds. Instead, the investigation is to determine how the runner length effect can be used at medium and high engine speeds to lower the pressure, and thus to lower the temperature as well.

DYNAMIC TEMPERATURE REDUCTION

At medium and high speeds, the runner length effect can be used to reduce both pressure and temperature. In order to obtain the same pressure at the intake valve as would be present without the resonance runner length effect, the wastegate closes further and the turbine speed of the turbocharger increases. The charge air pressure rises, and so does the average pressure around which the resonance runner pulsation oscillates. Part of the com-

❺ Torque curve and torque increase

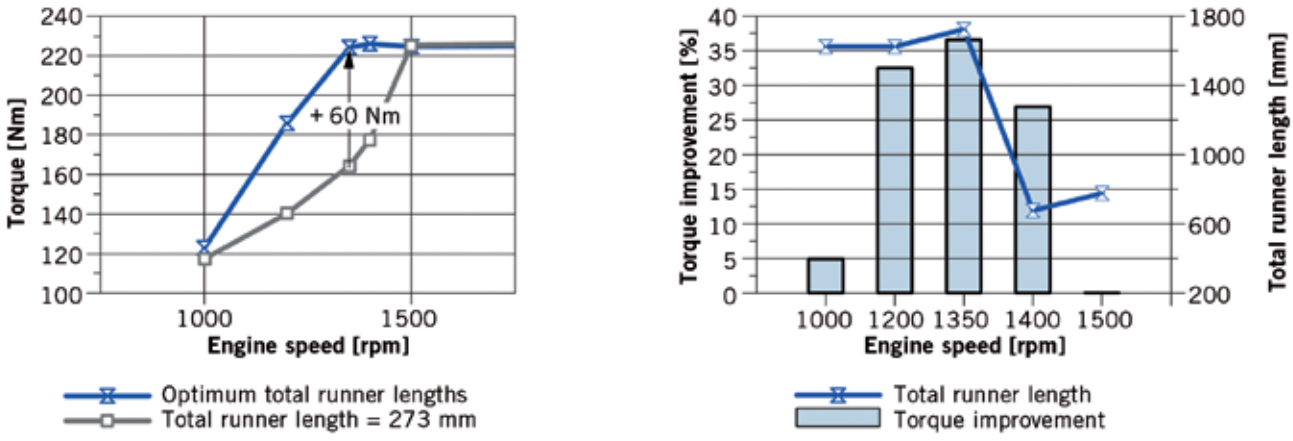

pression work is thereby transferred from the runner to the turbocharger.

The air compressed in the turbocharger first passes through the charge air cooler and then cools off further due to the effect of the dynamic temperature drop in the resonance runner. ❻ shows this effect, for example, at 4500 rpm. In the initial state, the intake pressure is 1.9 bar at the point when the intake valve closes. The variant with an optimised runner length achieves the same intake pressure when the average charge air pressure is increased and the intake pressure drops to the minimum pressure of the runner effect.

Medium pressure increases by about 0.4 bar. The amplitude of this pressure oscillation is also 0.4 bar. This effect reduces the intake air temperature. It is possible to shift the ignition to an earlier point due to the reduced tendency to knocking, resulting in a center of combustion mass that is closer to the efficiency optimum of 8° CA after the top dead center. Fuel consumption can thus be reduced by about 5 % (e.g., at 4500 rpm). The application of this effect at other engine speeds, with optimised runner lengths for each case, is shown in the measurement results in ❼.

1-D charge cycle simulations made a more precise analysis of the temperature drop possible. An existing GT-Power model of the engine was used to determine the temperature changes at 4500 rpm and 225 Nm. Compared to the original intake manifold, an increase in temperature of up to 9 Kelvin may occur at the closing point of the intake in case of an unfavorable design of the runner length. If the runner lengths are designed optimally as described above, then the simulation results show a drop in temperature of 15 K at the same point in time. The physical explanation of the test results was therefore confirmed by the simulation.

TRANSIENT RESPONSIVENESS

At low engine speeds, it was possible to raise the torque by increasing the volumetric efficiency, using the resonance effect. This effect was intended to be applied to transient behavior as well. For the test, a load step from 22.5 Nm to a full load of 225 Nm was performed at a constant 2000 rpm for various runner lengths. A fixed setting of the maximum valve overlap ensured that the intake valve opened early. ❽ shows the torque increase over time during the load step.

Compared to the base runner length of 273 mm, a faster torque increase was achieved by means of an optimised runner length of 1373 mm. Ninety percent of the maximum torque is already available

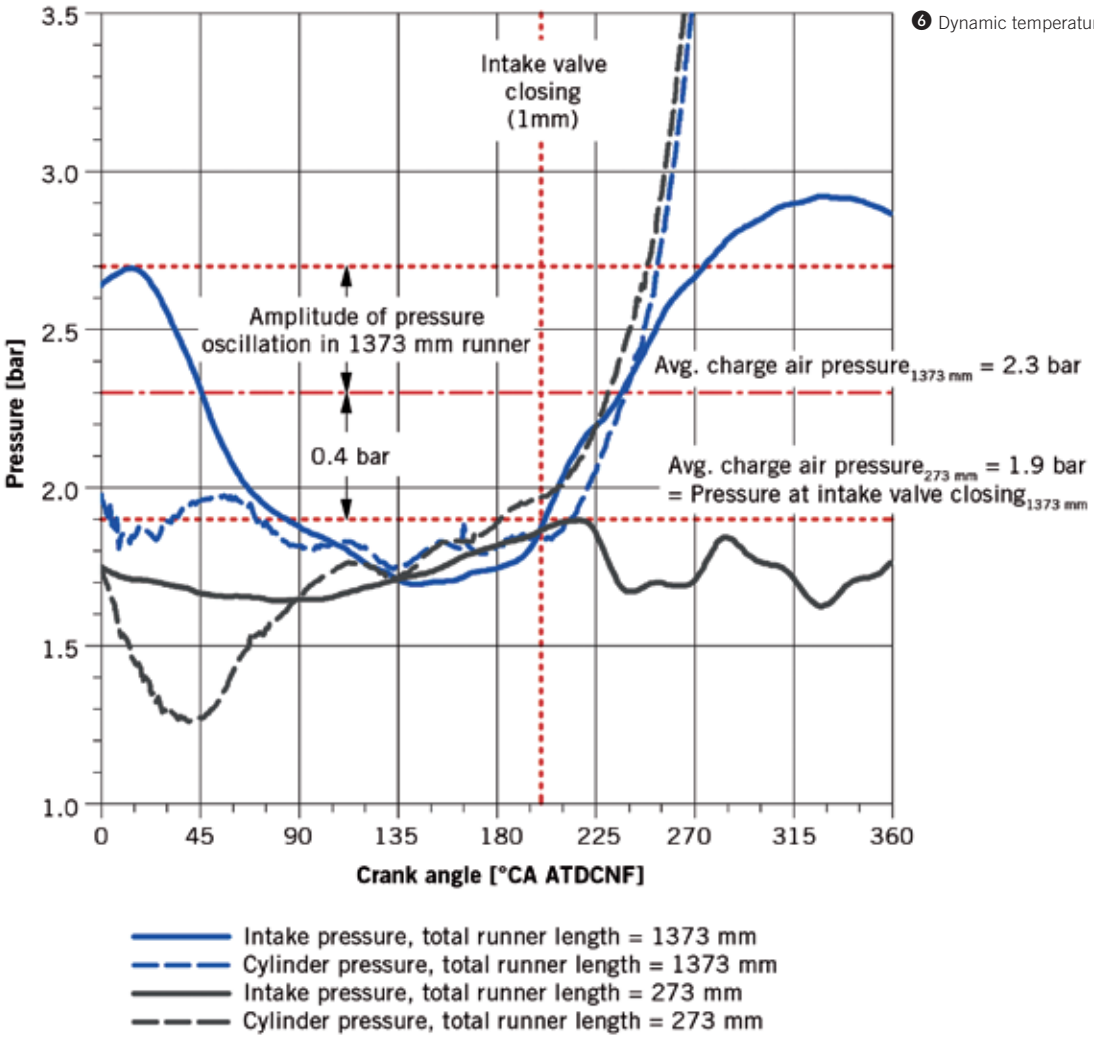

❻ Dynamic temperature reduction

❼ Optimised runner lengths at different engine speeds

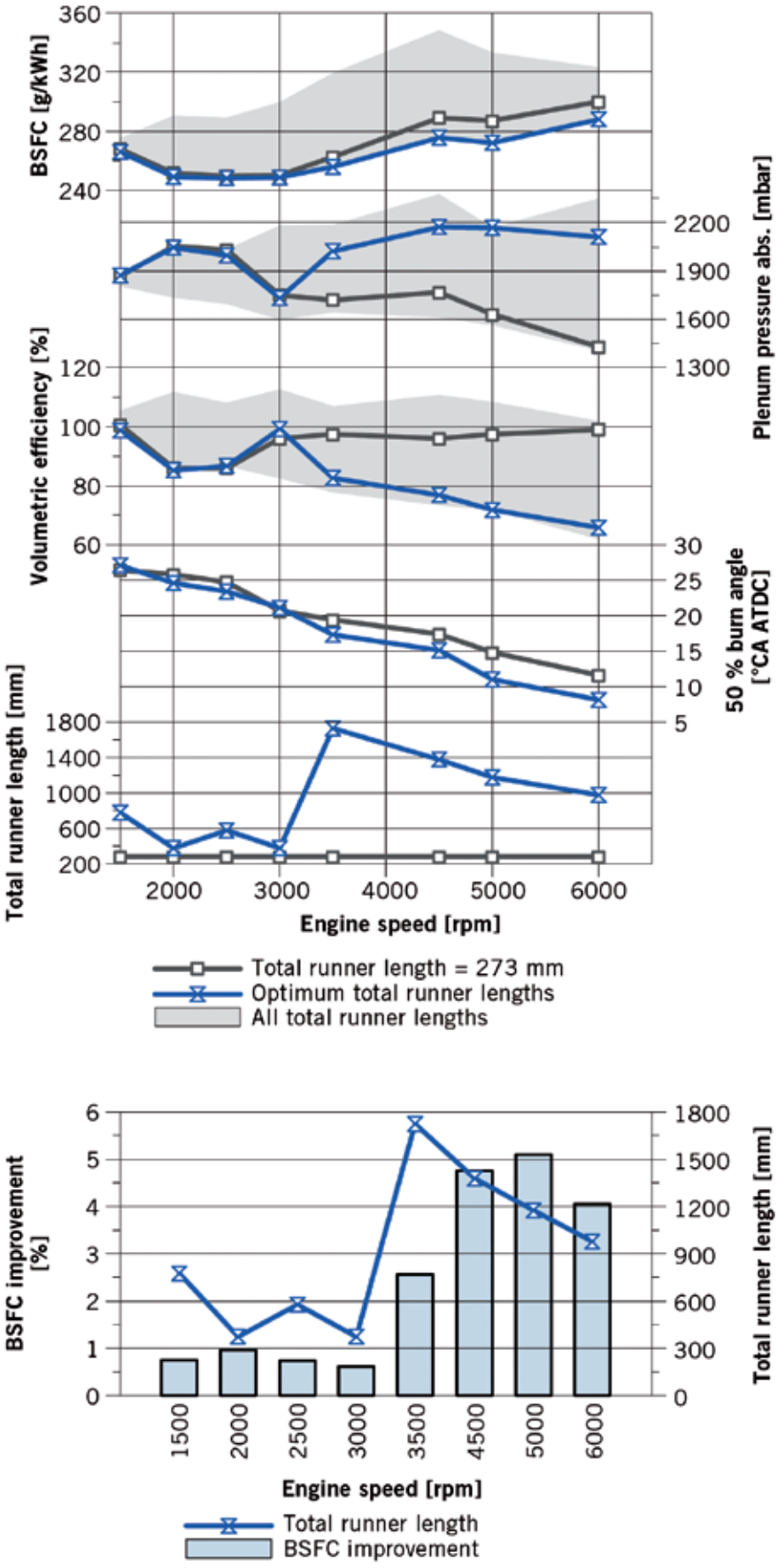

0.4 s earlier. The optimally tuned runner length increases the volumetric efficiency, and thus the mass flow through the engine. The pre-turbine enthalpy increases, which leads to a faster rise in the charge air pressure, and thus in the torque.

In a vehicle, a load step is typically also associated with an increase in engine speed, such as when accelerating. This must be taken into consideration when designing the runner lengths. ❾ shows the volumetric efficiency as a function of the engine speed and different runner lengths. The optimal design of the runner length is intended to ensure that as great a range as possible of the engine speed seen during the load step is located in the region of high volumetric efficiency. Using the torque curve from ⑧ as an example yields the band shown in grey in ⑨.

PREVENTING FUEL CONSUMPTION DISADVANTAGES UNDER PARTIAL LOAD

The runner length also has an effect on fuel consumption under partial load. Measurements indicated that fuel consumption increases at runner lengths greater than 800 mm. This can be attributed to an increase in gas exchange work. Using shorter runner lengths, the partial load can therefore be made neutral to fuel consumption.

SUMMARY

A test of engine performance was carried out for a mass-production, four-cylinder downsizing gasoline engine with single turbocharging, using an air intake module with variable runner lengths. The engine measurements showed the following:

- The torque can be increased by up to 60 Nm for the low engine speed range between 1000 and 1500 rpm by a combination of runner charging and a turbocharger.
- Runner charging also improves responsiveness. For example, for a load step at a constant 2000 rpm, the nominal torque is reached 0.4 s sooner.
- For engine speeds from 3500 to 6000 rpm, the goal is not to increase torque. Rather, the temperature can be reduced dynamically by means of the resonance effect in the runner. The intake temperature can be reduced by

up to 15 K, thus allowing fuel consumption to be reduced by up to 5 %.

: Under partial load, fuel consumption can be maintained at a neutral level.

OUTLOOK

With respect to a realistic application in a vehicle, the package must be considered. This means a limitation on the number of switching stages and a limit to the maximum potential runner length. A two-stage resonance runner length (373 and 750 mm) has been shown to be sensible here. This results in torque increases of up to 45 Nm at low engine speeds and improved responsiveness. The partial load can be implemented without affecting fuel consumption. The reduction in fuel consumption at high speeds is about one percent under these conditions. Based on the engine bench tests performed, the two-stage air intake module should be implemented in a vehicle package as a next step, and then evaluated in simulation. The results will then be validated using rapid prototype parts in a live engine in the vehicle.

❽ Torque increase over time during the load step at 2000 rpm

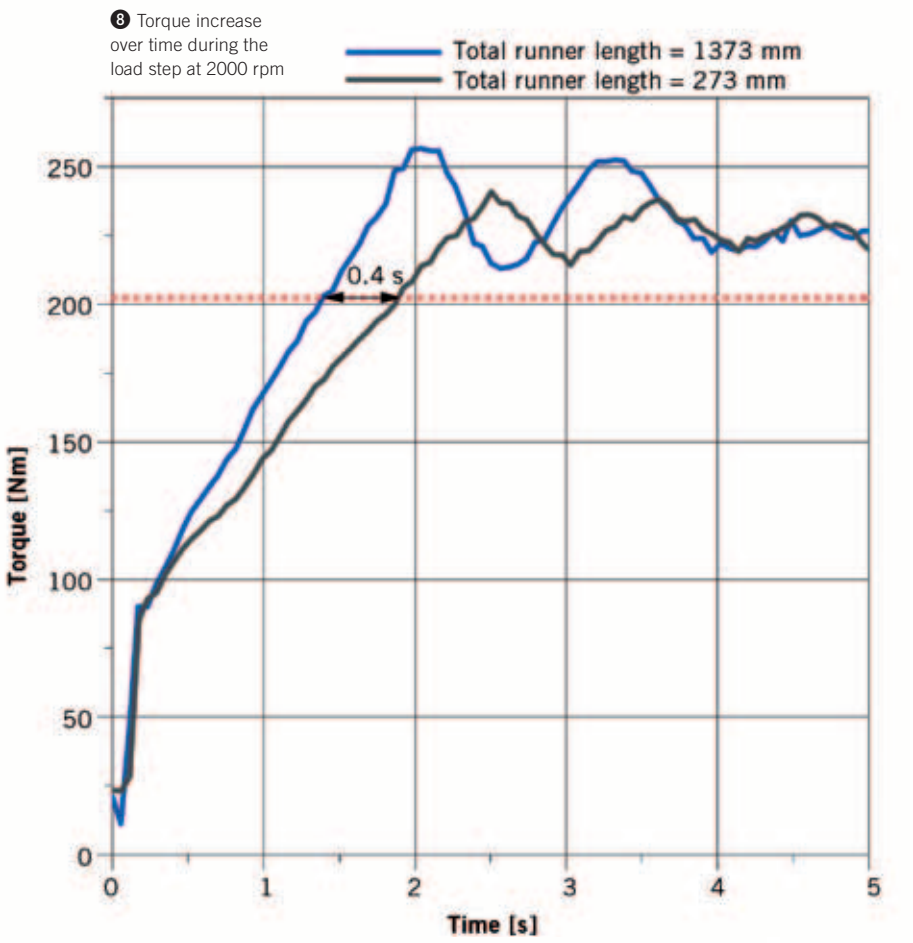

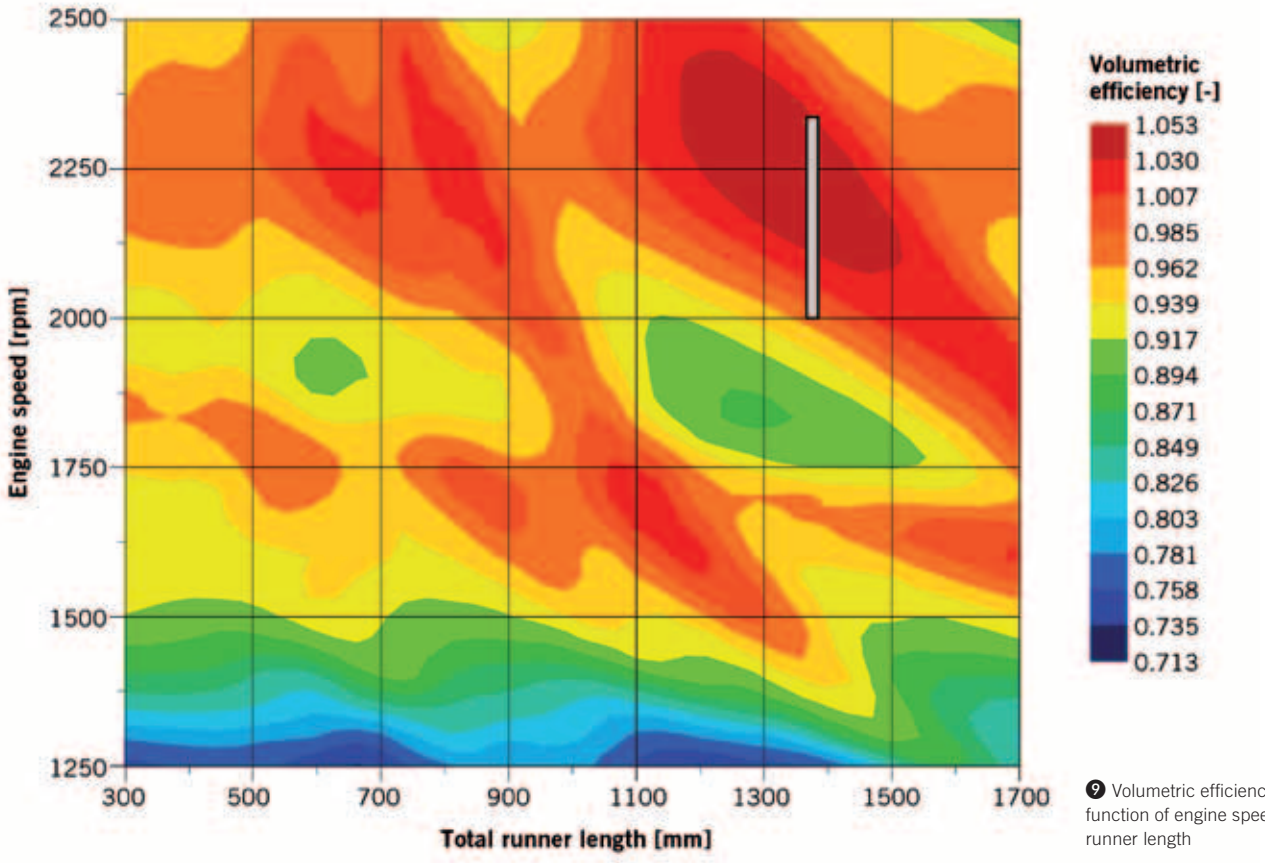

❾ Volumetric efficiency as a function of engine speed and runner length

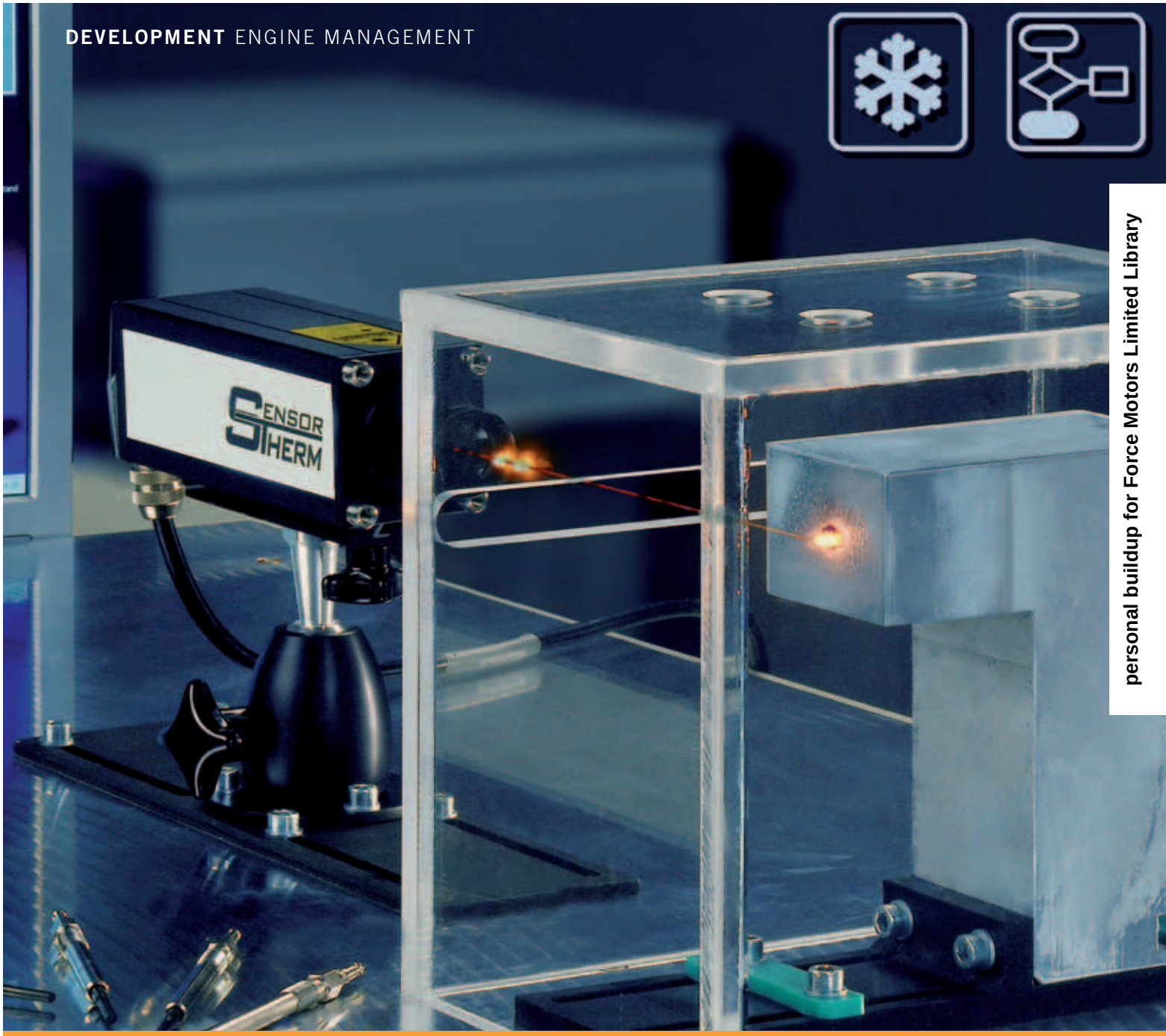

ENHANCING EFFICIENCY IN CALIBRATING DIESEL ENGINES FOR LOW TEMPERATURES

Diesel engine cold-starting is of high consumer relevance in relation to starting time, acoustics, emissions as well as running smoothness. This, of course, is also the focus of diesel engine developers. The need for efficient processes in validating cold-starting performance and optimizing cold idling is increasing, not least also in the wake of a trend toward reducing compression for emission reasons. In addition to conditioning, automation and data analysis, IAV investigated on determining and optimizing glow temperature.

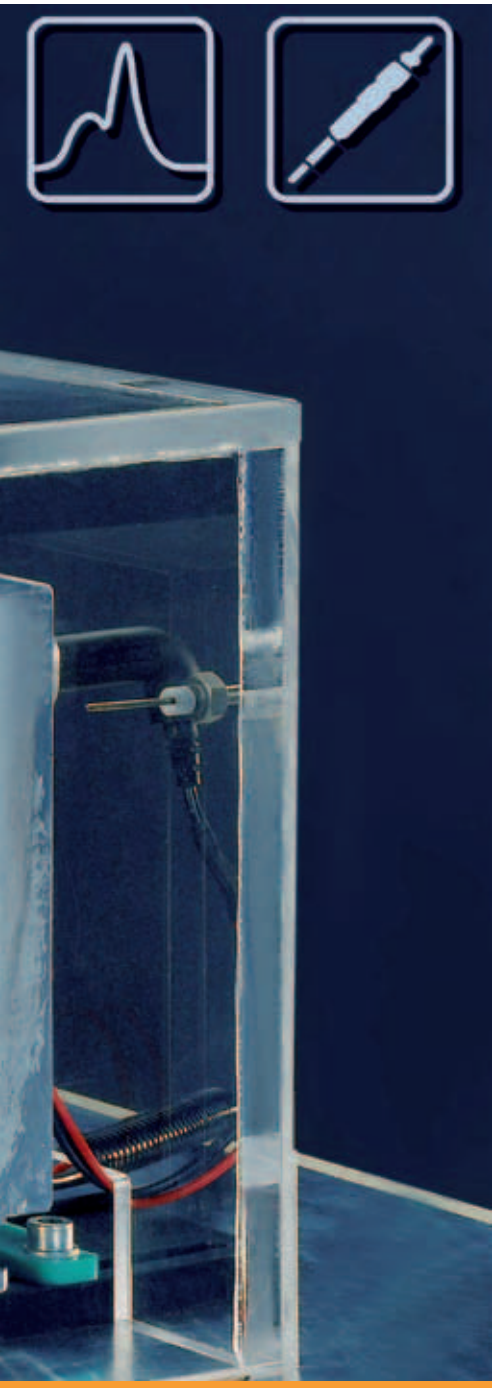

AUTHORS

DIPL.-ING. CARSTEN ENGE
is Development Engineer in Diesel Calibration at IAV GmbH's Development Center in Chemnitz (Germany).

DIPL.-ING. (FH) RALF STERNBERG
is Team Manager in Diesel Calibration at IAV GmbH's Development Center in Chemnitz (Germany).

DIPL.-ING. WOLFGANG TSCHIGGFREI
is Head of Diesel Engine Calibration in der IAV GmbH's Powertrain Mechatronics Business Area in Berlin (Germany).

OPTIMIZATION APPROACHES

In low-temperature diesel-engine calibration today, one to two cold-start tests are performed each working day in the temperature range from -10 to -30 °C. Whether on the engine test bench or in the form of vehicle measurement, time-consuming temperature conditioning makes gathering result-oriented data relatively slow in comparison with other development fields. The higher time and, also with this, cost factor is accompanied by quality-related demands on low-temperature calibration which, together with glowing strategy, pilot-injection characteristic and main-injection variation as key parameters, comes with a multi-dimensional variation space. Proceeding from primary investigations in the laboratory [1], many influences on the diesel combustion process in production engines, ❶, can only be defined with accuracy on the basis of test series and varying parameters. These must be regarded as engine-specific on the grounds of different injection systems and combustion-chamber geometries alone. This makes it necessary to intensify measurement-data recording. The potential here lies in increasing the number of tests and the efficiency of data analysis.

COLD-START TEST – ACTIVE CONDITIONING

Conditioning usually takes eight to twelve hours. Attempts to reduce this have already

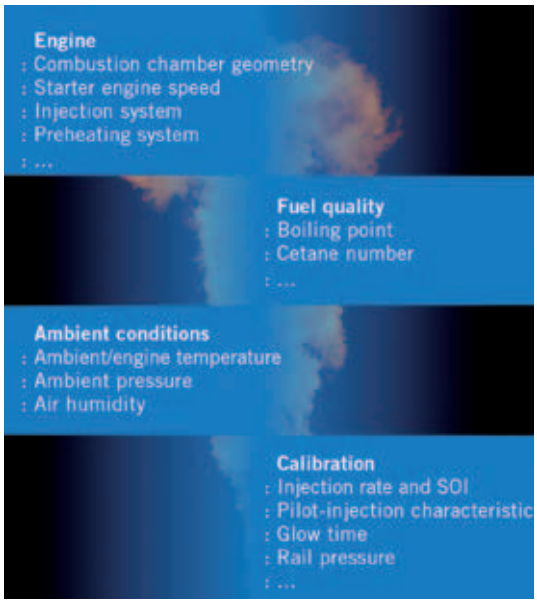

❶ Factors influencing the diesel combustion process

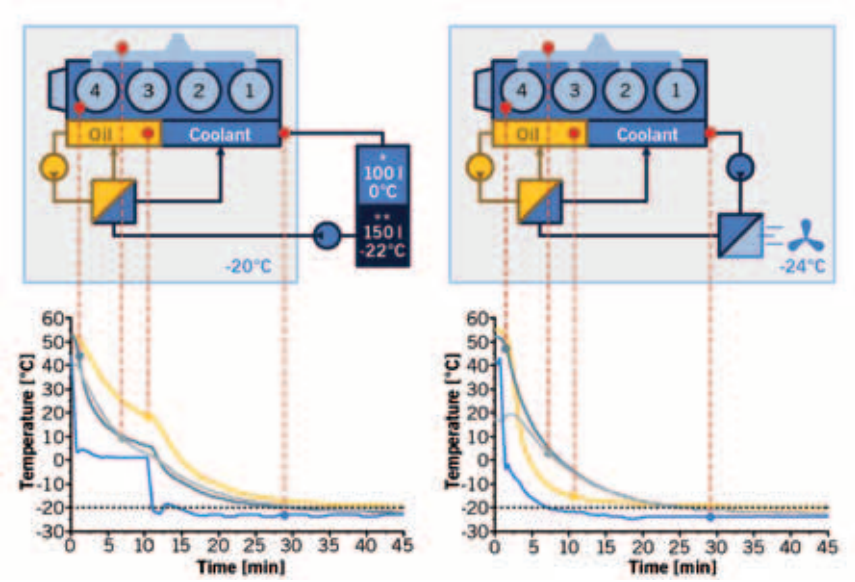

❷ Active engine conditioning by means of thermal-shock system (var. A, left) or vehicle radiator and blower (var. B, right)

been made under nominal conditions (25 °C) [2]. Two further methods have been applied using a 2.2-l four-cylinder in-line engine in the low-temperature chamber and compared with each other. The test setups are shown in schematic form, ❷.

In variant A, a thermal-shock system was integrated into the engine cooling circuit with two coolant reservoirs at different temperature levels. While the engine is at rest, coolant is passed through it by means of an external pump. To avoid damaging the engine, it was preconditioned to 0 °C and then cooled to -20 °C. Conditioning the engine oil, the viscosity of which has a significant influence on friction loss torque, is extremely important for providing near-reality test conditions. This is done by cooling it separately in a secondary circuit with a heat exchanger incorporated in the engine cooling circuit.

Variant B merely involves cooling with ambient air in the test chamber and manages without the use of any thermal-shock system. This was replaced with a regular radiator which, in combination with a blower, cools the coolant in the circuit down to the cold ambient temperature. External pumps are used and the engine is left at rest in this case as well. The compact setup can be mounted on an engine pallet or integrated into a vehicle.

For the purpose of monitoring temperatures, thermocouples were installed in the cylinder head, on the intake manifold, at the thermostat as well as in the oil sump. The temperature curves for both variants show that an oil temperature of -20 °C is reached after approx. 45 min if the setpoint values for variant A are reduced by 2 K and ambient air in the low-temperature chamber for variant B by 4 K. After stabilizing for a further 30 min, it was possible to ensure a temperature state corresponding to that achieved with conventional conditioning. In the temperature range down to -20 °C examined to date, it has not been possible to establish any side-effects of rapid conditioning.

Whereas it would be possible to speed up the process in variant A by shortening preconditioning and cooling the engine regardless of its ambient temperature, the far simpler setup with vehicle radiator is shown to be more cost-effective and offer greater flexibility. Both methods provided the capability of performing four cold starts (including heating-up phase) within eight hours, with about six hours being spent on conditioning.

AUTOMATION

Particularly with tests that take a long time to prepare, failed attempts result in additional cost, and divergent boundary conditions are reflected as uncertainties in the result. This makes improving reproducibility a further aspect of enhancing efficiency in low-temperature testing.

The idea of automating cold starting with the above-mentioned objectives therefore seems reasonable. INCA calibration in combination with the envisaged CaliAV automation software provides the technical

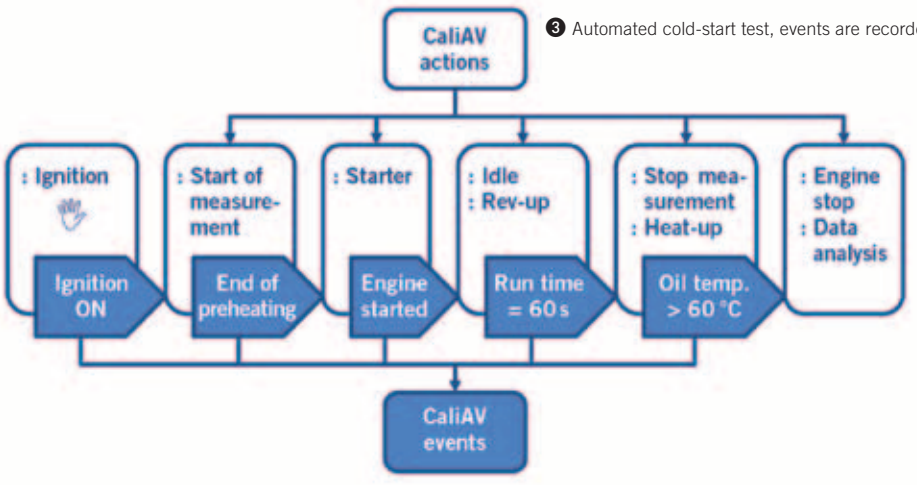

❸ Automated cold-start test, events are recorded and actions controlled by CaliAV

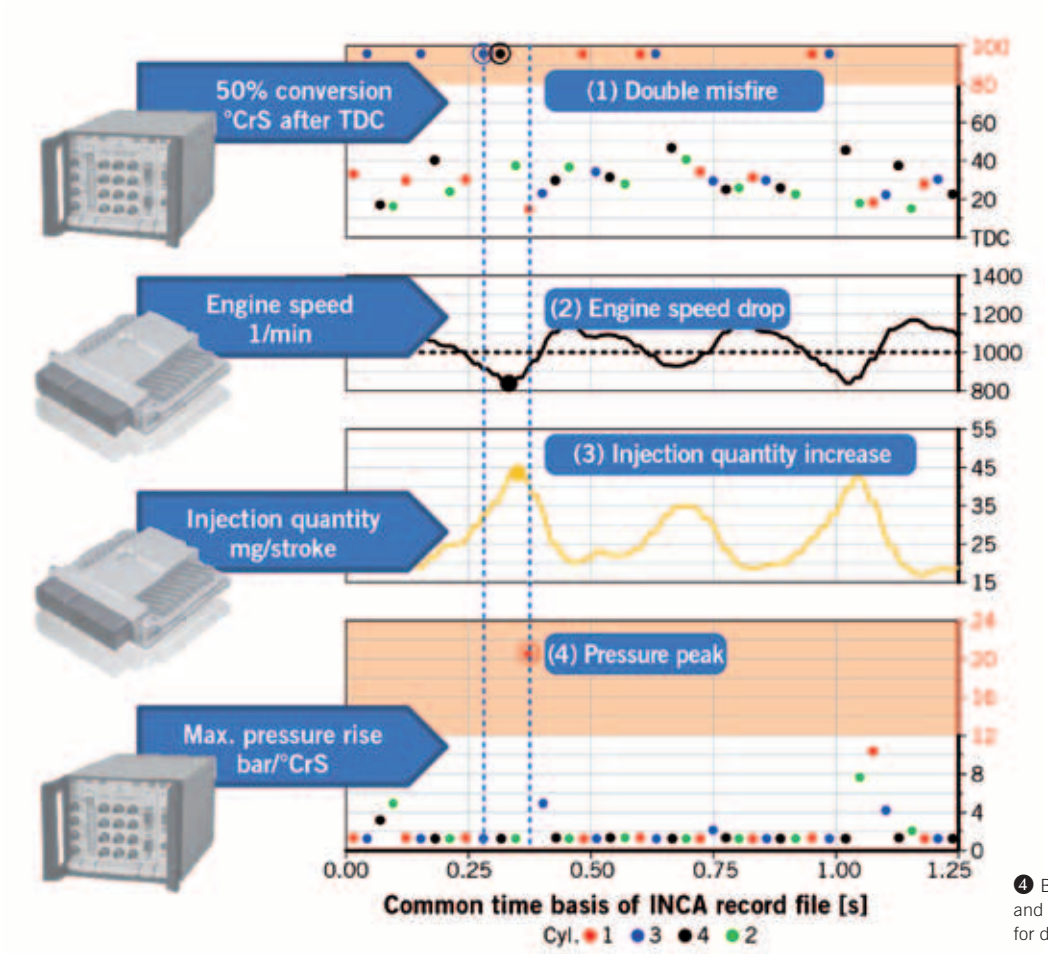

❹ Bringing together control unit and indication data (IAV Indicar) for detailed analysis

capability to do so. The test sequence can be put together on the basis of the modular system. Events, such as preheating or starting cutout as well as running times, are recorded, with individual phases of the cold-start test running through automatically. This is where the engine management system can be influenced actively using INCA and additional technology can be activated (e.g. sound recorder). The person in charge has an assistance system and can devote greater attention to subjective impression. By way of example, ❸ shows a program sequence for an automated cold start in which turning on the ignition is the only manual action.

A block for immediately analyzing the data recorded is integrated at the end of the automatic program. Conclusive parameters are computed for comparing the test results more quickly and for revealing anomalies. Examples of this include starting time, engine speed fluctuation or the frequency distribution of engine misfires as a result of thermodynamic analysis described in the next section.

REAL-TIME COMPUTATION IN CYLINDER-PRESSURE INDICATION

Combustion-chamber indication is standard procedure in low-temperature testing. Here, piezo pressure sensors are used for measuring cylinder pressures in high time resolution to form cycles of 0 to 720 °CA. These are analyzed statistically and thermodynamically for each specific cylinder with the aim, for example, of ascertaining the rise in pressure and the energy-conversion points. The Indicar indication system developed by IAV performs this computation in real time and supports the CAN protocol for data transfer. These two options provide the capability of merging results with values measured from the engine management system in INCA and in a file using the same time base. In this way, the combustion parameters can be integrated into the automatic test evaluation process and compared directly in the detailed analysis of engine management variables.

This is illustrated, ❹, using the example of cold idle. Control unit parameters (engine speed, injected fuel quantity) and indication parameters (pressure rise, 50 % energy conversion) are presented in context without post-process after the measurement. In the cold-idle cycles, with its high time resolution, it is possible to infer the cause of pressure peaks that result in harsh combustion noise. As a consequence of misfires in cylinder 3 and 4 that are detected with the help of the 50 % energy conversion point, engine speed falls below the desired idle speed. The idle controller responds to this by increasing the injection rate which produces a sharp rise in pressure in cylinder 1 during combustion. Looking at the two subsequent local inject-rate peaks and the associated rises in pressure, their correlation becomes clear. Superimposing the relevant acoustic recording over the indication data has shown that pressure rises in excess of 12 bar/°CA are clearly audible as “backfires”.

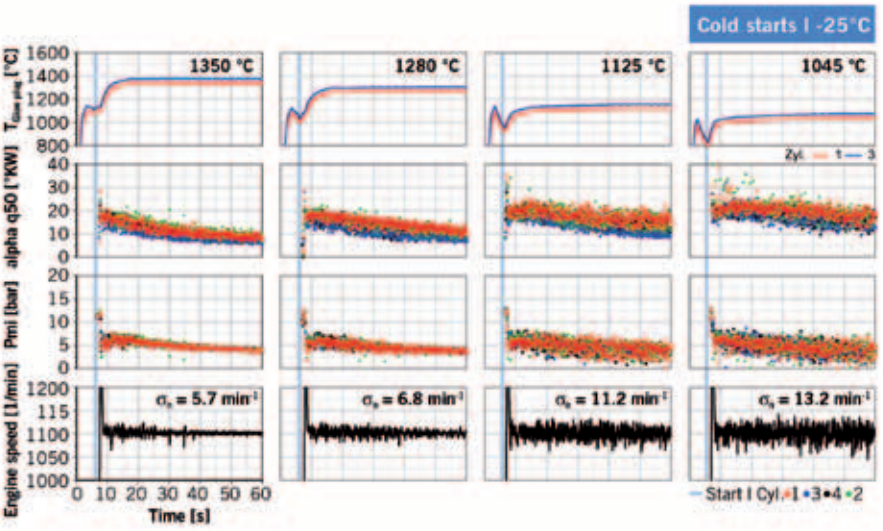

❺ Influence of glow temperature on combustion stability

GLOW TEMPERATURE AS CALIBRATION PARAMETER

The positive influence of high glow temperatures on combustion stability and the desire for short heating-up times are the reasons for advancing glow systems. The third generation uses ceramic plugs, the activation of which provides a new degree of freedom in diesel calibration. They can be used for purposes that range from assisting cold starting to reducing emissions. This is where the various temperature requirement profiles must be seen in relation to glow-plug life and energy requirement [3]. Hence, it is worthwhile knowing the influence of glow temperature from the aspect of optimizing glow strategy.

To this end, IAV GmbH has developed a test bench in which a pyrometer measures the temperature at the tip of the glow plug with pinpoint accuracy (cover picture). A computer-aided unit takes care of recording the data measured as well as supplying power to the glow plug. The latter is given in the form of an analog or PWM signal, and can, for example, be imported from a previously measured real-life cold start. The extent to which the temperature measured reflects reality depends on how accurately the glow-plug tip's degree of emission is known and on how precisely the ambient conditions are reproduced. Simulating gas exchange is a challenge that must still be overcome.

In a measurement series, the diagram, ❺, shows the influence of glow temperature on combustion stability during cold idle. For a four-cylinder engine from the 2 l category meeting Euro 5 with a compression ratio of 16, glow-plug activation was varied and sampled at 2 kHz for generating the PWM parameters in the post-process. Using these as input variables, temperature curves can be allocated to the different power output levels on the described glow-plug test bench.

The (T_{GSK}) temperature curves presented are divided up into the four phases: heating up (pushing), preheating, heating during engine start and postheating, with the level of power supplied being reduced in the preheating and postheating phase. Lower glow temperatures during the starting cycle resulted in a continuous deterioration in starting times. In the postheating phase, a mean temperature level of 1350 °C set in after activating the generator. This was lowered to 1045 °C in further starts. The resultant delay in combustion by up to 5° CA is shown by the 50 % energy-conversion point (alpha q50). Its increasing scatter to the point of misfiring (indicated mean cylinder pressure Pmi = 0) is manifest as higher engine speed fluctuation at idle.

Using the example of cylinders 1 and 3, the graph also shows the temperature scatter among glow plugs of the same type (approximately 35 K), this being reflected in a slight shift in the main centers of heat release. As an alternative to measurement glow plugs with thermocouples, this glow-plug test bench can therefore also be used for determining tolerance patterns and their influence on combustion.

SUMMARY

Reducing conditioning time was able to increase measuring frequency in cold-start testing. The use of automation software enhances the reproducibility of testing and improves analysis of the volume of data that grows as the number of tests increases. As a result, development time can be reduced or used more efficiently. These methods will be extended further in vehicle measurements. Determining glow temperature as an additional calibration tool provides potential for optimizing low-temperature calibration, with the particular focus being on the actuation profile of ceramic glow plugs.

REFERENCES

[1] Graf, M.: Diesel Kaltlauf. Aachen, Rheinisch-Westfälische Technische Hochschule, FVV Final Report, Vol. 920-2010

[2] Lewis, A; Brace, C. J.; Cox, A.: The Effect of Forced Cool Down on Cold Start Test Repeatability. University of Bath, SAE Paper 2009-01-1976

[3] Ketteler, H. B.; Ernst, S.; Dressler, W.: Vom Kaltstarthilfsmittel zum adaptiven Glühsystem. In: MTZ 69 (2008), No. 7-8, pp. 592-596

IMPRINT

MTZ

WORLDWIDE

www.MTZonline.com

Founded 1939 by Prof. Dr.-Ing. E. h. Heinrich Buschmann and
Dr.-Ing. E. h. Prosper L'Orange

Organ of the Fachverband Motoren und Systeme im VDMA, Verband Deutscher Maschinen- und Anlagenbau e.V., Frankfurt/Main, for the areas combustion engines and gas turbines
Organ of the Forschungsvereinigung Verbrennungskraftmaschinen e.V. (FVV)
Organ of the Wissenschaftliche Gesellschaft für Kraftfahrzeug- und Motorentechnik e.V. (WKM)
Organ of the Österreichischer Verein für Kraftfahrzeugtechnik (ÖVK)
Cooperation with the STG, Schiffbautechnische Gesellschaft e.V., Hamburg, in the area of ship drives by combustion engine

01 I 2012 _ January 2012 _ Volume 73
Springer Vieweg I Springer Fachmedien Wiesbaden GmbH
P. O. Box 15 46 · 65173 Wiesbaden · Germany I Abraham-Lincoln-Straße 46 · 65189 Wiesbaden · Germany
Amtsgericht Wiesbaden, HRB 9754, USt-IdNr. DE811148419

Managing Directors Dr. Ralf Birkelbach (Chairman), Armin Gross, Albrecht Schirmacher I **Director Advertising** Armin Gross
Director Marketing + Individual Sales Rolf-Günther Hobbeling I **Director Production** Christian Staral

EDITORS-IN-CHARGE
Dr. Johannes Liebl, Wolfgang Siebenpfeiffer

EDITORIAL STAFF

EDITOR-IN-CHIEF
Johannes Winterhagen (win)
phone +49 611 7878-342 · fax +49 611 7878-462
johannes.winterhagen@springer.com

VICE EDITOR-IN-CHIEF
Ruben Danisch (rd)
phone +49 611 7878-393 · fax +49 611 7878-462
ruben.danisch@springer.com

CHIEF-ON-DUTY
Kirsten Beckmann M. A. (kb)
phone +49 611 7878-343 · fax +49 611 7878-462
kirsten.beckmann@springer.com

SECTIONS
Electrics, Electronics
Markus Schöttle (scho)
phone +49 611 7878-257 · fax +49 611 7878-462
markus.schoettle@springer.com
Engine
Ruben Danisch (rd)
phone +49 611 7878-393 · fax +49 611 7878-462
ruben.danisch@springer.com
Production, Materials
Stefan Schlott (hlo)
phone +49 8726 9675972
Redaktion_Schlott@gmx.net
Service, Event Calendar
Martina Schraad (mas)
phone +49 611 7878-276 · fax +49 611 7878-462
martina.schraad@springer.com
Research, Transmission
Dipl.-Ing. Michael Reichenbach (rei)
phone +49 611 7878-341 · fax +49 611 7878-462
michael.reichenbach@springer.com
Dipl.-Ing. (FH) Moritz-York von Hohenthal (mvh)
phone +49 611 7878-278 · fax +49 611 7878-462
moritz.von.hohenthal@springer.com

PERMANENT CONTRIBUTORS
Richard Backhaus (rb), Andreas Burkert (ab), Prof. Dr.-Ing. Stefan Breuer (sb), Dipl.-Ing. (FH) Andreas Fuchs (fu), Jürgen Grandel (gl), Ulrich Knorra (kno), Prof. Dr.-Ing. Fred Schäfer (fs), Roland Schedel (rs)

ENGLISH LANGUAGE CONSULTANT
Paul Willin (pw)

ONLINE I ELECTRONIC MEDIA
Managing Editor
Gernot Goppelt (gg)
phone +49 611 7878-121 · fax +49 611 7878-462
gernot.goppelt@springer.com

Editorial Staff
Caterina Schröder (cs)
phone +49 611 7878-190 · fax +49 611 7878-462
caterina.schroeder@springer.com

Katrin Pudenz M. A. (pu)
phone +49 6172 301-288 · fax +49 6172 301-299
redaktion@kpz-publishing.com

SPECIAL PROJECTS
Managing Editor
Markus Bereszewski (mb)
phone +49 611 7878-122 · fax +49 611 7878-462
markus.bereszewski@springer.com

Editorial Staff
Christiane Brünglinghaus (chb)
phone +49 611 7878-136 · fax +49 611 7878-462
christiane.bruenglinghaus@springer.com

ASSISTANCE
Christiane Imhof
phone +49 611 7878-154 · fax +49 611 7878-462
christiane.imhof@springer.com

Marlena Strugala
phone +49 611 7878-180 · fax +49 611 7878-462
marlena.strugala@springer.com

ADDRESS
Abraham-Lincoln-Straße 46 · 65189 Wiesbaden
P. O. Box 1546 · 65173 Wiesbaden, Germany
redaktion@ATZonline.de

MARKETING I OFFPRINTS

PRODUCT MANAGEMENT AUTOMOTIVE MEDIA
Sabrina Brokopp
phone +49 611 7878-192 · fax +49 611 7878-407
sabrina.brokopp@springer.com

OFFPRINTS
Martin Leopold
phone +49 2642 9075-96 · fax +49 2642 9075-97
leopold@medien-kontor.de

ADVERTISING

HEAD OF SALES MANAGEMENT
Britta Dolch
phone +49 611 7878-323 · fax +49 611 7878-140
britta.dolch@best-ad-media.de

KEY ACCOUNT MANAGEMENT
Rouwen Bastian
phone +49 611 7878-399 · fax +49 611 7878-140
rouwen.bastian@best-ad-media.de

SALES MANAGEMENT
Volker Hesedenz
phone +49 611 7878-269 · fax +49 611 7878-140
volker.hesedenz@best-ad-media.de

MEDIA SALES
Frank Nagel
phone +49 611 7878-395 · fax +49 611 7878-140
frank.nagel@best-ad-media.de

DISPLAY AD MANAGER
Petra Steffen-Munsberg
phone +49 611 7878-164 · fax +49 611 7878-443
petra.steffen-munsberg@best-ad-media.de

AD PRICES
Advertising ratecard from October 2011

PRODUCTION I LAYOUT
Heiko Köllner
phone +49 611 7878-177 · fax +49 611 7878-464
heiko.koellner@springer.com

YOUR HOTLINE TO MTZ

Editorial Staff
☎ +49 611 7878-393
Customer Service
☎ +49 6221 345-4303
Advertising
☎ +49 611 7878-395

SUBSCRIPTIONS
Springer Customer Service Center GmbH
Haberstraße 7 • 69126 Heidelberg, Germany
phone +49 6221 345-4303 • fax +49 6221 345-4229
Monday to Friday, 8 a.m. to 6 p.m.
springervieweg-service@springer.com

SUBSCRIPTION CONDITIONS
The eMagazine appears 11 times a year at an annual subscription rate 199 € for private persons and 299 € for companies. Special rate for students on proof of status in the form of current registration certificate 98 €. Special rate for VDI/ÖVK members on proof of status in the form of current member certificate 172 €. Special rate for studying VDI members on proof of status in the form of current registration and member certificate 71 €. Annual subscription rate for combination MTZworldwide (eMagazine) and MTZ (print) 398 €. All prices include VAT at 7%. Every subscription comes with access to the ATZonline archive. However, access is only available for the individual subscription holder. To obtain access for your entire company/library/organisation, please contact Rüdiger Schwenk (ruediger.schwenk@springer.com or phone +49 611 7878-357). The subscription can be cancelled in written form at any time with effect from the next available issue.

HINTS FOR AUTHORS
All manuscripts should be sent directly to the editors. By submitting photographs and drawings the sender releases the publishers from claims by third parties. Only works not yet published in Germany or abroad can generally be accepted for publication. The manuscripts must not be offered for publication to other journals simultaneously. In accepting the manuscript the publisher acquires the right to produce royalty-free offprints. The journal and all articles and figures are protected by copyright. Any utilisation beyond the strict limits of the copyright law without permission of the publisher is illegal. This applies particularly to duplications, translations, microfilming and storage and processing in electronic systems.

NOISE ABSORPTION CLOSE TO THE ENGINE WITH POSITIVE THERMAL EFFECTS

Effective high-temperature insulation systems reduce noise emissions, increase the hot gas temperature in the diesel exhaust system by up to 10 % and reduce the surface temperatures of the insulated components from 850 to 400 °C in the case of diesel engines. Since September 2011, BMW has been using special insulation systems developed by Isolite for the acoustic encapsulation of diesel particulate filters.

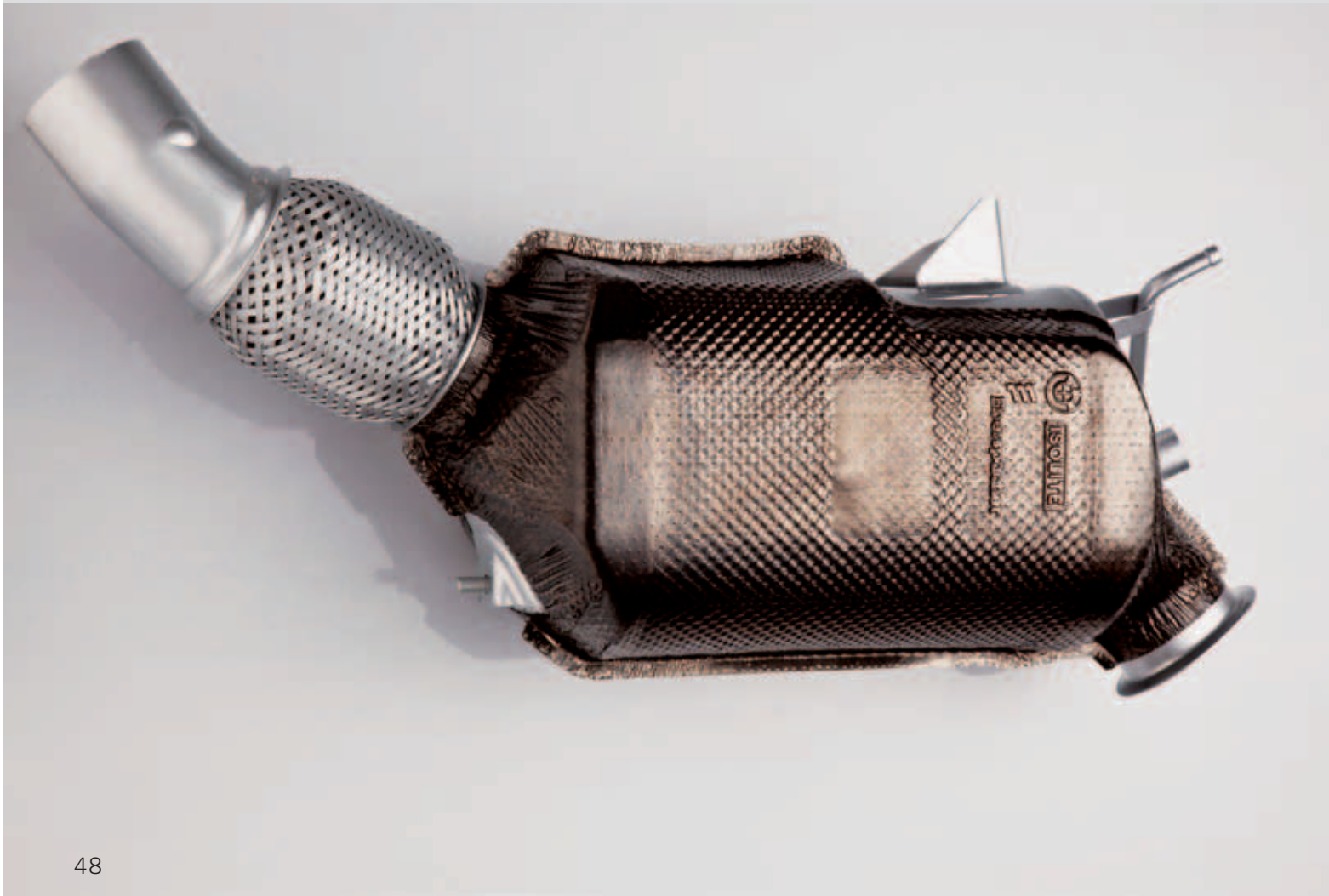

AUTHORS

MATTHIAS KROLL
is Director and Head of Engineering, Development and Sales at Isolite Automotive GmbH in Ludwigshafen (Germany).

GERO SEYDLER
is Sales Manager and works at the Team Engineering at Isolite Automotive GmbH in Ludwigshafen (Germany).

REQUIREMENTS

The demands of automotive customers for comfort and the demands of legislators with regard to noise emissions are on the increase. Against this backdrop, components besides the weight which further reduce the noise emissions of petrol and diesel engines are becoming more and more important. The acoustic and thermal high-temperature insulation systems from Isolite described in this article do not only reduce the noise emissions – they also reduce the temperature in the engine compartment and additionally provide for the increase in the temperature of the hot gases aimed for in diesel vehicles.

BENEFITS OF HIGH-TEMPERATURE INSULATION SYSTEMS

Whereas the engines belonging to modern automobile generations are already encapsulated to a high degree and thus soundproofed, a search for suitable insulation materials for exhaust gas systems is still going on in many cases. One of the reasons for this are the high temperatures arising at the components containing hot gases – especially in the case of diesel engines. Only a few noise-absorbing materials are suitable for this high-temperature range. Nevertheless, the benefits of the relevant insulation measures are undisputed. For example, BMW uses insulation systems for the acoustic encapsulation of the particle filter (DPF) in its diesel engines [1]. According to the Munich automotive manufacturer, this ensures a high perceivable reduction of the noise level inside and outside of the vehicle. Also, the new encapsulation of the DPF has not only an acoustic insulation effect but a thermal insulation effect too. An encapsulated particle filter reaches its optimum operating temperature more rapidly after a cold start. Studies conducted at Isolite Automotive GmbH have shown that the temperature in the hot gas system is increased by up to 10 % as a result of the high-temperature insulation systems developed by the Ludwigshafen manufacturer. At the same time, the surface temperature of the component is reduced from 850 to 400 °C in the case of diesel engines. Thus, in the current Audi Q7 with its 3.0-l TDI engine, a suitable Isolite thermal insulation of the exhaust system led to a considerable reduction in fuel consumption while simultaneously reducing the NO_x emissions by 15 %.

DIRECT INSULATION

To optimize the acoustic properties the concept of direct insulation of components containing exhaust gases is recommended [2]. According to this concept, the insulation material is directly applied to the component in a permanent way, allowing a high thermal and acoustic efficiency to be achieved. However, the changes in the thermal flow and the loss of the option of ventilating encapsulated components lead to new geometrical and thermomechanical challenges. It is for example necessary to precisely observe the specific effect on the temperatures of the individual components. If these requirements are taken into account, however, it is possible to design an encapsulation which is tailor-made for a certain vehicle. In this way, we can generate a thermal insulation effect which achieves the desired temperature reduction in the engine compartment as well as the intended temperature increase in the hot gas system. In addition, the emission of airborne sound is reduced considerably as a result of the mechanical properties of these direct insulation concepts. It is also possible to design the surface of the insulation systems in such a way that it provides an additional absorption surface in the engine compartment. As a result, the insulation element used in the four-cylinder diesel engine from BMW allows synergies in the fields of thermics and acoustics. At the same time, it reduces the weight of the vehicle as it integrates several functions in one insulation component.

STRUCTURAL PROPERTIES

The high-temperature insulation systems consist of a combination of a temperature-resistant, sound-absorbing corpus with a highly heat-resistant, sound-absorbing and porous/perforated liner. In this composition, the acoustic absorption behaviour of the insulation systems known as Isolite-Akustop and Isolite-Akuflex have improved considerably in comparison with the corpus on its own. At the same time, the thermal radiation is reduced further, a higher self-insulation of the material is achieved, thermal stresses are reduced and the operational stability of the system under load is

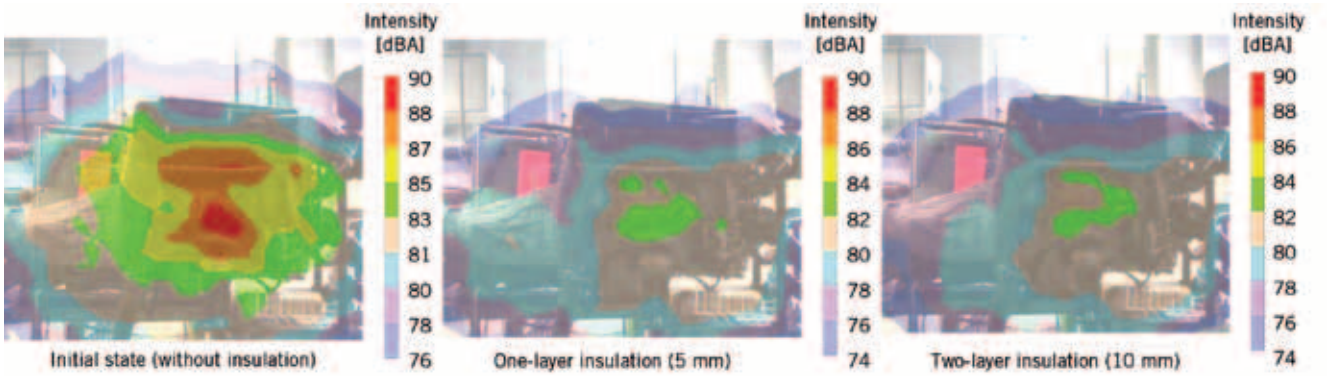

❶ Acoustical measurements on the motor outlet side of a series engine

increased. The sound-absorbing properties of the insulation system are illustrated in ❶, which shows the acoustic measurement at the outlet side of a series engine in which the outlet manifold has been equipped with various different insulations. It is soon obvious that a significant noise reduction is achieved at an insulation thickness of as low as 5 mm. This reduces peak values of 90 dBA to 84 dBA. A further reduction in sound emissions is achieved at an insulation thickness of 10 mm. The results of measurement shown in ❷ demonstrate that the sound pressure can be reduced considerably over virtually the entire frequency range above the 1000 Hz limit by using high-temperature insulation systems. Worthy of note here is the fact that the two-layer insulation (10 mm) only has very few advantages in comparison with one-layer insulation (5 mm). In a few frequency ranges, one-layer insulation even achieved better test results.

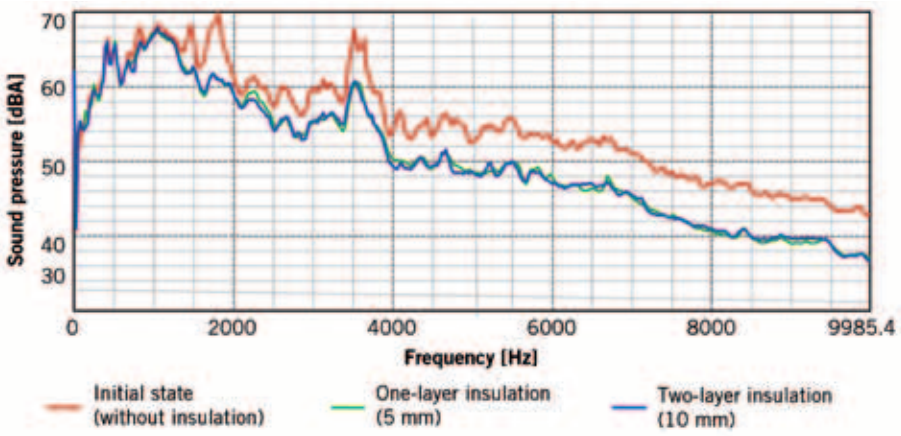

❷ Results of measurement for an insulated outlet manifold

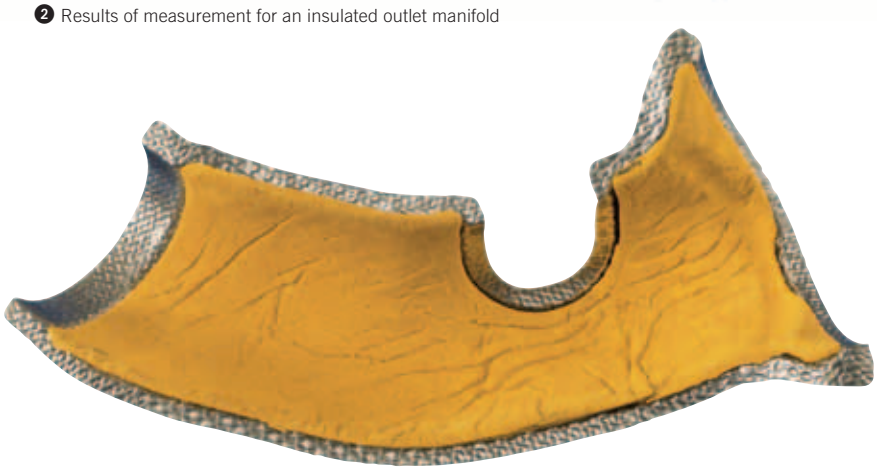

❸ REF-ISO fibre skins with a special pigment coating for improved thermal insulation characteristics

CORPUS

The corpus consists of fibrous, high-temperature materials such as bio-soluble silicate fibres. These materials have already been used for pure thermal insulation in the past and they allow a temperature resistance of up to 1200 °C and more to be achieved. The insulation body is specially and reproducibly designed in fibre skin technology for the relevant application and directly dimensioned for the necessary parameters. It is a permanently defined component reproducible with a precision of +/- 0,25 mm in which material thicknesses of between 2 mm and 10 mm can be realized. Here are some of the properties of fibre skins from Isolite:

: non-flammable
: sound-absorbing (ISO 10534-1)
: good physical properties
: skin-friendly
: very low thermal conductivity λ (DIN 52612)
: resistant to chemicals
: high mechanical resilience
: good handling.

REF-ISO FIBRE SKINS

The fibre skin with a so-called REF-ISO coating (REF-ISO = reflection – insulation) is a technological improvement on the conventional skin, ❸. Here the thermal insulation properties are deliberately changed by mixing in pigments. The thermal absorption and thermal reflection of the material is increased again considerably by this. For example,

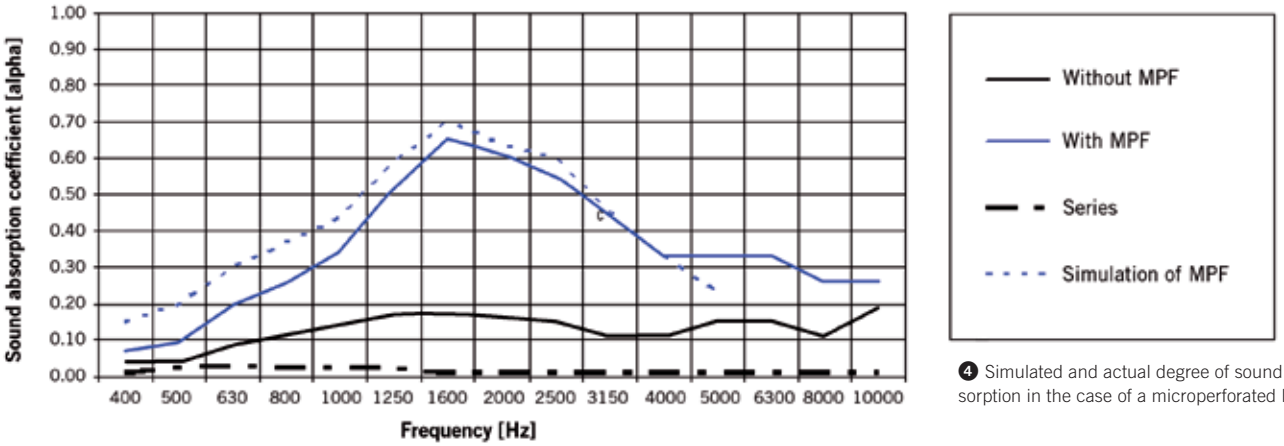

❹ Simulated and actual degree of sound absorption in the case of a microperforated liner

black colour pigments are used where the task is temperature compensation or the maintenance of a certain temperature. Yellow colour pigments are used where the heat is to be reflected back to the heat carrier. However, both types of colour pigments cause for example exhaust gases to be heated up to the necessary operating temperature for subsequent components (such as a turbocharger or catalyser) after engine start. The colour pigments used have good impermeability to UV and visible light and are chemically inert as well as being resistant to heat and ultraviolet radiation. They also have a high endurance strength, opacity, light fastness and an adequate resistance to acids and alkalis.

LINER

In order to increase the thermomechanical strength of the fibre body and reinforce its sound-absorbing properties, it is covered on one side with a liner made of a porous highly heat resisting (metal or mineral) filament tissue. If the liner is additionally quilted with the corpus, this allows the encapsulation of the corpus, which consists of fibres, and increases its strength still more. An additional improvement of the properties mentioned is the result if the corpus is equipped with a liner on the second side too. The liner consists of a heat-resistant metal – such as alloyed steel – or a mineral material. These materials can be equipped with the required porosity in a

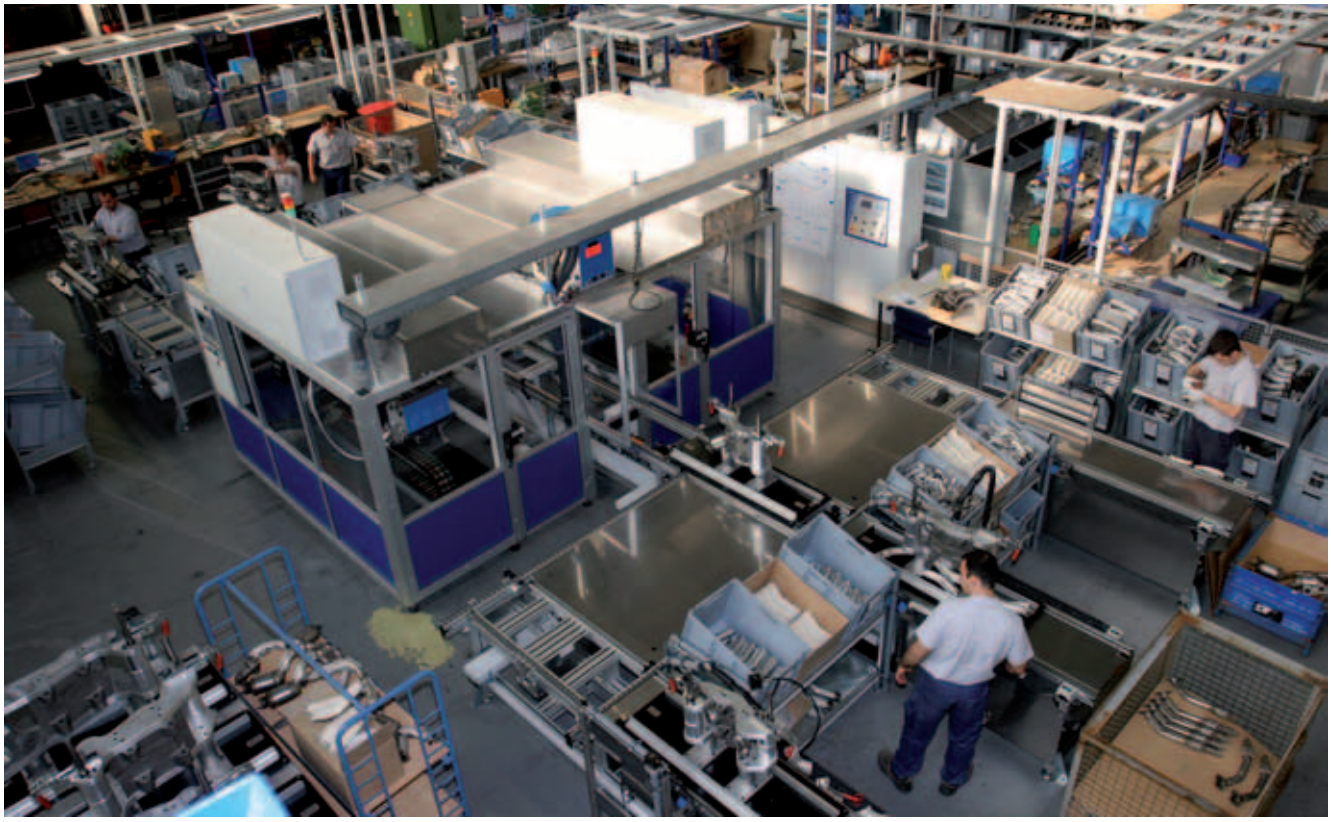

❺ A look at the production procedure

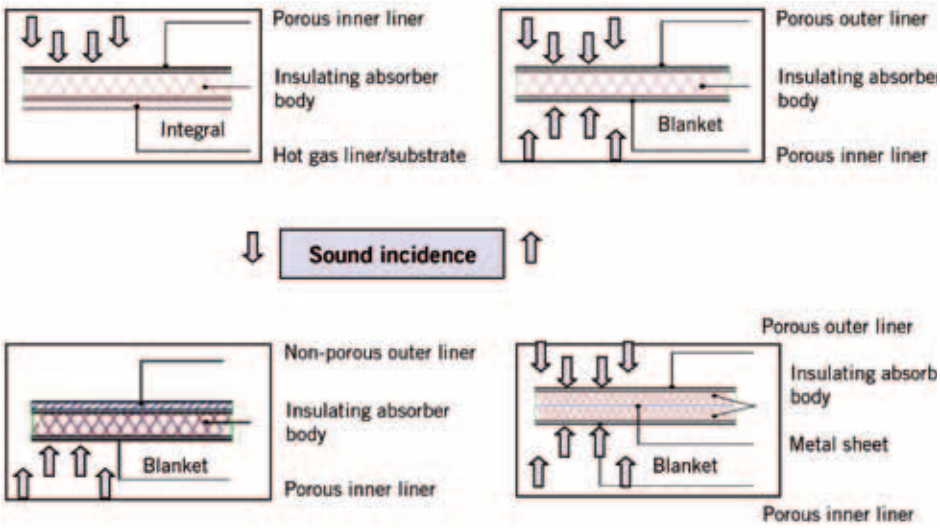

❻ Various versions of the insulation systems: integral liner and blanket

relatively problem-free way and offer the necessary heat resistance as well as the desired (and necessary) sound absorption. A special advantage is the fact that the porous liner consists of sheet metal manufactured from a sintered metal tissue.

SOUND ABSORPTION THROUGH PERFORATION

The perforation of the liners is primarily there to ensure that the sound energy is able to penetrate into the fibre insulating body. However, measurements performed in an acoustical laboratory have shown that the proportion of perforations in the liner can be designed to have a sound-absorbing effect within a defined frequency field, ❹. The degree of absorption depends on size, shape, diameter and number of holes. These parameters determine the degree of sound absorption within a certain frequency range. If the frequency changes, the parameters mentioned must be adapted. In this way, the perforation in the outer liner can be designed to fit the frequency range required for the application in question. Production technology at Isolite makes it possible to deliberately integrate certain degrees of perforation into areas in which it is necessary. For example, the margin and the vicinity of the weld remain unperforated. Instead, the proportion of perforations is increased accordingly in areas in which it makes sense. The compound of non-woven fabric and perforated sheet steel has proven its worth in numerous comparison measurements performed in the laboratory. The Kundt's tube (for measuring the non-woven fabric), the calculation model for microperforated absorbers and the calculation model for porous absorbers are used as a basis for calculation.

OUTLOOK

The high-temperature insulation systems have the advantage that automotive manufacturers can do without part of the sound insulation used in the underfloor panelling, the front wall and the front axle up to now, thus reducing the overall weight of the vehicle thanks to the effective encapsulation of the particulate filter. The acoustical and thermal high-temperature insulation systems from Isolite are still mainly being used as a permanently installed application. For this purpose, the supplier delivers the hot gas component to Isolite production, ❺. There it is equipped with a permanent insulation and then supplied to the automotive manufacturer. This causes high costs for logistics. In addition, the insulation element cannot be removed in the case of a defective hot gas component. For this reason, the method is to be increasingly replaced by the blanket design in future, ❻. These detachable and replaceable blankets have a liner on both sides, are produced at Isolite and are delivered to the assembly lines of the OEMs as ready-to-mount components. The completing equipment necessary for assembly is then also available to Isolite.

REFERENCES
[1] BMW Group Innovationstag 2011: Efficient Dynamics. BMW Medieninformation 4/2011
[2] Weber, F.: Acoustic relevance of exhaust gas components in terms of airborne noise. Lecture at the Automotive Acoustics Conference 2011, Zurich

PEER REVIEW ATZ | MTZ

PEER REVIEW PROCESS FOR RESEARCH ARTICLES IN ATZ AND MTZ

Scientific articles of universities in ATZ Automobiltechnische Zeitschrift and MTZ Motortechnische Zeitschrift are subject to a proofing method, the so-called peer review process. Articles accepted by the editors are reviewed by experts from research and industry before publication. For the reader, the peer review process further enhances the quality of the magazines' content on a national and international level. For authors in the institutes, it provides a scientifically recognised publication platform.

In the ATZ | MTZ Peer Review Process, once the editors has received an article, it is reviewed by two experts from the Advisory Board. If these experts do not reach a unanimous agreement, a member of the Steering Committee acts as an arbitrator. Following the experts' recommended corrections and subsequent editing by the author, the article is accepted.

In 2008, the peer review process utilized by ATZ and MTZ was presented by the WKM (Wissenschaftliche Gesellschaft für Kraftfahrzeug- und Motorentechnik e. V. / German Professional Association for Automotive and Motor Engineering) to the DFG (Deutsche Forschungsgemeinschaft / German Research Foundation) for official recognition.

ONLINE OIL DILUTION MEASUREMENT AT GASOLINE ENGINES

AUTHORS

DIPL.-ING. (FH) CHRISTINA ARTMANN, M.SC.
is Scientific Assistant in the Laboratory for Combustion Engines and Emission Control at the University of Applied Sciences Regensburg (Germany).

PROF. DR.-ING. HANS-PETER RABL
is Head of the Laboratory for Combustion Engines and Emission Control at the University of Applied Sciences Regensburg (Germany).

PROF. DR.-ING. MARTIN FAULSTICH
is Head of the Institute of Resource and Energy Technology at the Technical University of Munich and Managing Director of the Science Center Straubing (Germany).

Due to the increasing usage of fuels containing ethanol in combustion engines one important issue at the development of new combustion engines is the consideration of the influence of the new fuels on the engine operation and durability. Especially the impact of the new fuels on the engine oil is one essential topic. For the FVV project “Lube Oil Dilution with Ethanol Fuels during Cold Start Boundary Conditions” a new measurement technique for the online determination of the lube oil dilution at gasoline engines has been developed in the Laboratory for Combustion Engines and Emission Control at the University of Applied Sciences Regensburg.

THE SEAL OF APPROVAL FOR SCIENTIFIC ARTICLES IN MTZ.
MTZ PEER REVIEW
RECEIVED 2011-07-20
REVIEWED 2011-08-26
ACCEPTED 2011-10-03
REVIEWED BY EXPERTS FROM RESEARCH AND INDUSTRY.

1 INTRODUCTION
2 BASIC ANALYSIS
3 EXPERIMENTAL SETUP
4 EVALUATION OF THE MEASUREMENT SIGNALS
5 EXPERIMENTAL PROCEDURE
6 SUMMARY AND OUTLOOK

1 INTRODUCTION

In April 2009 the European Parliament and Council enacted the "Renewable Energy Directive" (2009/28/EG) that regulates an increase of the rate of renewable energy up to 20 % of the total final energy consumption in all EU member states. This enactment also affects the development of modern combustion engines because the principle schedules especially for the transport sector a minimum rate of renewable energy of 10 % [1].

In Germany the implementation of this directive is carried out by the German Federal Government through the "Biofuel-Sustainability Regulation" from 20.09.2009 and results in an increasing addition of renewable fuels to the conventional fuels [2]. Thus Super E10 has been introduced in Germany in February 2011 as a new fuel that contains up to 10 % biogenic ethanol fuel. The new fuel has been seen very critically by the public and the fear of engine damage prevented lots of people from using the new, cheaper fuel.

Previous findings show that an increasing percentage of ethanol in fuel can affect the engine in several ways. For example it can damage fuel carrying parts or lead to an increased ware due to a faster lubricant aging [3, 4]. Also higher fuel input in the engine oil can appear which reduces the lubrication characteristic of the oil and thus leads to an insufficient lubrication and a damage of the engine. Compared to regular gasoline ethanol has a higher evaporation enthalpy and a lower vapor pressure and therefore fuels containing a higher percentage of ethanol have worse preconditions for the mixture formation which gains significance particularly during cold start and warm up operation. Thereby especially during these operation points the potential of increased fuel input in the engine oil exists [3, 5].

At the development of new gasoline engines it is therefore necessary to consider the ethanol compatibility of the engines. In this process the knowledge of the amount of fuel in the engine oil is very important in order to determine the fuel in oil sorption and desorption. One conventional method for the measurement of the oil dilution is the offline analysis of the oil samples. Here, oil samples are taken from the engine and analyzed by means of gas chromatography in chemical laboratories. This has on the one hand the disadvantage that the required sample volume allows only a limited number of taken samples without influencing the oil balance of the engine and on the other hand the analysis of the samples takes a rather long time.

The new developed method permits online a quantitative determination of the sorption and desorption of low boiling fuel components in and out of the engine oil without influencing the oil balance of the engine significantly. The oil samples are analyzed by a mass spectrometer in order to offer a fast and specific measurement of the single hydrocarbon molecules. So particularly transient engine operation points like engine start and warm up procedures can be evaluated.

2 BASIC ANALYSIS

For the realization of the online measurement technique basic analysis are necessary to investigate the applicable analyzing opportunities for the fuel components in the oil sample by means of a mass spectrometer and the required physical preparation of the oil sample for the analysis are examined.

2.1 SELECTION OF THE TARGET COMPONENTS

The analysis of the fuel in oil sorption process is done by measuring single hydrocarbon molecules representing the fuel. For this hydrocarbon molecules are selected that are contained in significant quantities in the fuel and in the oil only in trace amounts. In addition molecules with different physical properties are to be considered because these are determining the desorption behavior of the fuel components from the engine oil.

For the selection of the target components the pure fluids gasoline and oil are examined by headspace technique with the mass spectrometer. The headspace technique allows the separation of the to be analyzed volatile molecules from the liquid sample and the transfer to gaseous phase, so that they can be analyzed with the mass spectrometer. The used mass spectrometer "Airsense" works with chemical ionization and thus enables a mostly fragment free measurement of the molecules [6]. The results of these measurements are shown in ❶. The measurement signal of the detector of the mass spectrometer is shown in "counts per second" (cps).

The mass spectrum of the analyzed fuel "Super Plus" (RON 98) shows significant differences to the engine oil 5W-30 in the mass range until 130 amu, in which the engine oil only generates minimal signal increases because the longer-chain hydrocarbons of the oil occur primarily at higher mass ranges. Most of the oil also remains liquid in the headspace vial. Based on the measured mass spectra the molecules benzene, toluene and xylene are selected for the analysis of the fuel content in the oil. For the investigation of fuels containing ethanol additionally the ethanol content is examined, ①.

The selected molecules are suitable for the investigation of the fuel content in oil because they are contained in significant amounts

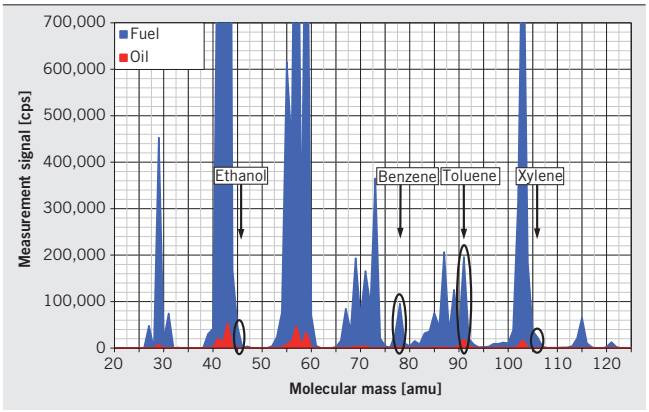

❶ Mass spectra of fuel and oil

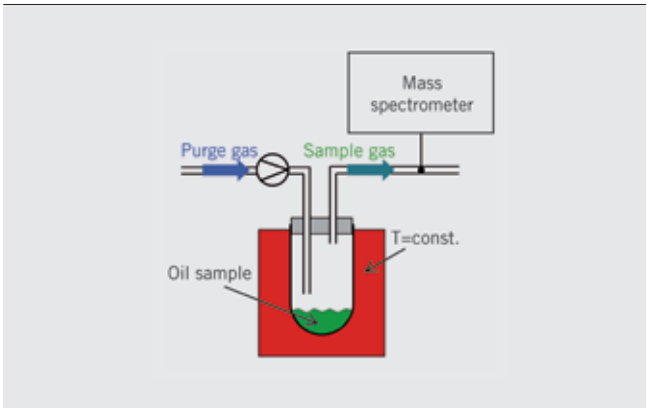

❷ Experimental setup with headspace technique

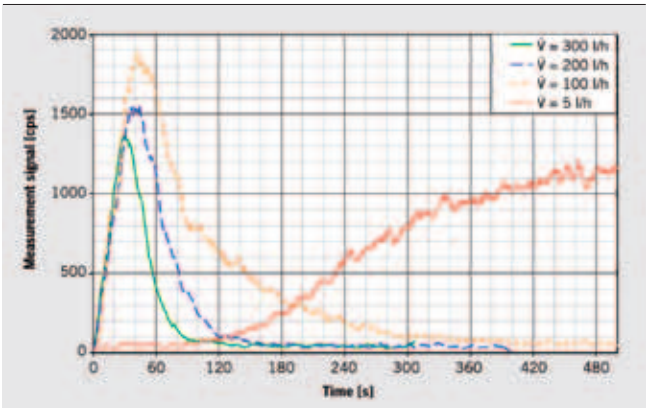

❸ Measurement of toluene with headspace for variable purge gas flow rates

in the fuel and can be definitely assigned to the fuel. Due to their different physical properties the bandwidth of the evaporation behavior of the gasoline fuel can be investigated.

2.2 ANALYSIS AND CONFIGURATION OF THE SEPARATION PROCESS

For the analysis with the mass spectrometer the selected molecules have to be separated from the liquid sample and transfered in the gaseous phase. Important for the measurement is the complete dissolution of the volatile fuel components from the oil sample. In order to investigate an applicable technique, fuel/oil-mixtures produced under laboratory conditions are examined with headspace technique at first. The used test setup is schematically shown in ❷.

In the studies the oil sample volume, the amount of fuel in the oil sample, the evaporation temperature and the purge gas flow rate are varied. ❸ shows exemplary the desorption of toluene from oil samples with constant fuel content for different purge gas flow rates. The measurements show that the duration and the yield of the desorption process of the fuel components mainly depend on the purge gas flow rate.

As for the quasi-continuous measurement of the lubrication oil dilution the measurement intervall is supposed to be as short as possible not only the complete but also the fast extraction of the volatile molecules is important. Fundamental studies of the evaporation process show that besides a high purge gas flow rate also high temperatures have a positive influence. A high flow rate promotes the complete desorption of the volatile molecules particullarly through the mixing and surface renewal of the liquid oil sample in the headspace vial.

With the headspace technique however the automated continuous exchange of the samples is unfavorable. Therefore an adapted thermo-desorption unit is designed for the measurement device, in which both the sample applicaton, the complete and fast desorption of the measured molecules as well as the deposition of the remaining liquid sample are optimized.

In the developed thermo-desorption unit, ❹, a two-phase flow is generated in a micro channel that achieves an intensive mixing of injected oil sample and purge gas and thus an optimal desorption of the volatile molecules. The sample to be analyzed is injected into the micro channel and after the desorption process the residual liquid oil is deposited before the gaseous sample is led into the mass spectrometer (MS).

To optimize the desorption process of the volatile fuel components with the thermo-desorption unit the purge gas flow rate, the oil sample volume and the temperature of the thermo-desorption unit are analyzed and adapted. The temperature is chosen so that it is higher than the boiling temperatures of the analyzed molecules.

This thermo-desorption unit is integrated into the experimental setup described below in order to measure the fuel content in the engine oil.

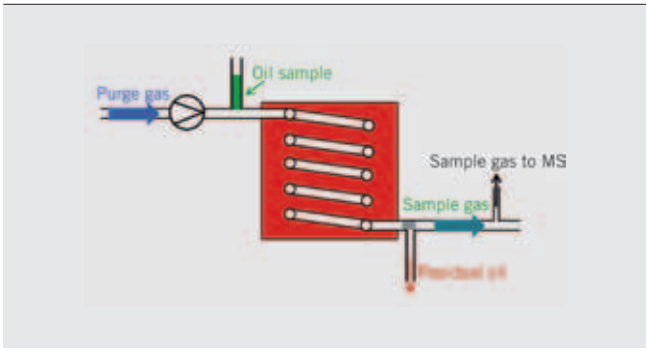

❹ Schematic setup of the thermo desorption unit

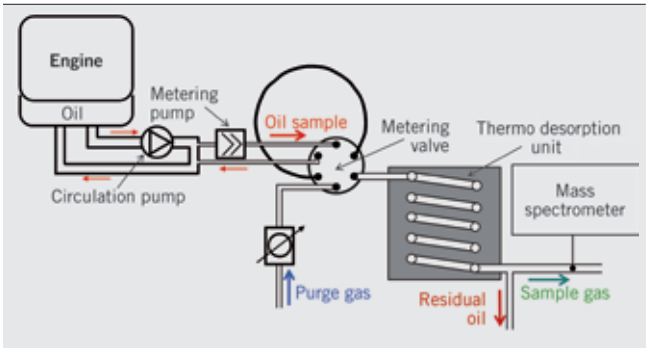

❺ Schematic experimental setup

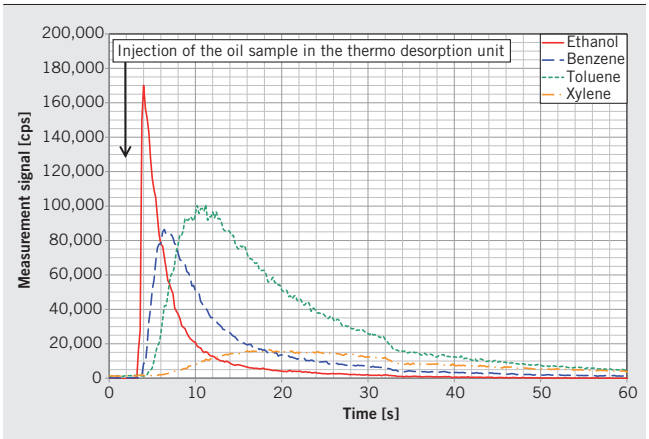

❻ Measurement signal of the oil dilution measurement

3 EXPERIMENTAL SETUP

The measurement of the oil dilution is performed with the experimental setup shown in ❺. This setup is divided into three main tasks:

- extraction of a representative oil sample from the engine
- separation of the volatile target components from the liquid sample
- determination of the concentration of the evaporated fuel components.

For the extraction of representative oil samples from the engine a circulating pump is connected to the oil pan that mixes the engine oil and feeds the following metering pump with a current oil sample. The metering pump takes the required oil volume for the analysis and pumps it through a metering valve.

In the second part of the experimental setup the oil sample is injected into the thermo-desorption unit described in section 2.2 with the metering valve and the gaseous components are fed with the purge gas into the analyzer. Simultaneously the residual liquid oil is derived separately in order to allow the performance of multiple analysis at short time intervals.

The requirement for the quantitative determination of the fuel concentration in the sample is the exact dosage of the oil sample and a constant purge gas flow rate. These are ensured by the metering pump and the metering valve for the oil sample and a mass flow controller (MFC) for the purge gas.

4 EVALUATION OF THE MEASUREMENT SIGNALS

For the online measurement of the oil dilution oil samples are taken and analyzed every 60 s. The resulting measuring signal of the mass spectrometer is shown in ❻. The desorption characteristics result from the physical properties of the molecules and the selected operating parameters of the thermo-desorption unit.

In order to calculate the fuel concentration from the measured desorption curves of the molecules the area of the measuring signal (scps = sum counts per second) is integrated. The calibration is done with calibration curves for the used fuels and engine oils. These are generated with calibration solutions of known composition. Exemplary the calibration curves for the four target components for E20 fuel are summarized in ❼. The nonlinearity of the calibration curve for ethanol results from the saturation of the detector at higher measurement signals, ⑥. The measurement signal generated by ethanol compared to the other measured molecules is higher, as ethanol is dissolved from the oil sample very fast.

The calibration curves are generated for fuel contents in the oil from 0 % up to 15 %. Thus a very large measuring range can be covered.

5 EXPERIMENTAL PROCEDURE

With the developed oil dilution measurement technique measurements on the engine test bench and with a Flex Fuel vehicle are performed in order to validate the new technique. At the engine test bench the ideal settings for the mass spectrometer and the delay time of the measurement process are examined. Subsequently the entire measurement technique is examined during cold starts with a FlexFuel vehicle.

5.1 MEASUREMENTS AT A GASOLINE ENGINE

To determine the delay time of the measurement process the measurement technique is installed at a six-cylinder gasoline engine

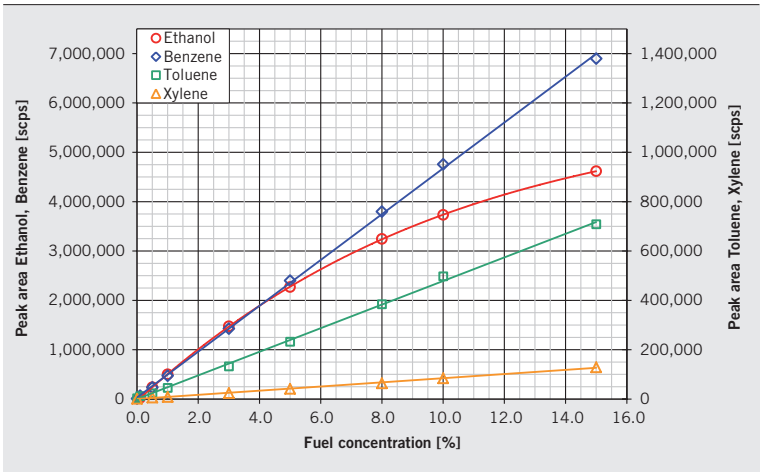

❼ Calibration curves for E20 fuel

run on "Super Plus" fuel. At idle speed fuel is added manually to the oil via the oil filler neck. ❽ shows the measurement result for this experiment.

The test results allow the determination of the delay time that occurs from the entry of the fuel into the engine and the response of the signal from the mass spectrometer and also confirm the applicability of the measurement technique at the engine.

5.2 MEASUREMENTS AT THE FLEX FUEL VEHICLE

The cold start tests are performed on a 1.6 l Flex Fuel MPI vehicle. The objective of the measurements is the determination of the fuel sorption and desorption behavior during cold start and warm-up phase and the influence of different ethanol contents of the fuel.

❾ shows the ethanol measurements for cold starts with E40 and E60 fuel. Both measurements show cold starts of the engine followed by engine warm up at idle speed. The deviation of the oil temperatures arise out of varying environmental conditions. The higher ethanol input into the engine oil during the cold start with E60 can clearly be seen.

In addition to cold starts with fuels containing varying contents of ethanol several cold starts without intermediate heating up of the engine oil are carried out. At the cold start shown in ❿ two prior cold starts with E85 were carried out without heating the engine oil over 50 °C resulting in the increased ethanol content at the beginning of the measurement. An additional ethanol input occurs during the cold start phase; during the warm up of the engine the ethanol evaporates from the oil and the ethanol content is reduced to the original value.

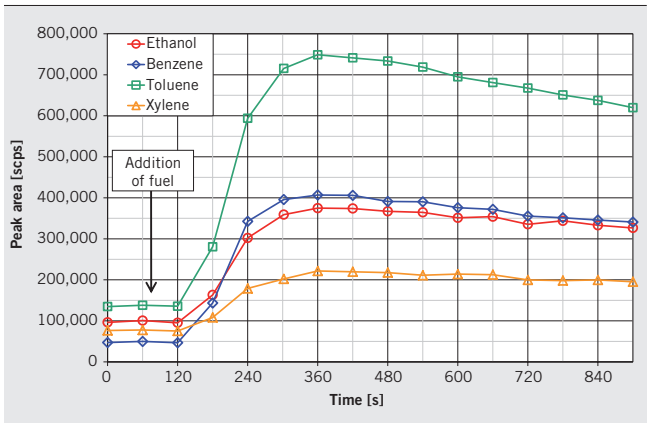

❽ Oil dilution measurement at a gasoline engine with addition of fuel at idle speed

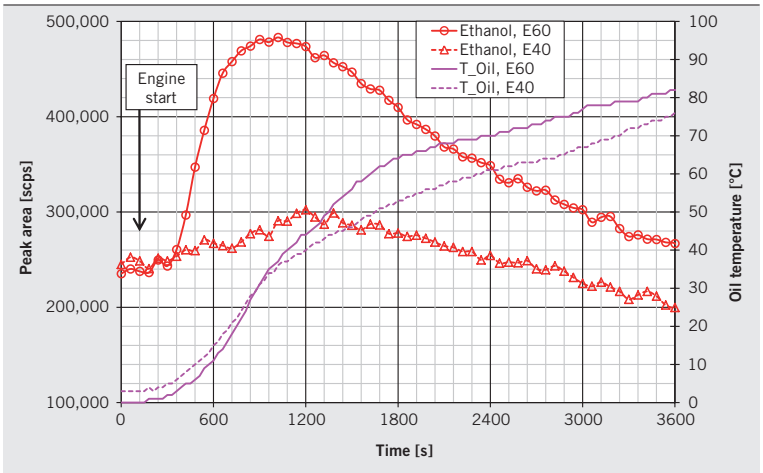

❾ Oil dilution measurement at a FlexFuel vehicle with E40 and E60 fuel

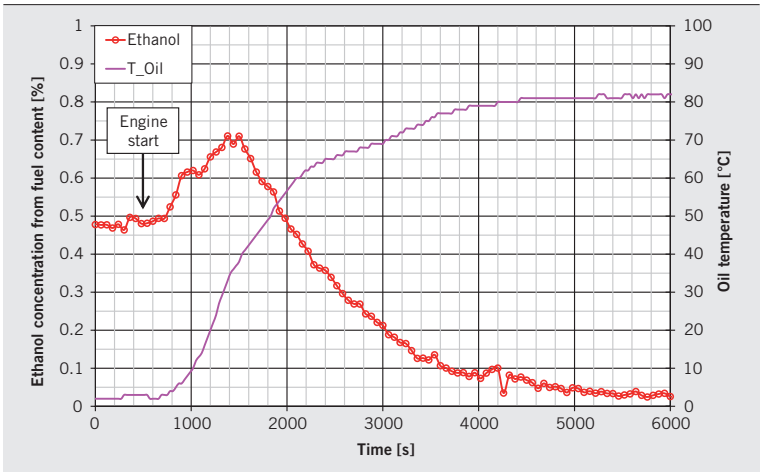

❿ Oil dilution measurement at a FlexFuel vehicle with E85

6 SUMMARY AND OUTLOOK

The FVV project "Lube Oil Dilution with Ethanol Fuels during Cold Start Boundary Conditions" is executed in collaboration of the Institute for Combustion Engines at the RWTH Aachen and the Laboratory for Combustion Engines and Emission Control at the University of Applied Sciences Regensburg. In the first part of the project the technique for the online measurement of the lube oil dilution via low boiling fuel components has been developed and built up in Regensburg.

Now, in the second part of the project the online measurement technique is used at the RWTH Aachen to study the oil dilution with different fuels and corresponding cold start calibrations.

A measurement technique is now available that allows online a fast analysis of the fuel content in engine oil both for conventional gasoline fuel as well as for ethanol containing fuels.

The existing measurement technique will now be further developed in order to realize a continuous determination of the oil dilution. Besides the analysis of fuel in the engine oil a target for the future is the integration of the determination of the water content of the oil with the measurement technique.

REFERENCES

[1] N.N.: Richtlinie 2009/28/EG zur Förderung der Nutzung von Energie aus erneuerbaren Quellen. Parlament und Rat der Europäischen Union, 23.04.2009
[2] N.N.: Verordnung über Anforderungen an eine nachhaltige Herstellung von Biokraftstoffen (Biokraftstoff-Nachhaltigkeitsverordnung – Biokraft-NachV), 30.09.2009
[3] Menrad, H.; König, A.: Alkoholkraftstoffe. Springer Verlag Wien, 1982
[4] Schwarze, H.; Brouwer, L.; Knoll, G.: Auswirkung von Ethanol E85 auf Schmierstoffalterung und Verschleiß im Ottomotor. In: MTZ 04/2010
[5] Kapus, P. E.; Fuerhapter, A.: Ethanol Direct Injection on Turbocharged SI Engines – Potential and Challenges. SAE 2007-01-1408, 2007
[6] Villinger, J.; Federer, W.: SIMS 500 – Rapid Low Energy Secondary Ion Mass Spectrometer for In-Line Analysis of Gaseous Components – Technology and Applications in Automotive Emission Testing. SAE 932017, 1993

THANKS

The authors would like to thank the "Forschungsvereinigung Verbrennungskraftmaschinen e.V." (FVV) for facilitating the research project "Lube Oil Dilution with Ethanol Fuels during Cold Start Boundary Conditions" and the working group of the project, particularly the chairman Dipl.-Ing. Eberhard Holder of the Daimler AG.
The IGF-project 16483 N/2 of the "Forschungsvereinigung Forschungskuratorium Maschinenbau e.V. – FKM", Lyonder Straße 18, 60528 Frankfurt am Main was financed by the AiF as part of the "Programm zur Förderung der industriellen Gemeinschaftsforschung und -entwicklung (IGF)" by the Federal Ministry of Economics and Technology following a decision by the German Bundestag.

PRECHAMBER IGNITION CONCEPTS FOR STATIONARY LARGE BORE GAS ENGINES

AUTHORS

DR.-ING. CHRISTOPH HEINZ worked as Scientific Assistant at the Institute of Thermodynamics at the Technical University of Munich until October 2010. Currently he works in the Department of Gas Engine Development at MTU Friedrichshafen GmbH (Germany).

DIPL.-ING. STEFAN KAMMERSTÄTTER works as Scientific Assistant at the Institute of Thermodynamics at the Technical University of Munich (Germany) since June 2008.

PROF. DR.-ING. THOMAS SATTELMAYER is Head of the Institute of Thermodynamics at the Technical University of Munich (Germany).

A testing facility for the optical investigation of ignition and combustion in large bore gas engines is described. The test rig was developed at the Institute of Thermodynamics at Technical University of Munich. Core element of the setup is an optically accessible high pressure combustion cell which can be charged, ignited, and discharged repeatedly according to the cycle times of a real engine. Until now the apparatus was used for the investigation of two different prechamber concepts.

THE SEAL OF APPROVAL FOR SCIENTIFIC ARTICLES IN MTZ.
MTZ PEER REVIEW
RECEIVED 2011-15-8
REVIEWED 2011-22-8
ACCEPTED 2011-3-10
REVIEWED BY EXPERTS FROM RESEARCH AND INDUSTRY.

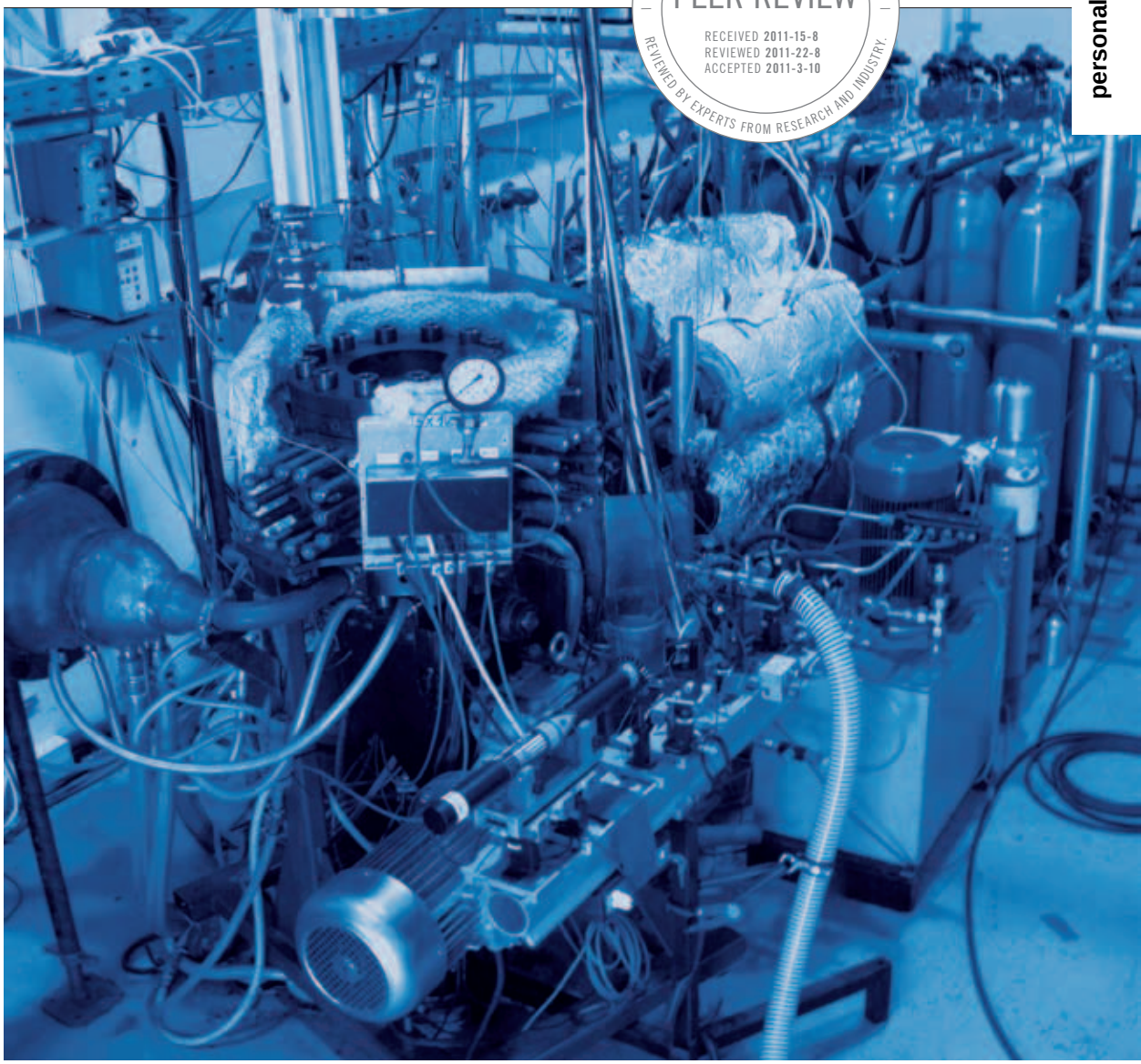

1 INTRODUCTION
2 TESTING FACILITY
3 MEASUREMENT TECHNIQUES
4 TEST PROCEDURE
5 PRECHAMBER CONCEPT
6 RESULTS
7 OPTICAL MEASUREMENTS
8 SUMMARY

1 INTRODUCTION

In the recent past the significance of the gas engine has increased significantly in the area of decentralized power supply. A well-established combustion process to obtain high power densities and efficiencies as well as low nitrogen oxide emissions is the homogeneously premixed lean combustion combined with high charging pressures. To ignite lean mixtures in the small operation range between engine-knock and misfire securely, e.g. scavenged prechambers may be used to increase ignition energy. For a better understanding of the underlying physical mechanisms of such concepts optical measurement techniques can make substantial contributions. Up to now mainly fiber-optical techniques [1] were used in the field of large engines since optically accessible engines of such dimensions are difficult to build and expensive. Improved optical access is provided by constant volume bombs (CVB). Their main disadvantages, however, are the unrealistic operating conditions compared to real engine behavior. A balance between optical accessibility and engine-like operating conditions is provided by rapid compression machines (RCM) [2, 3]. However, a drawback of RCMs is that the investigation of several consecutive cycles is not possible, which might be useful e.g. for the analysis of cycle to cycle variations. Against this background a testing facility was developed which allows for the optical investigation of a periodic sequence of up to 60 combustion cycles under engine-like conditions. In the following the test rig will be described and experimental results from a recently completed research project will be presented. The prechamber concept under investigation is based on the PGI concept from MAN Diesel & Turbo [4], which applies high pressure pilot gas injection and glow plug ignition. Currently the apparatus is used to investigate a scavenged prechamber concept with conventional spark ignition. Corresponding results can be found in Kammerstätter et al. [5].

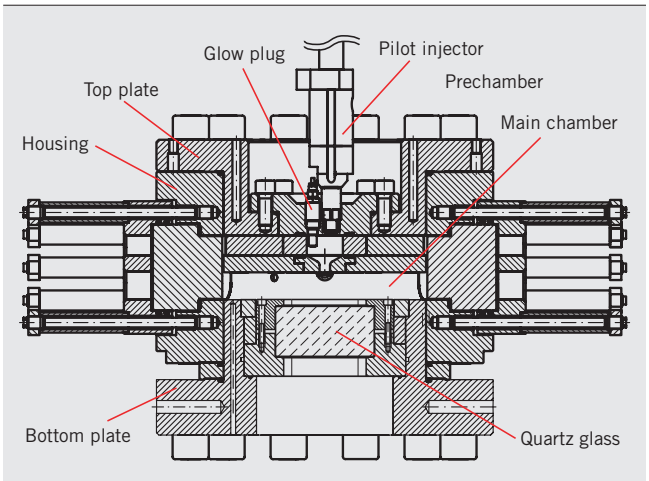

❶ Sectional view of the pressure cell with prechamber setup according to the PGI concept

2 TESTING FACILITY

The central part of the test rig is a heatable high pressure cell (T_{max} = 300 °C, p_{max} = 200 bar) whose combustion chamber can be divided into a pre- and a main chamber. The geometric setup of the main chamber (diameter D = 252 mm, height h = 25 or 35 mm) is based on an engine's combustion chamber with the piston in TDC position. The modular setup allows for an operation with different prechamber inserts as well as without prechamber. Optical access to the main chamber is possible through three side windows as well as the bottom plate. The prechamber is optically accessible via an optionally insertable quartz glass ring. The alignment of the side windows allows for the application of light-sheet-based measurement techniques as well (e. g. the Planar Laser Induced Fluorescence – PLIF). ❶ shows a sectional view of the cell with optical access through the bottom plate.

Charging and discharging of the cell are accomplished by three intake and outlet valves respectively, which are actuated by two camshafts via a chain drive (not shown in ①). The cycle times for the periodical operation were derived from a real engine's working cycle at a speed of 750 rpm, which results in a duration of 40 ms per single stroke. This leads to a period of 40 ms each for the charging and the combustion cycle. Due to the longer duration of the discharging cycle (80 ms) a pressure level close to atmospheric pressure is reached before the beginning of the subsequent charging cycle. A higher exhaust residual percentage as it arises from the increased exhaust gas back pressures in turbocharged engines cannot be realized for safety reasons. Valve overlap as another means to control the gas exchange cycle and the residual gas percentage can be accomplished by freely adjustable camshafts. However, the influence of varying exhaust residual gas levels on the process was not scope of the present work and therefore will not be discussed further.

Despite the lacking compression stroke realistic values of pressure and temperature have to be reached by the end of the charging cycle. To provide these conditions the mixture flowing into the cell has to be preconditioned externally. This is accomplished with the peripheral setup shown in ❷. Air is provided by six identical units of a pressure reservoir and an air heater. The heaters consist of electrically heatable steel liners filled with packed beds of stainless steel balls. The design of the heaters allows for a constant outlet temperature of max. T = 500 °C for a period of up to 15 s at a mean air mass flow rate of approximately 1 kg/s. To minimize heat losses all tubing downstream the gas mixer can be heated up to a temperature of T_{max} = 500 °C as well, which ensures that the mixture enters the cell at the desired preheating temperature. Thus, in the rig's design point a compression temperature of T ≈ 750 K can be reached at the end of the charging process (estimate of the charging process, see [6]). In the gas mixer the six mass flows merge and mix with the fuel gas. The hydraulically controlled gas valve [7] is opened at the same time as the inlet valves. Due to its

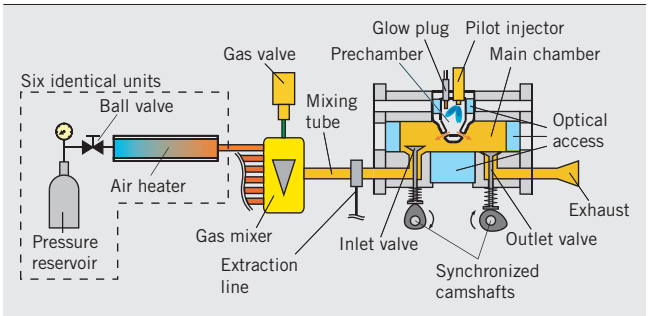

❷ Sketch of the supply system with the cell

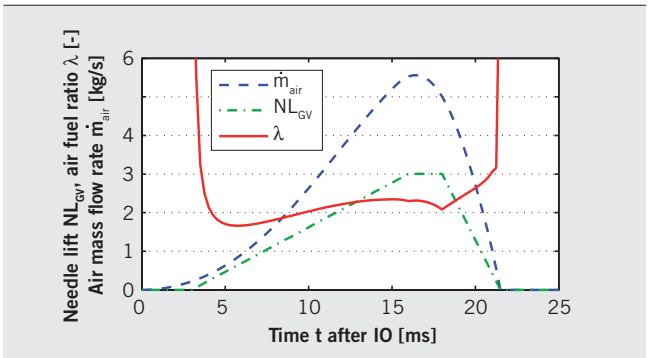

❸ Air fuel ratio λ, air mass flow rate and needle lift NL_{GV} of the gas valve during the charging process

variable needle lift it provides a gas flow rate proportional to the air flow rate. In this way a nearly constant air fuel ratio can be provided throughout the charging process, ❸. Homogenization of the mixture is enhanced by means of so called "Delta Vortex Mixers" [8] inside the gas mixing chamber. The mixers as well as the mixing tube downstream the gas mixer were designed with the help of 3D CFD simulations to provide optimum mixture homogenization. Before entering the cell, a small portion of the mixture mass flow leaves the system via an extraction line and is analyzed using an air fuel ratio metering device.

3 MEASUREMENT TECHNIQUES

Conventional measurement techniques are the pressure indication in pre- and main chamber (sampling rate f = 50 kHz) as well as the metering of fresh gas pressure and temperature in the mixing tube (f = 20 kHz). The glow plug temperature can be determined from the temperature-dependent ohmic resistance of the heating coil. A corresponding resistance-temperature characteristic was derived from previously conducted pyrometric measurements. However, a control or limitation of the glow plug temperature is not possible due to the continuously repeated heat input into the plug during each prechamber combustion cycle (a valuation of the glow plug temperature's influence on the combustion process is given in [6]). The air fuel ratio λ of the fresh mixture can be obtained from optical measurements using an infrared absorption method [6]. The technique allows for the time resolved (f = 1 kHz) determination of hydrocarbon concentration in the fresh gas which can subsequently be converted into corresponding values of air fuel ratio. For the visualization of the prechamber jets as well as the main chamber combustion a high speed camera system is available. The images of the OH*-chemiluminescence emissions shown in this article were taken at a frame rate of 8 kHz. To separate the OH*-specific spectral range around 306 nm from the background, a bandpass filter was used. For further details regarding the test rig and the employed measurement techniques the reader is referred to Mittermayer et al. [9] and Heinz [6] as well as the references therein.

4 TEST PROCEDURE

In order to illustrate the test procedure, ❹ shows a chronological sequence of the most important trigger signals. During a test the periodically repeated input trigger signals from the intake and outlet valves, i.e. "intake open" (IO), "intake closed" (IC), "outlet open" (OO) and "outlet closed" (OC) are used to actuate other time relevant events. Examples shown in ④ are the pulse-width-modulated (PWM) signals to trigger the gas injectors as well as the trigger for the camera system. The latter records a previously defined number of pictures each time an IC trigger event occurs.

❺ shows the pressure and needle lift profiles for a single cycle within an experiment. Between IO and IC fuel gas is added to the air entering the combustion cell (see ③). At IC the pilot injector is activated and initiates the prechamber combustion. During the subsequent combustion process in the main chamber the pressure profiles in pre- and main chamber are nearly identical. After OO the cycle ends with the discharge phase of the cell.

5 PRECHAMBER CONCEPT

The PGI concept from MAN Diesel & Turbo [4] works as follows: During the compression stroke lean fresh mixture from the main chamber enters the prechamber. To invoke ignition, the prechamber mixture is enriched by the injection of high pressurized fuel gas and ignited at the hot surface of a glow plug. Ignition of the main charge is accomplished by flame jets entering the main

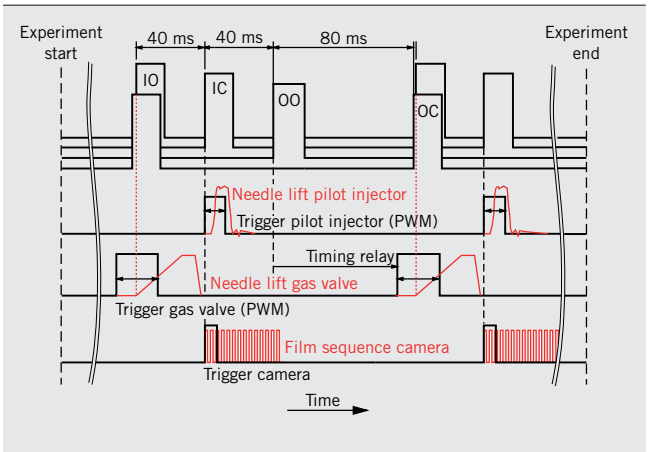

❹ Flow diagram of an experiment; black: input trigger signals from the intake and outlet valves and output signals to trigger gas injectors and camera system; red: needle lift of gas injectors and recording sequence of the camera system

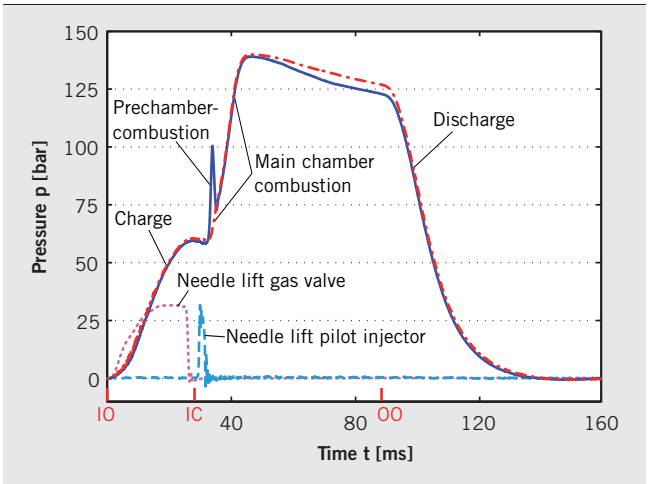

❺ Pressure profiles in prechamber (blue) and main chamber (red) together with needle lift profiles of gas valve and pilot injector for a single cycle

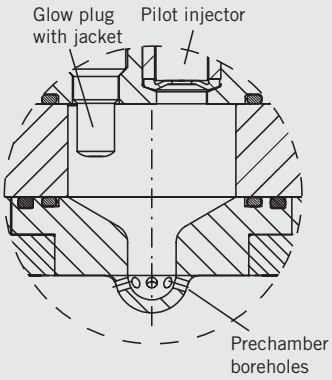

❻ Sectional view of the prechamber setup and geometry

chamber via boreholes in the prechamber tip. The original PGI prechamber geometry was modified to fit the demands of the cell experiments and is shown in ❻. Geometric variations of the prechamber setup (e.g. prechamber volume, diameter, number and alignment of the boreholes etc.) were not investigated in the present work but are currently being examined in further studies at the Institute of Thermodynamics.

6 RESULTS

The scope of the experiments on the PGI concept was the investigation of the prechamber ignition process, the injection characteristics of the flame jets as well as the ignition and combustion behavior in the main chamber. The main focus was on the influence of the fresh mixture's air fuel ratio on the phenomena mentioned above.

The air fuel ratio of the fresh mixture was varied in the range of $2.0 < \lambda < 2.6$ while the air fuel ratio of the prechamber mixture was constantly kept at $\lambda \approx 1$. The ignition behavior observed can be categorized into four operating or ignition regimes respectively.

: Misfire regime I ($\lambda \geq 2.5$)
The retarded prechamber combustion is followed by incomplete combustion in the main chamber or even by no combustion at all.

: Regular ignition regime II ($\lambda \approx 2.3...2.4$)
Prechamber combustion starts after the end of pilot injection and is followed by combustion in the main chamber. In this regime the highest fuel conversion rates can be observed.

: Transition regime III ($\lambda \approx 2.2...2.3$)
Prechamber ignition already starts during the pilot injection and is accompanied only by weak prechamber pressure peaks. Heat release in the main chamber is slightly lower than in the regular regime (II).

: Preignition regime IV ($\lambda < 2.2$)
Advanced prechamber ignition occurs before the beginning of the pilot injection. Control of the ignition timing is no longer possible.

❼ shows an overlay of the prechamber pressure profiles from regimes I to IV as well as the corresponding fuel conversion rates from main chamber combustion. In the misfire regime (I) the fresh mixture in the main chamber is too lean to be ignited by the prechamber flame jets. Due to the long delay time between pilot injection and prechamber ignition the turbulent energy introduced by the pilot gas is already largely dissipated before the start of the prechamber combustion [10]. This becomes noticeable in a reduced turbulent flame speed and accordingly low pressure rise rates. In the main chamber heavily retarded combustion establish-

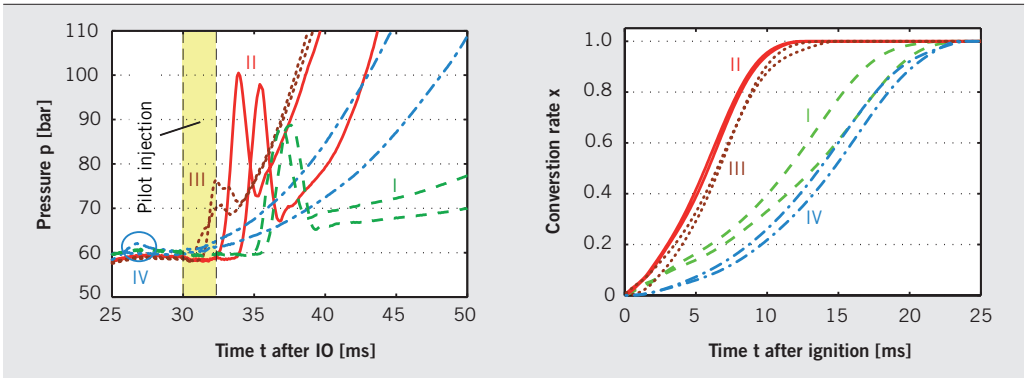

❼ Prechamber pressure profiles (left) and fuel conversion rates of main chamber combustion (right) for regimes I to IV

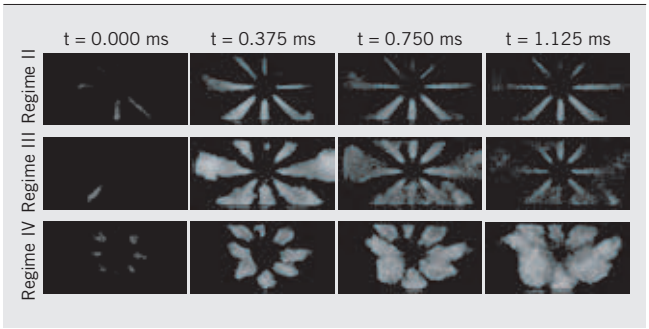

❽ OH*-recordings of the prechamber jets for regimes II to IV; the first occurrence of OH*-emissions is denoted by t = 0 ms individually for each ignition regime

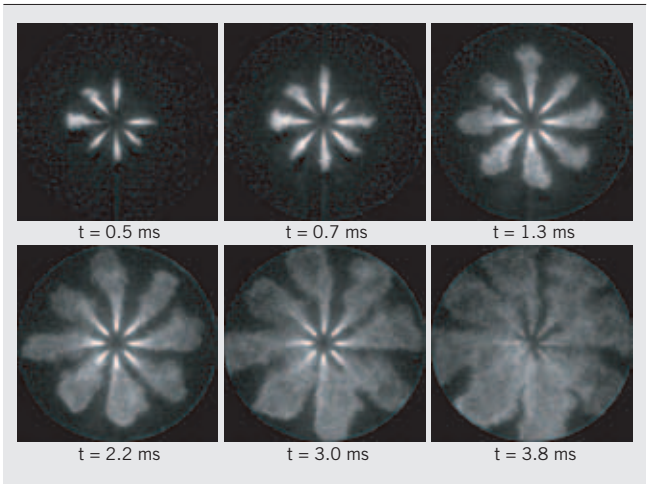

❾ OH*-chemiluminescence of the regular ignition regime with optimized optical access

es for air fuel ratios $\lambda \leq 2.5$. For a real engine it can be assumed that main chamber combustion fails completely due to the deteriorating ignition conditions during the expansion stroke after TDC.

Regular ignition (II) can be observed in the range of $\lambda \approx 2.3...2.4$. Prechamber ignition starts earlier than in regime I. The remaining turbulent energy from the pilot injection results in a more intensive prechamber combustion. Improved ignition behavior and faster fuel conversion in the main chamber is caused by the higher momentum of the prechamber flame jets.

Further reduction of air fuel ratio ($\lambda \approx 2.2...2.3$) leads into the transition regime (III). Prechamber combustion already starts before the end of the pilot injection and the prechamber pressure peaks show a significantly degraded shape. Since the pilot fuel is not completely injected yet, the global fuel composition in the prechamber is leaner than in the regular case. Additionally, strong fuel stratification with lean and rich zones is present due to the short mixing time between injection and ignition [10]. This again leads to a low burning rate and consequently to weak prechamber combustion. Despite the richer fresh gas composition compared to the regular regime, heat release in the main chamber is slower. This can be explained by the weak prechamber flame jets as well: Due to the lower jet momentum the introduction of turbulence into the main chamber decreases, which consequently results in a lower turbulent flame speed as well. Under real engine conditions this effect may not observable to the same extent since the turbulent charge motion in the pressure cell is not fully comparable to engine-like conditions. However, the flow character in the cell is advantageous for fundamental investigations, since the impact of single phenomena (e.g. the mentioned influence of flame jet turbulence) can be analyzed more precisely.

Air fuel ratios of $\lambda < 2.25$ in the fresh mixture lead into the preignition regime (IV). Since combustion in the prechamber begins even before the start of pilot injection (see marker in ⑦) the ignition timing can no longer be controlled. With further decreasing values of λ ignition occurs more and more advanced. This finally results in the uncontrolled self-ignition of the whole mixture already during the charging cycle of the cell (not shown in ⑦).

7 OPTICAL MEASUREMENTS

❽ shows the OH*-chemiluminescence of the prechamber jets for regimes II, III and IV. In the regular ignition regime (II) compact prechamber jets enter the main chamber with a high momentum. The jets break up outside the visible area of the cell. From there a flame front propagates further through the combustion chamber (not shown). In the transition regime (III) the momentum of the flame jets is lower than in the regular case due to the weaker prechamber combustion. The lower momentum results in an earlier jet break-up inside the visible area. This behavior can be seen best by looking at the jets oriented to the left and to the right respectively (t = 0.375 ms and t = 0.750 ms). In the preignition regime (IV) the turbulent-free-jet-like character of the flame jets gets lost due to the very low momentum. Ignition of the main charge does no longer begin at the tip of the jets but emerges radially from the nested flame areas around the prechamber at a rather low speed. All pictures show a non-uniform distribution of flame jet intensity over the prechamber boreholes. This is a result of the eccentric assembly of pilot injector and glow plug in the prechamber, ⑥, which causes the flames to pass earlier through the boreholes closer to the glow plug (bottom holes in ⑧) [5, 6, 10]. This effect is further enhanced by a strong charge stratification caused by the excentric injector position noted above as well as the short mixing time between gas injection and ignition [6, 10].

After initial tests the limited optical access to the main chamber, ⑧ (window size 48 mm x 102 mm), was improved significantly by changes in the combustion cell's design (combustion chamber completely visible). As an example ❾ contains a film sequence showing the prechamber flame jets as well as the main chamber combustion for the regular ignition regime. A first break-up at the jets' tips can be observed about halfway between the combustion chamber's center and walls (t = 0.5 und 0.7 ms). After the beginning of the main chamber combustion (t = 1.3 ms) the flames propagate primarily in radial direction. Further flame propagation through the combustion chamber only happens after the flames' impingement on the chamber walls (3.8 ms).

8 SUMMARY

A new test rig was developed at the Institute of Thermodynamics at Technical University of Munich which allows for the optical investigation of ignition concepts of large bore gas engines. Due to its operation characteristics the test rig can be categorized between con-

ventional constant volume bombs and experimental engines. While real engine-like processes cannot exactly be simulated (e.g. compression and expansion), the periodically repeatable chargeability of the combustion cell turns out to be a valuable improvement over simple bomb experiments. The compromise with respect to deviations from real engine performance seems to be acceptable or even advantageous for fundamental research since interfering effects may be isolated and investigated separately. After improvements of the initial cell and periphery design high operational reliability of the rig was obtained. For a prechamber concept similar to MAN Diesel & Turbo's PGI concept a strong dependency of ignition behavior on the air fuel ratio of the fresh mixture could be found and four ignition regimes were identified. Regular ignition was only observed in a relatively narrow range of air fuel ratios. It was shown by means of high speed recordings of the OH*-chemiluminescence that the momentum and burning characteristics of the jets are extremely sensitive to the air fuel ratio and the ignition regime. Hence, the newly developed test rig of the Institute of Thermodynamics of Technical University of Munich has been shown to be suitable for fundamental research in the field of large bore gas engine combustion.

REFERENCES

[1] Kogler, G.; Wimmer, A.; Jauk, T.: Optische Analyse der Flammenausbreitung und Detektion von Verbrennungsanomalien bei Großgasmotoren. In: 10. Tagung „Der Arbeitsprozess des Verbrennungsmotors", Graz, 2005

[2] Dorer, F.: Kompressionsmaschine zur Simulation von Brennraumvorgängen in Wasserstoff-Großdieselmotoren, Technische Universität München, Dissertation, 2000

[3] Eisen, S.; Ofner, B; Mayinger, F.: Schnelle Kompressionsmaschine – Eine Alternative zum Transparentmotor? In: MTZ 62 (2001), No. 9, pp. 680-685

[4] Hanenkamp, A.; Terbeck, S.; Köbler, S.: 32/40 PGI – Neuer Otto-Gasmotor ohne Zündkerzen. In: MTZ 67 (2006), No. 12, pp. 932-941

[5] Kammerstätter, S.; Heinz, C.; Mittermayer, F.; Sattelmayer, T.: Experimentelle Untersuchung des Einflusses von Zündquelle, Zündzeitpunkt und Gemischzusammensetzung auf Zündung und Verbrennung in mager betriebenen Erdgas-Großmotoren mit Vorkammerzündung, In: Berichte zur Energie- und Verfahrenstechnik, Motorische Verbrennung, Vol. 11.1, 2011

[6] Heinz, C.: Untersuchung eines Vorkammerzündkonzepts für Großgasmotoren in einer Hochdruckzelle mit repetierender Verbrennung, Technische Universität München, Dissertation, 2011

[7] Prechtl, P.: Analyse und Optimierung der innermotorischen Prozesse in einem Wasserstoff-Dieselmotor, Technische Universität München, Dissertation, 2000

[8] Grünwald, J.; Sattelmayer, T.; Steinbach, S.: Wirbelmischer für SCR-Verfahren im Pkw. In: MTZ 66 (2005), No. 1, pp. 44-48

[9] Mittermayer, F.; Heinz, C.; Sattelmayer, T.; Hanenkamp, A.; Wilke, I.: Periodisch beladbare Hochdruckzelle zur Untersuchung der Verbrennung in vorkammergezündeten Großgasmotoren, In: Berichte zur Energie- und Verfahrenstechnik, Motorische Verbrennung, Vol. 9.1, 2009

[10] Mittermayer, F.: CFD-Simulation der Zündung und Verbrennung in einem vorkammergezündeten Großgasmotor, Technische Universität München, Dissertation, 2011

THANKS

The authors would like to thank MAN Diesel & Turbo for the fruitful collaboration within the project. Furthermore, the financial support of the Bavarian Research Fund (Bayerische Forschungsstiftung – BFS) is gratefully acknowledged.